EGE UNIVERSITY GRADUATE SCHOOL OF APPLIED AND NATURAL SCIENCES

(MASTER OF SCIENCE THESIS)

BORON REMOVAL FROM REVERSE OSMOSIS DESALINATED SEAWATER BY ION EXCHANGE-OPTIMIZATION STUDIES

ÖZLEM KIRMIZISAKAL

Department of Chemical Engineering
Department Code : 603.01.00

Date of Presentation :26.08.2008

Supervisor : Prof. Dr. Nalan KABAY

ÖZLEM KIRMIZISAKAL tarafından **Yüksel Lisans** tezi olarak sunulan "**Boron Removal from Reverse Osmosis Desalinated Seawater by Ion Exchange-Optimization Studies**" başlıklı bu çalışma, E.Ü. Lisansüstü Eğitim ve Öğretim Yönetmeliği ile E.Ü. Fen Bilimleri Enstitü Eğitim ve Öğretim Yönergesi'nin ilgili hükümleri uyarınca tarafımızdan değerlendirilerek savunmaya değer bulunmuş ve **26.08.2008** tarihinde yapılan tez savunma sınavında aday oybirliği/oyçokluğu ile başarılı bulunmuştur.

		İmza
Jüri Başkanı	: Prof. Dr. Nalan KABAY	.....
Raportör Üye	: Prof. Dr. Ümran YÜKSEL	.....
Üye	: Prof. Dr. Mithat YÜKSEL	.....

ÖZET

İYON DEĞİŞTİRME YÖNTEMİYLE DENİZ SUYUNUN TERS OZMOS SÜZÜNTÜSÜNDEN BOR GİDERİLMESİ-OPTİMİZASYON ÇALIŞMALARI

KIRMIZISAKAL, Özlem

Yüksek Lisans Tezi, Kimya Mühendisliği Bölümü

Tez Yöneticisi: Prof. Dr. Nalan KABAY

Ağustos 2008, 130 sayfa

Ters ozmos desalinasyon prosesi, deniz suyundan içme suyu üretmek için güvenilir ve etkin bir yöntemdir. Dünya Sağlık Örgütü'nün belirlediği düzenlemelere göre, içme suyundaki bor konsantrasyonu 0.5 mg/L yi geçmemelidir. Bu değer hali hazırda işletilmekte olan ters ozmos tesisleri için ulaşılması çok zor bir değerdir. Bu nedenle deniz suyu ters ozmos süzüntüsünden borun ikinci bir ayırma prosesi yardımıyla uzaklaştırılması gerekmektedir.

Bu çalışmada, borun farklı çözeltilerden; model bor çözeltisi (2ppm) ve doğal deniz suyundan elde edilmiş ters ozmos çıkış suyundan, şelatlayıcı, ticari reçineler (Diaion CRB 02 ve Dowex-XUS 43594.00) yardımıyla uzaklaştırılması incelenmiştir.

Çalışmalar; kesikli yöntemle gerçekleştirilmiştir.

Bu çalışmalarda, optimum reçine miktarı, kinetik testler ve sorpsiyon-sıyırma deneyleri yapılmıştır. Bu çalışmalardan elde edilen verilerle;

- Reçinelerin kesikli çalışma performansları,
- Reçinelerin kinetik performansları,

  - Sıcaklığın bor ayrılmasına etkisi (25°C, 30°C ve 35°C)
  - Tanecik boyutunun bor ayrılmasına etkisi (45-125 µm, 125- 250 µm ve 0.355-0.500 mm),
  - Karıştırma hızının bor ayrılmasına etkisi (200 RPM, 250 RPM ve 300 RPM)
- Adsorpsiyon izotermleri (Freundlich ve Langmuir, Dubinin-Radushkevich modelleri),
- İyon değiştirme kinetik basamakları,
- İyon değiştirme hızı tayin basamakları (Sonsuz Çözelti Hacmi ve Reaksiyona Girmemiş Çekirdek Modelleri)
- Ters osmos süzüntüsünün kinetik performansı,
- Reçinelerin sorpsiyon-sıyırma performansı incelenmiştir.

Anahtar Sözcükler: Bor, bor seçimli reçine, deniz suyu, desalinasyon, iyon değiştirme, modelleme, ters ozmos.

ABSTRACT

BORON REMOVAL FROM REVERSE OSMOSIS DESALINATED SEAWATER BY ION EXCHANGE-OPTIMIZATION STUDIES

KIRMIZISAKAL, Özlem

Master Science Thesis, Department of Chemical Engineering

Supervisor: Prof. Dr. Nalan KABAY

August 2008, 130 pages

Reverse osmosis (RO) membrane desalination process is an efficient and reliable technology for the production of drinking water from seawater. According to the WHO regulations, the boron concentration should be lower than 0.5 mg/L in drinking water. In the literature it was reported that, the concentration limit of boron in drinking water is very low which is quite difficult to be reached for conventional reverse osmosis desalination plants equipped with commercially available membranes. For this reason, removal of boron from reverse osmosis desalinated seawater by a secondary seperation process is needed.

In this study, removal of boron from different solutions (model B solution and model RO permeate with two commercial chelating resins (Diaion CRB 02 and Dowex-XUS 43594.00) was studied.

Experiments were performed with batch methods.

In these studies, determination of optimum resin amount and the sorption-elution conditions were examined.

According to these studies:

- Batch performance of the resins,

- Kinetic performance of the resin,
    - Temperature effect on boron removal (25°C, 30°C ve 35°C),
    - Particle size effect on boron removal (45-125 µm, 125-250 µm and 0.355-0.500 mm),
    - Stirring rate effect on boron removal (200 RPM, 250 RPM and 300 RPM),
- Effect of the boron concentration on kinetic performances of resins with model B solution,
- Adsorption isotherms (Freundlich and Langmuir Dubinin-Radushkevich models),
- Rate determining steps of the ion exchange (Infinite Solution Volume and Unreacted Core Models)
- Kinetic performance of resin with seawater reverse osmosis permeates.
- Sorption-elution performance of resins were investigated.

Key words: Boron, boron selected resin, desalination, ion exchange, modelling, seawater, reverse osmosis.

TEŞEKKÜR

Tez çalışmamın başarıya ulaşmasında büyük bir özveri ile bütün imkanlarını önüme seren, bana yeni ufuklar açan tez danışman hocam Sayın Prof. Dr. Nalan KABAY'a; tezimi inceleyerek verdikleri katkılardan ötürü Sayın Prof. Dr. Mithat Yüksel ve Sayın Prof. Dr. Ümran Yüksel'e teşekkürlerimi sunarım.

Avicenne Proje Laboratuarı'ndaki yardımlarından ve dostuklarından dolayı Yard. Doç. Müşerref Arda'ya, Araştırma Görevlileri İdil Yılmaz ve Özgür Arar'a, doktora öğrencisi Evrim Orhan'a ve Yüksek lisans öğrencileri Enver Güler, Deniz Özakdağ ve Sümbül Yavuz'a teşekkür ederim.

Bu noktaya gelmemdeki büyük emeklerinden ve özverilerinden dolayı aileme, desteklerini hiç esirgemeyerek hep yanımda olan ve bundan sonra da yanımda olmalarını istediğim arkadaşlarıma sonsuz teşekkürler.

Özlem KIRMIZISAKAL

TABLE OF CONTENTS

LIST OF FIGURES

LIST OF TABLES

NOMENCLATURE

a	:	specific surface area (m^2/m^3), stoichiometric coefficient
b	:	constant in Langmuir equilibrium (m^3/kg)
C	:	concentration of the solute in the solvent (kg/m^3)
C_{A0}	:	solute concentration in the bulk solution (M)
C_0	:	initial concentration (mg/L)
C_{s0}	:	concentration of the solid reactant at the bead's unreacted core (M)
d_p	:	particle diameter (m)
D	:	diameter of the packed bed column (m)
$\bar{D}$	:	inter-diffusion coefficient in the ion exchange resin
D_0	:	inter-diffusion coefficient in the film
$D_{e,r}$	:	effective diffusion coefficient in the solid phase (m^2/s)
F	:	surface area (m^2)
H	:	height of the sorbent layer in packed bed column (m)
J	:	permeate flux (m^3/m^2s)
k	:	kinetic constant (s^{-1})
K_{mA}	:	mass-transfer coefficient of the solute through the liquid film (m/s)
k_s	:	reaction constant based on surface (m/s)
m	:	mass of the solute (kg)
P	:	pressure drop during the flow in the column (Pa)
q	:	solute concentration in the sorbent (kg/kg)
r_0	:	average particle radius (mm)
X	:	concentration of fixed groups

v	:	superficial velocity of the feed in columns
V_b	:	Breakthrough volume (mL)
V_{eq}	:	Equilibrium volume (mL)

Greek Letters

δ	:	film thickness (m)
ε	:	porosity
η	:	membrane-sorption efficiency
μ	:	viscosity (Pa s)
τ	:	tortuosity
α_B^A	:	separation factor

1. INTRODUCTION

Nowadays, due to increasing for water, both potable and for irrigation, coupled with a decrease in suitable water sources suppliers have to turn to find alternatives. Seawater desalination or treatment of high saline and contaminated surface water was a known method. By using those alternative sources that have more trace contaminants start to appear in the final product. One of these contaminants is boron (Yılmaz et al, 2006).

Boron is an essential micronutrient for plants to complete certain metabolic activities. On the other hand, higher boron levels accelerate plants decay and expiration. Boron compounds passing to soil, surface waters and ground waters form many complexes with heavy metals such as Pb, Cd, Cu, Ni, etc. and these complexes are more toxic than heavy metals forming them. Seawater contains an average of 5 mg/L of boron presence as boric acid. The World Health Organization has given a recommendation of below 0.3 mg/L of boron for drinking water and 0.3-0.5 mg/L for irrigational water. So, there is a need for removal of boron from water and wastewater to obtain the limit concentration value for environmental pollution control (Yılmaz et al, 2006).

The membranes are available presently for seawater desalination remove only 60-80% of boron in the first pass of reverse osmosis system. This means that the first pass permeate contains between 1 and 2 mg/L of boron, depending on the water temperature and membrane conditions (Jacob, C., 2006).

1.1 Importance of Water for Our Life

As seen from space, one of the most unique features of our home planet is the water, in both liquid and frozen forms, that covers approximately 75% of the Earth's surface. Believed to have initially arrived on the surface through the emissions of ancient volcanoes, geologic evidence suggests that large amounts

of water have likely flowed on Earth for the past 3.8 billion years, most of its existence. As a vital substance that sets the Earth apart from the rest of the planets in our solar system, water is a necessary ingredient for the development and nourishment of life (Gleick, 1996).

Most of the earth's surface is covered by water, and most of the human body is composed of water two facts illustrating the critical linkages between water, health and ecosystems (Gleick, 1996).

Water in our body has a very important role and an excellent water circulating system is established in our digestive tract. The human body consists of around 65% water and if we lose 3% of it, we will have symptoms of dehydration. If we lose 10~15% of it, we lose sound body conditions (BDA, 2003).

Table 1.1 Recommendations for daily requirements of drinking water (WHO, 2003)

	Average conditions	Manual labour in high temperatures	Total needs in pregnancy/lactation
Female adults	2.2 litres	4.5 litres	4.8 litres (pregnancy) 5.5 litres (lactation)
Male adults	2.9 litres	4.5 litres	-

As seen in Table 1.1, usually adults drink around 2~3 liters of water every day, of water every day, but in our body approximately 6~7 liters of water is circulated in our digestive tract to digest and absorb the nutrients of foods. In the lower parts of the large intestine, there exist intestinal microorganisms which produce short chain fatty acids, of which butyric acid is attributed to be an energy source to absorb water into the large intestine, to give the feces an

adequate water content of 70~80%. Water is the most important constituent of our body and a splendid water recycling system is established. The availability of clean, fresh water is one of the most important issues facing humanity today – and will be increasingly critical for the future, as growing demand outstrips supplies and pollutioncontinues to contaminate rivers, lakes and streams (BDA, 2003).

1.2 Water Resources

Water is an odourless, colourless, and tasteless compound that is also considered to be a renewable resource. It is a renewable resource since it has been continually recycled through the water cycle (also known as the hydrologic cycle) for millions of years (Figure 1.1). Water is recycled through the processes of evaporation and precipitation (Figure 1.1). Even though water is constantly being recycled, only a small amount is available for use by humans. (Bauder et al., 2007).

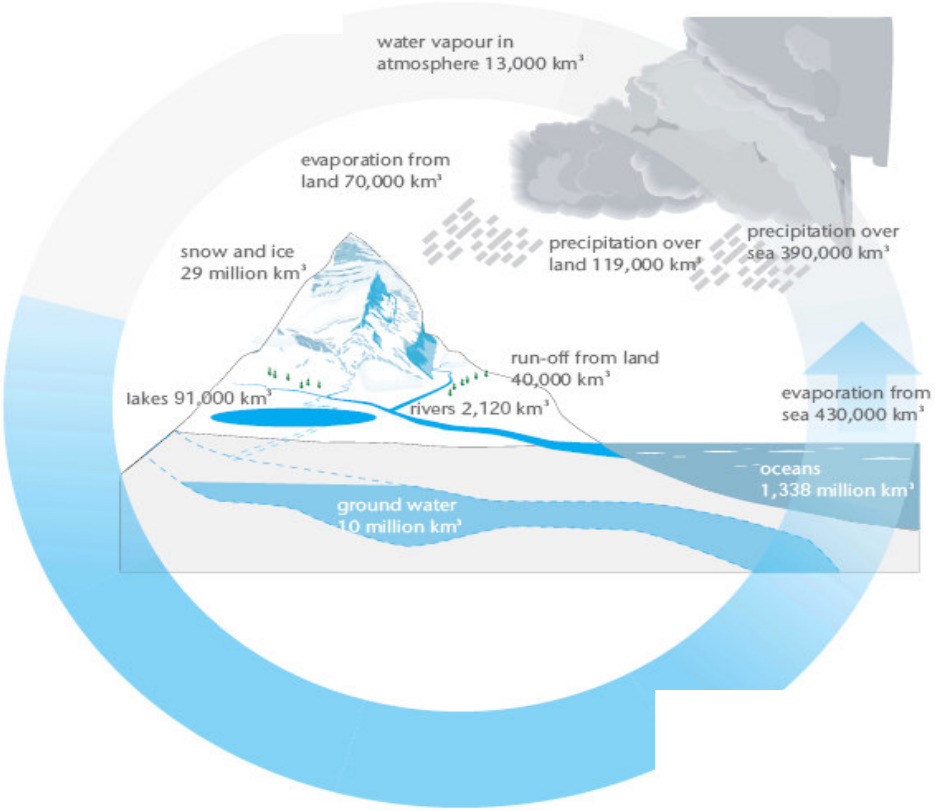

Figure 1.1 The big water cycle (WBCSD and UNEP, 1998).

1.2.1 The Water Cycle

Since water is in a cycle that is in constant motion, let's begin with evaporation. Evaporation is the process of converting water into water vapor through the application of heat. The main source of heat when discussing surface water is the sun. The water vapor then becomes part of the atmosphere. Precipitation occurs when atmospheric water vapor combines to form water droplets. When the droplets are large enough, they fall from the clouds. Depending on the weather conditions, the forms of precipitation can be rain, snow, hail, sleet, dew or frost (Bauder et al., 2007).

1.2.2 Ground Water, Surface Water and Seawater

Although water is the most widely occurring substance on earth, only 2 percent is fresh water while the remainder is salty water (see in Figure 1.2). Some two thirds of this freshwater is locked up in glaciers and permanent snow cover. In addition to the accessible freshwater in lakes, rivers and aquifers, man-made storage in reservoirs adds a further 8,000 cubic kilometres (km^3) (The Environment Agency, 2008).

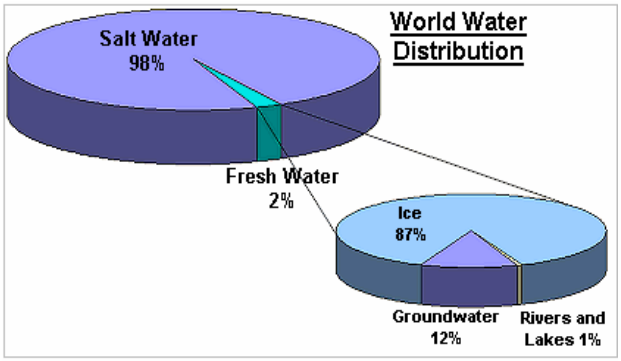

Figure 1.2 World Water Distribution Diagram

In order to understand drinking water contamination, it is necessary to first understand from where our drinking water comes. For most urban residents, relying upon municipal water systems, drinking water comes from two major sources: groundwater and surface water. On the other hand, seawater is not accepted as drinking water in literature. Because of the sources of drinking water is decreasing, seawater is used as drinking water and irrigation water after membrane and/or resin processes in most countries (Dasch, 1996).

Groundwater is the largest available reservoir of fresh water. The 'World Water Distribution' diagram shows that the majority of fresh water is locked away as ice in the polar ice caps, continental ice sheets and glaciers. Water in rivers and lakes has only accounts for less than 1% of the world's fresh water reserves (Dasch, 1996).

Most people are unaware of the part groundwater plays in the water cycle-water falls as rain and snow on the land (precipitation); and soaks into the soil, with excess rainfall flowing overland to rivers. Once the needs of plant roots and soil moisture have been satisfied, the remaining water continues its journey downward to rock layers beneath the soil. These underground rock layers have the capacity to let water flow through them, either through large cracks and openings in the rock, or through tiny inter-connected spaces between individual rock grains Dasch, 1996). The water contained in these rocks is groundwater; and such bodies of rock are known as aquifers, shown in Figure 1.3.

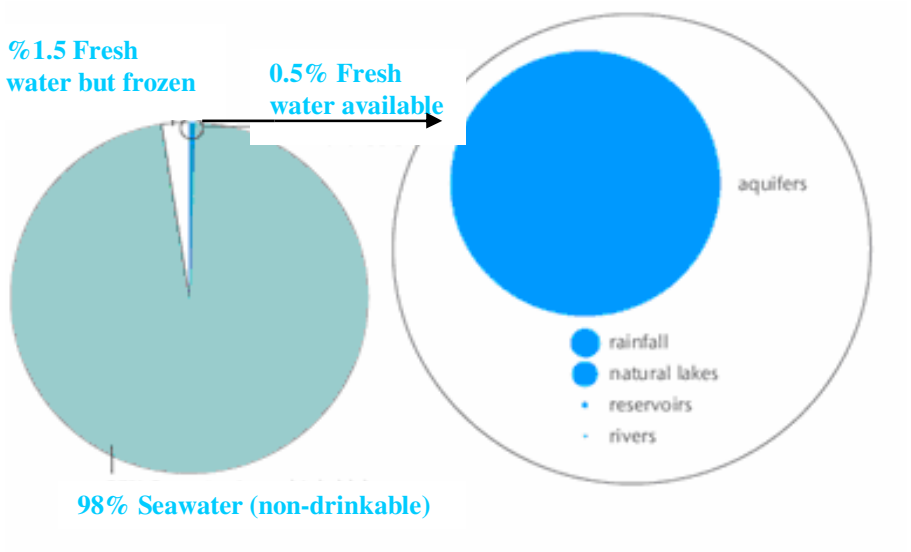

Figure 1.3 Fresh water available (UNESCO, 2003).

Perhaps the best way of imaging an aquifer is as a giant sponge. Water aided by gravity naturally fills the aquifer from the bottom upwards. This bottom part of the aquifer has spaces that are completely filled by water termed the 'saturated zone' of the aquifer. In the top part of the aquifer the rock spaces contain air as well as water; here the aquifer zone is called 'unsaturated' (Dasch, 1996).

Water in an aquifer does not sit still it flows through the spaces and cracks in the rock, being pulled by gravity; and pushed by the force of the water above and behind it. The water moves from an area where water enters the aquifer (a recharge zone) to an area where water exits the aquifer (a discharge zone). Where discharge happens, springs may appear, and the aquifer will contribute groundwater to support the flow of rivers and maintain important habitats like fens and marshlands (Dasch, 1996).

The movement of groundwater through the aquifer has the effect of removing a lot of impurities from the water, filtering it through the rock so that groundwater is generally much cleaner than surface water. As groundwater is generally very clean it often requires little or no treatment before being used, the level of treatment depends on what it is to be used for. This makes groundwater a very cheap source of 'raw water' for public supply. This freshwater can be accessed by drilling down into the water-bearing rock layers and pumping the water out (Dasch, 1996).

Aquifers close to, or outcropping at, the ground surface are more vulnerable to pollution or physical damage that could harm both the quality and flow of the groundwater. The flow of groundwater is slower than surface water, and the deeper into an aquifer the water is, the slower it moves. This means that if groundwater becomes polluted and the pollution moves deep into the aquifer, the water can potentially remain polluted for a very long time This could subsequently led to a deterioration in the quality of drinking water supplied from a groundwater source or damage vulnerable groundwater dependent rivers and ecosystems (Dasch, 1996).

Surface water refers to water occurring in lakes, rivers, streams, or other fresh water sources used for drinking water supplies.

Although the only natural input to any surface water system is precipitation within its watershed, the total quantity of water in that system at

any given time is also dependent on many other factors. These factors include storage capacity in lakes, wetlands and artificial reservoirs, the permeability of the soil beneath these storage bodies, the runoff characteristics of the land in the watershed, the timing of the precipitation and local evaporation rates. All of these factors also affect the proportions of water lost (Miles, 1979).

Human activities can have a large impact on these factors. Humans often increase storage capacity by constructing reservoirs and decrease it by draining wetlands. Humans often increase runoff quantities and velocities by paving areas and channelizing stream flow (Miles, 1979).

Seawater is (impure) water from a sea or ocean. An aqueous solution of salt of a rather constant composition of elements whose presence determines the climate and makes life possible on the Earth and which constitutes the oceans, the Mediterranean seas, and their embayment. Water is most often found in nature as seawater (about 98%). The rest is ice, water vapour, and fresh water (Pilson, 1998).

On average, seawater in the world's oceans has a salinity of about 3.5%, or 35 parts per thousand as seen Table 1.2. This means that every 1 kg of seawater has approximately 35 grams of dissolved salts (mostly, but not entirely, the ions of sodium chloride: Na^+, Cl^-). The average density of seawater at the surface of the ocean is 1.025 g/ml; seawater is denser than fresh water (which reaches a maximum density of 1.000 g/ml at a temperature of 4°C) because of the added weight of the salts (Fry, 2006).

Table 1.2 Major constituents of seawater (salinity 35 psu)* (Pilson, 1998).

Cations	Amount, g/kg	Anions	Amount, g/kg
Sodium	10.7520	Chloride	19.3450
Magnesium	1.2950	Bromide	0.0660
Potassium	0.3900	Fluoride	0.0013
Calcium	0.4160	Sulfate	2.7010
Strontium	0.0130	Bicarbonate	0.1450
		Boric acid	0.0270

*PSU: practical salinity unit, 35g salt/1000g water

As can be seen in Table 1.2, seawater with TDS of 35,000 mg/L is considered standard seawater constituting, by far, the largest amount of water worldwide. The composition is nearly the same all over the world. The actual TDS content may, however, vary within wide limits from the Baltic Sea with 7,000 mg/L to the Red Sea and Arabian Gulf with up to 45,000 mg/L. The actual compositions can be proportionally estimated from the standard seawater composition (Table 1.2). The water from seashore wells, however, depending on the soil, influx from inland, etc., can often have salinity and composition quite different from water taken from the sea itself (Charles, 2006).

1.2.3 Water Use

Water is important recource for domestical, industrial, irrigational uses. As shown in Figure 1.4, industrial use of water increases with country income, going from 10% for low- and middle- income countries to 59% for high-income countries (UNESCO, 2003).

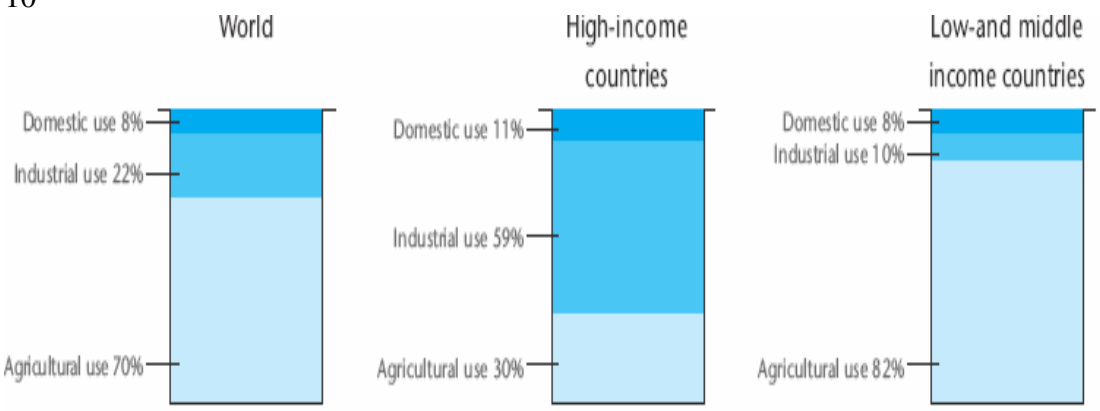

Figure 1.4 Usage of water as a parameter of country income (UNESCO, 2003).

1.2.3.1 Agriculture

In many developing nations, irrigation accounts for over 70% of water withdrawn from available sources for use. In UK, where rain is aboundant year round, water used for agriculture accounts less than 1 % of human usage. Yet even on the same continent, water used for irrigation in Spain, Portugal and Greece exceededs 70% of total usage. (percentage of total usage of irrigation for some other countries is shown in Figure 1.5). Irrigation has been a key component of the green revolution that has enabled many developing countries to produce enough food to feed everyone. But increasing competition for water and inefficient irrigation practices could constrain future food production.

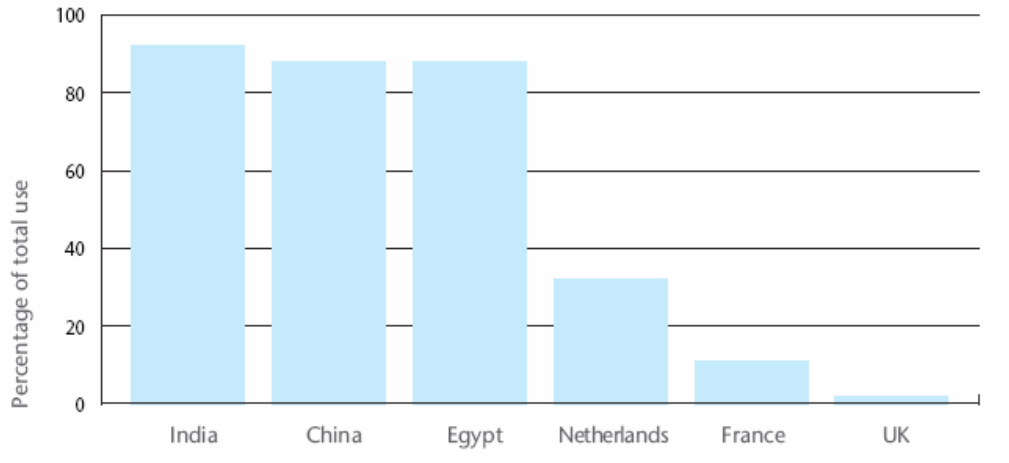

Figure 1.5 Percentages of total water used for irrigation (Saeijs and Van Berkel, 2003)

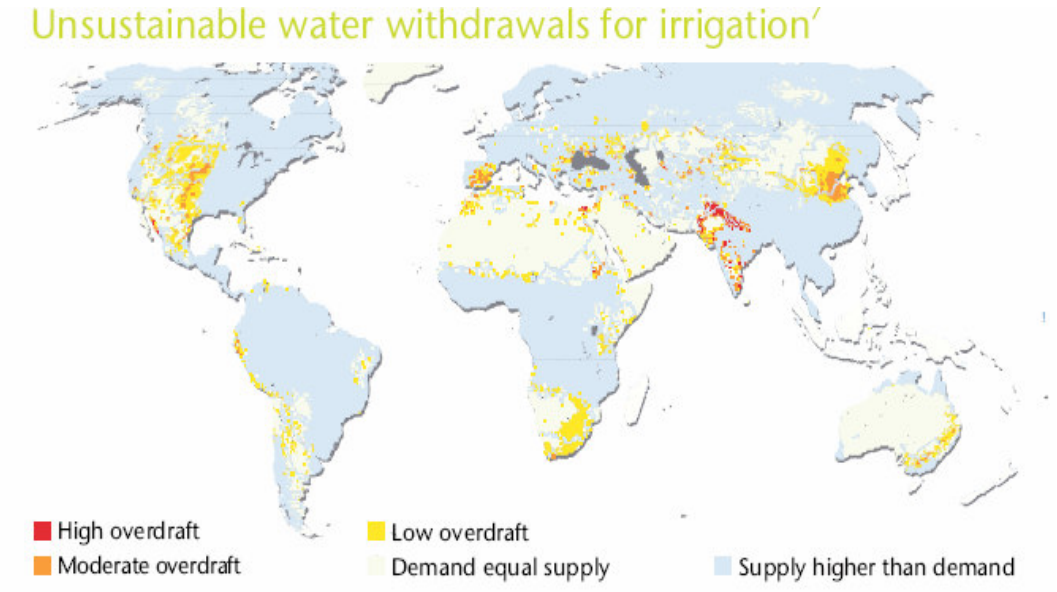

Figure 1.6 Unsustainable water withdrawals for irrigation.

As shown in Figure 1.6, globally, roughly 15-35% of irrigation withdrawals are estimated to be unsustainable. The map indicates where there is insufficient freshwater to fully satisfy irrigated crop demands. (Key: high overdraft, > 1 cubic kilometer per year; moderate, 0.1–1 cubic

kilometer per year; low, 0–0.1 cubic kilometer per year. All estimates made on about 50-kilometer resolution. Though difficult to generalize, the imbalances translate into water table drawdowns >1.6 meters per year or more for the high overdraft case and <0.1 meter per year for low, assuming water deficits are met by pumping unconfined aquifers with typical dewatering potentials (specific yield = 0.2)) (Millennium Ecosystem Assessment, 2005).

1.2.3.2 Industry

After agriculture, industry is the second largest user of water. However the amount of water used varies widely from one type of industry to another.

Cooling water: The largest single use of water by industry is for cooling in thermal power generation steam to atmosphere to fall (Fry, 2006).

Water for energy: Multi purpose hydro projects manage water for many interests: flood control, irrigation, recreation and drinking water, as well as energy (Fry, 2006).

Process water: Industry uses water to make steam for direct drive power and for use in various production processes or chemical reactions (Fry, 2006).

Water for products: Many businesses, notably the food, beverage and pharmaceutical sectors consume water by using it as an ingredient in finished products for human consumption. Think of dairy products, soups, beverages and medicines that are delivered in liquid form. Some water experts are using the term “virtual water” to describe the water that is embedded both in agricultural and manufactured products, as well as the water used in the growing or manufacturing process. When a country exports goods, it is exporting “virtual water” (Fry, 2006).

1.3 Water for Irrigation-Quality Standards

One of the major concerns with water used for irrigation is decreased crop yields and land degradation as a result of excess salts being present in water and in soils. Salinity is the term used when referring to the presence of soluble salts in or on soils, or in waters (Bauder et al., 2007).

To assess the suitability of irrigation water in regards to salinity management, other factors must be considered besides water quality. These include salt tolerance of the crop being cultivated and the characteristics of the soil under irrigation. Climate, soil management and water management practices can also impact on the extent of salinity (Bauder et al., 2007).

Soil scientists use the following categories to describe irrigation water effects on crop production and soil quality:

- Salinity hazard - total soluble salt content
- Sodium hazard - relative proportion of sodium (Na^{+}) to calcium (Ca^{2+}) and magnesium (Mg^{2+}) ions
- pH
- Alkalinity - carbonate and bicarbonate
- Specific ions: chloride (Cl), sulfate (SO_4^{2-}), boron (B), and nitrate-nitrogen (NO_3-N).
- Other potential irrigation water contaminants that may affect suitability for agricultural use include heavy metals and microbial contaminants.

1.3.1 Salinity Hazard

The most influential water quality guideline on crop productivity is the water salinity hazard as measured by electrical conductivity (EC_w). The primary effect of high EC_w water on crop productivity is the inability of the plant to compete with ions in the soil solution for water (physiological drought). The higher the EC, the less water is available to plants, even though the soil may appear wet. Because plants can only transpire "pure" water, usable plant water in the soil solution decreases dramatically as EC increases (Bauder et al., 2007).

Table 1.3 Suggested criteria for irrigation water use based upon conductivity (Bauder et al., 2007).

Classes of water	**Electrical Conductivity**
	(dS/m)*
Class 1, Excellent	≤0.25
Class 2, Good	0.25 - 0.75
Class 3, Permissible[1]	0.76 - 2.00
Class 4, Doubtful[2]	2.01 - 3.00
Class 5, Unsuitable[2]	≥3.00

*dS/m at 25ºC = mmhos/cm

[1]Leaching needed if used.

[2]Good drainage needed and sensitive plants will have difficulty for obtaining standards.

Other terms that laboratories and literature sources use to report salinity hazard are: salts, salinity, electrical conductivity (EC_w), or total dissolved solids (TDS). These terms are all comparable and all quantify the amount of dissolved “salts” (or ions, charged particles) in a water sample. However, TDS is a direct

measurement of dissolved ions and EC is an indirect measurement of ions by an electrode (Bauder et al., 2007).

Although people frequently confuse the term “salinity” with common table salt or sodium chloride (NaCl), EC measures salinity from all the ions dissolved in a sample. This includes negatively charged ions (e.g., Cl^-, NO_3^-) and positively charged ions (e.g., Ca^{++}, Na^+). Another common source of confusion is the variety of unit systems used with EC_w. The preferred unit is deci siemens per meter (dS/m), however millimhos per centimeter (mmho/cm) and micromhos per centimeter (µmho/cm) are still frequently used (Bauder et al., 2007).

1.3.2 Sodium Hazard

While EC_w is an assessment of all soluble salts in a sample, sodium hazard is defined separately because of sodium's specific detrimental effects on soil physical properties. The sodium hazard is typically expressed as the sodium adsorption ratio (SAR). This index quantifies the proportion of sodium (Na^+) to calcium (Ca^{++}) and magnesium (Mg^{++}) ions in a sample. Calcium will flocculate (hold together), while sodium disperses (pushes apart) soil particles. This dispersed soil will readily crust and have water infiltration and permeability problems (Bauder et al., 2007).

1.3.3 pH and Alkalinity

These two are important factors in determining the solubility of water for irrigating ornamental plants. pH is a measure of the concentrations of hydrogen ion (H^+) in water or other liquids. pH is an important chemical property related to plant growth because of its effect on nutrient availability. It is therefore important to monitor and control pH during the growth of your crop. Water for irrigation should have a pH between 5.0 and 7.0. However, it is the relationship between water pH and alkalinity, namely the presence of high alkalinity that will

have a more significant impact on pH control of soils and growing media. Alkalinity is a measure of the water's ability to neutralize acidity. An alkalinity test measures the level of bicarbonates, carbonates and hydroxides in water. The results are expressed as ppm of calcium carbonate ($CaCO_3$). Levels between 30 and 60 ppm are considered optimum for most plants (Bauder et al., 2007).

1.3.4 Chloride

Although chloride is essential to plants in very low amounts, it can cause toxicity to sensitive crops at high concentrations. Like sodium, high chloride concentrations cause more problems when applied with sprinkler irrigation. Leaf burn under sprinkler from both sodium and chloride can be reduced by night time irrigation or application on cool, cloudy days. Drop nozzles and drag hoses are also recommended when applying any saline irrigation water through a sprinkler system to avoid direct contact with leaf surfaces (Bauder et al., 2007).

1.3.5 Sulfate

As with boron, sulfate in irrigation water has fertility benefits, and irrigation water in Colorado often has enough sulfate for maximum production for most crops. Exceptions are sandy fields with <1 percent organic matter and <10 ppm SO_4-S in irrigation water (Bauder et al., 2007).

1.3.6 Nitrogen

Water high in N can cause quality problems in crops such as barley and sugar beets and excessive vegetative growth in some vegetables. However, these problems can usually be overcome by good fertilizer and irrigation management. Regardless of the crop, nitrate should be credited toward the fertilizer rate especially when the concentration exceeds 10 ppm NO_3-N (45 ppm NO_3^-) (Bauder et al., 2007).

1.3.7 Boron

Boron is an essential element for plant growth. Boron is needed in relatively small amounts, however, and if present in amounts appreciably greater than needed, it becomes toxic. For some crops, if 0.2 mg/l boron in water is essential, 1 to 2 mg/l may be toxic. Surface water rarely contains enough boron to be toxic but well water or springs occasionally contain toxic amounts, especially near geothermal areas and earthquake faults. Boron problems originating from the water are probably more frequent than those originating in the soil. Boron toxicity can affect nearly all crops but, like salinity, there is a wide range of tolerance among crops (Ayers and Westcot, 1994).

Boron toxicity symptoms normally show first on older leaves as a yellowing, spotting (Figure 1.7), or drying of leaf tissue at the tips and edges. Drying and chlorosis often progress toward the centre between the veins (interveinal) as more and more boron accumulates with time. On seriously affected trees, such as almonds (Figure 1.8) and other tree crops which do not show typical leaf symptoms, a gum or exudate on limbs or trunk is often noticeable (Ayers and Westcot, 1994).

Figure 1.7 Boron effect on leaves

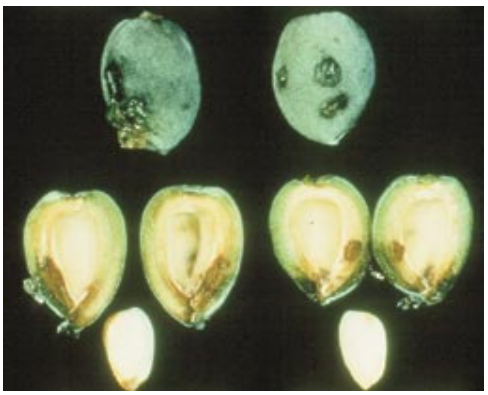

Figure 1.8 Boron effect on almond

Most crop toxicity symptoms occur after boron concentrations in leaf blades exceed 250–300 mg/kg (dry weight) but not all sensitive crops accumulate boron in leaf blades. For example, stone fruits (peaches, plums, almonds, etc.), and pome fruits (apples, pears and others) are easily damaged by boron but they do not accumulate sufficient boron in the leaf tissue for leaf analysis to be a reliable diagnostic test. With these crops, boron excess must be confirmed from soil and water analyses, tree symptoms and growth characteristics (Ayers and Westcot, 1994).

A wide range of crops was tested for boron tolerance by using sand-culture techniques (Eaton 1944). As seen in Table 1.4, boron tolerance tables in general use have been based for the most part on these data. This table reflected boron tolerance at which toxicity symptoms were first observed and, depending on crop, covered one to three seasons of irrigation (Maas 1984). It is not based on plant symptoms, but upon a significant loss in yield to be expected if the indicated boron value is exceeded (Ayers and Westcot, 1994).

Table 1.4 Tolerance amounts of boron for agricultural crops (ANZECC, 1992)

Tolerance	Concentration of boron in soil water (mg/L)	Agricultural crop
Very sensitive	<0.5	Blackberry
Sensitive	0.5-1.0	Peach, cherry, plum, grape, cowpea, onion, garlic, sweet, potato, wheat, barley, sunflower, sesame, strawberry
Moderately sensitive	1.0-2.0	Red pepper, pea, carrot, radish, potato, cucumber
Moderately tolerant	2.0-4.0	Lettuce, cabbage, celery, turnip, oat, corn, artichoke, tobacco, mustard, squash
Tolerant	4.0-6.0	Tomato, alfalfa, purple, parsley, sugar-beet
Very tolerant	6.0-15.0	Asparagus

1.4 Desalination of Seawater by Membrane Processes

Desalination of seawater and treatment of high saline surface waters are important processes for producing potable and irrigation water. However, saline water sources also contain other trace contaminants, like boron, which may appear in the final product water (Charles, 2006).

Figure 1.9 gives an approximate representation of the salinity range to which the main desalination processes can be generally applied economically (Dow Tech Manual, 2006).

The most typical operating range of the four major desalination processes is also shown in Figure 1.9 (Dow Tech Manual, 2006).

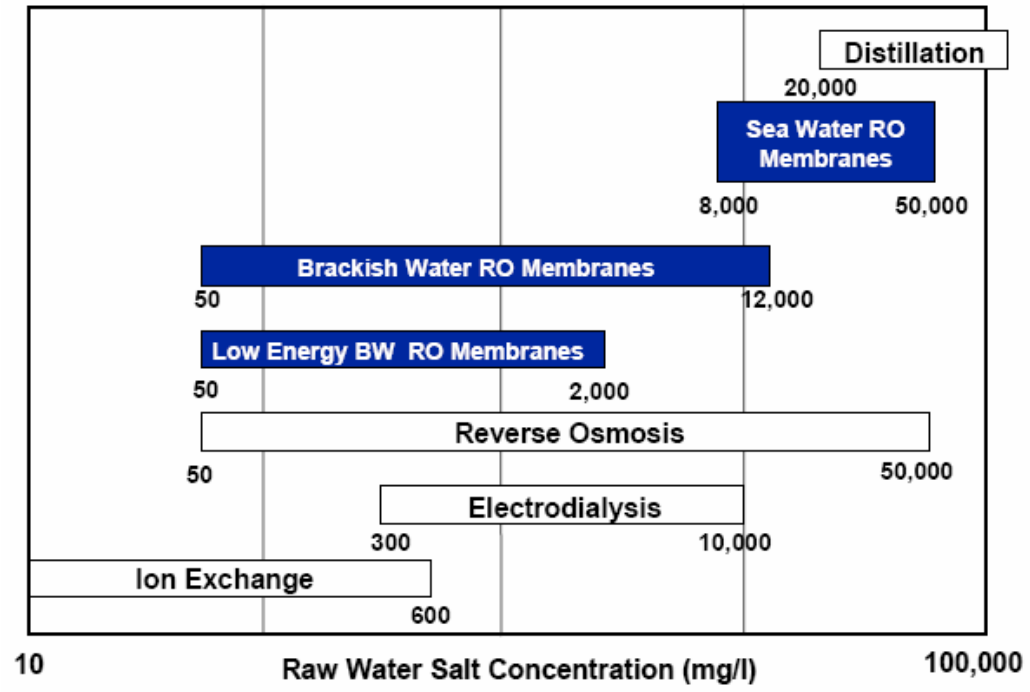

Figure 1.9 Major Desalination Process (Dow Tech Manual, 2006).

The various filtration technologies which currently exist can be categorized on the basis of the size of particles removed from a feed stream. Conventional macrofiltration of suspended solids is accomplished by passing a feed solution through the filter media in a perpendicular direction. The entire solution passes through the media, creating only one exit stream. Examples of such filtration devices include cartridge filters, bag filters, sand filters, and multimedia filters. Macrofiltration separation capabilities are generally limited to undissolved particles greater than 1 micron (Dow Tech Manual, 2006).

1.4.1 Membrane Separation Processes

Membrane technologies have been established as very effective and commercially attractive options for separation and purification processes (TIFAC, 1997).

The membrane can be defined essentially as a barrier, which separates two phases and restricts transport of various chemicals in a selective manner. A membrane can be homogenous or heterogeneous, symmetric or asymmetric in structure, solid or liquid can carry a positive or negative charge or be neutral or bipolar. Transport through a membrane can be affected by convection or by diffusion of individual molecules, induced by an electric field or concentration, pressure or temperature gradient. The membrane thickness may vary from as small as 100 micron to several mms (TIFAC, 1997).

1.4.1.1 Membrane Separation Technology

In a membrane separation process, a feed consisting of a mixture of two or more components is partially separated by means of a semipermeable barrier (the membrane) through which one or more species move faster than another or other species. The most general membrane process is shown in Table 1.5 where the feed mixture is separated into a retentate that part of the feed that does not pass through the membrane, i.e., is retentate, and a permeate that part of the feed that does pass through the membrane Although the feed, retentate and permeate are usually liquid or gas, they may also be solid. The barrier is most often a thin, nonporous polymeric film, but may also be porous polymer, ceramic or metal materials, or even a liquid or gas. The barrier must not dissolve, disintegrate, or break (Seader and Hendley, 1998).

Membrane separation process enjoys numerous industrial applications with the following advantages:

- Appreciable energy savings
- Environmentally benign
- Clean technology with operational ease
- Replaces the conventional processes like filtration, distillation, ion-exchange and chemical treatment systems
- Produces high, quality products
- Greater flexibility in designing systems

Table 1.5 Industrial application of membrane separation processes (Seader and Henley, 1998).

1. Reverse osmosis:
   - Desalinization of brackish water
   - Treatment of wastewater to remove a wide variety of impurities
   - Treatment of surface and ground water
   - Concentration of foodstuffs
   - Removal of alcohol from beer and wine
2. Dialysis:
   - Separation of nickel sulfate from sulfuric acid
   - Hemodialysis (removal of waste metabolites, excess body water, and restoration of electrolyte balance in blood)
3. Electrodialysis:
   - Production of table salt from seawater
   - Concentration of brines from reverse osmosis
   - Treatment of wastewaters from electroplating
   - Demineralization of cheese whey
   - Production of ultrapure water for the semiconductor industry
4. Microfiltration:
   - Sterilization of drugs
   - Clarification and biological stabilization of beverages
   - Purification of antibiotics
   - Separation of mammalian cells from a liquid
5. Ultrafiltration:
   - Preconcentration of milk before making cheese
   - Clarification of fruit juice
   - Recovery of vaccines and antibiotics from fermentation broth
   - Color removal from Kraft black liquor in paper-making
6. Prevaporation:
   - Dehydration of ethanol–water azeotrope
   - Removal of water from organic solvents
   - Removal of organics from water
7. Gas permeation:
   - Separation of CO_2 or H_2 from methane and other hydrocarbons
   - Adjustment of the H_2/CO ratio in synthesis gas
   - Separation of air into nitrogen- and oxygen-enriched streams
   - Recovery of helium
   - Reocvery of methane from biogas
8. Liquid membranes:
   - Recovery of zinc from wastewater in the viscose fiber industry
   - Recovery of nickel from electroplating solutions

1.4.1.2 Types of Membranes

The following section explains the types of membranes commonly used.

Microporous Membranes

The membrane behaves almost like a fibre filter and separates by a sieving mechanism determined by the pore diameter and particle size. Materials such as ceramics, graphite, metal oxides, polymers etc. are used in making such membranes. The pores in the membrane may vary between 1 nm-20 microns (TIFAC, 1997).

Homogeneous Membranes

This is a dense film through which a mixture of molecules is transported by pressure, concentration or electrical potential gradient. Using these membranes, chemical species of similar size and diffusivity can be separated efficiently when their concentrations differ significantly (TIFAC, 1997).

Asymmetric Membranes

An asymmetric membrane comprises a very thin (0.1-1.0 micron) skin layer on a highly porous (100-200 microns) thick substructure. The thin skin acts as the selective membrane. Its separation characteristics are determined by the nature of membrane material or pore size, and the mass transport rate is determined mainly by the skin thickness. Porous sub-layer acts as a support for the thin, fragile skin and has little effect on the separation characteristics (TIFAC, 1997).

Electrically Charged Membranes

These are necessarily ion-exchange membranes consisting of highly swollen gels carrying fixed positive or negative charges. These are mainly used in the electro-dialysis (TIFAC, 1997).

Liquid Membranes

A liquid membrane utilizes a carrier to selectively transport components such as metal ions at relatively high rate across the membrane interface (TIFAC, 1997).

1.4.1.3 Membrane Modules

The following membrane modules are largely used for industrial applications.

a) *Hollow fiber:* resembles a shell-and-tube heat exchanger. The pressure feed enters the shell side at one end. While flowing over the fibres toward the other end, permeate passes through the fibre walls into the central fiber channels as in Figure 1.10. Typically fibres are sealed at one end and embedded into a tube sheet with epoxy resin at the other end. A commercial module might be 1 m long and 0.1 ar 5 m in diameter and contain more than one million hollow fibres (Seader and Henley, 1998).

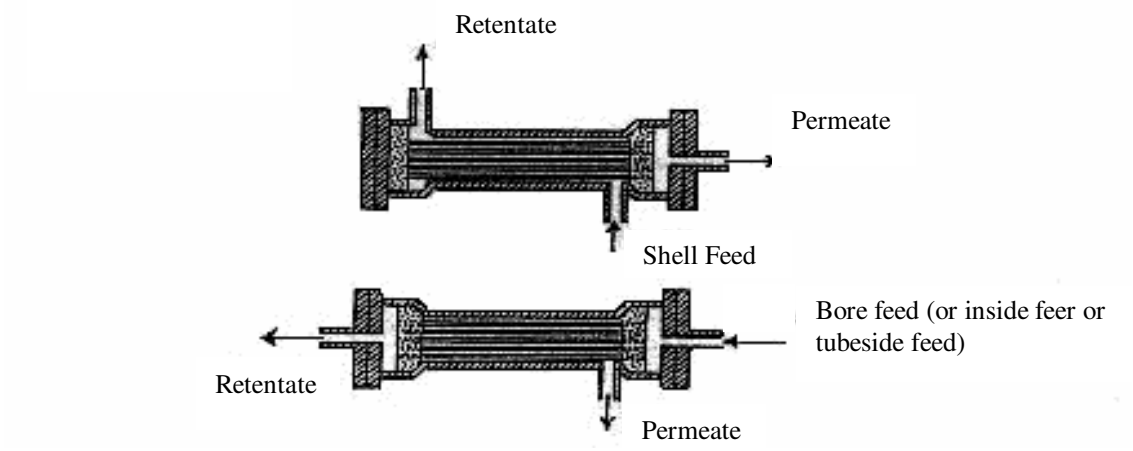

Figure 1.10 Hollow-Fibre type membranes (Seader and Henley, 1998).

b) Plate and frame module : plate sheets used in plate-and- frame modules are circulari squarei or rectangular in cross-section.the sheets are separated by support plates that channel the permeate. In Figure 1.11.a, a feed of brackish water flows across the surface of each membrane sheet in the stack. Pure water is permeate product, whereas the retentate is a concentrated brine solution (Seader and Henley, 1998).

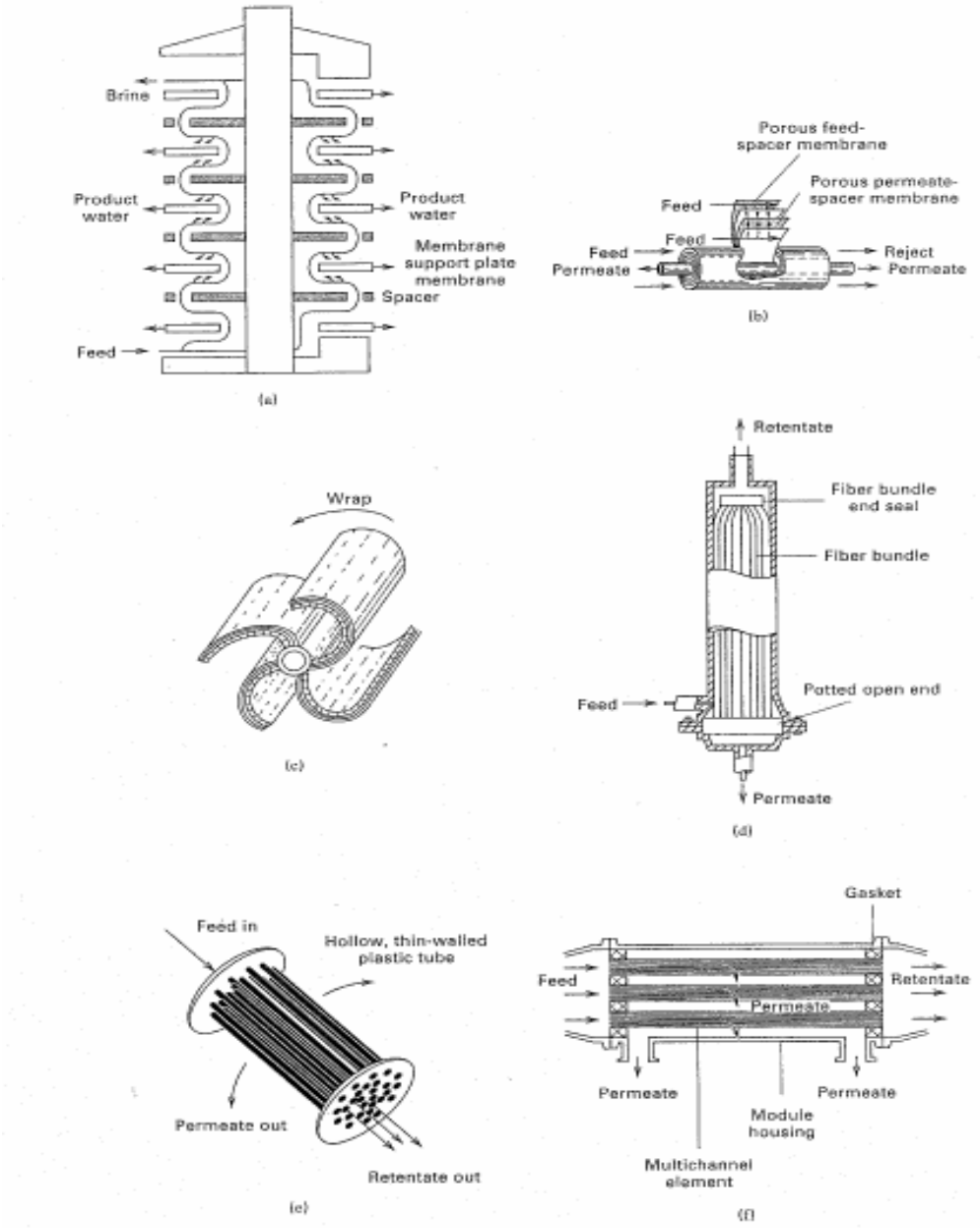

Figure 1.11 Common membrane modules: a) plate and frame b) spiral wound c) four-leaf spiral wound d) hollow fibre e) tubular f) monolithic (Seader and Henley, 1998).

c) Spiral wound module: flat sheets are also fabricated into spiral-wound modules shown in Figure 1.12. A laminate, consisting of two membrane sheets separated by spacers for the flow of the fees and permeate, is wound around a central perforated collection tube to form a module that is inseted into a pressure vessel. The feed flows axially in the channels created between the membranes by the porous spacers. Permeate passes through the membrane, travelling inward in spiral path to the central collection tube. From there, the permeate flows in either axial direction through and of the central tube. A typical spiral-wound module is 0.1 to 0.3 m in diameter and 3 m long six such modules are often placed in series (Seader and Henley, 1998).

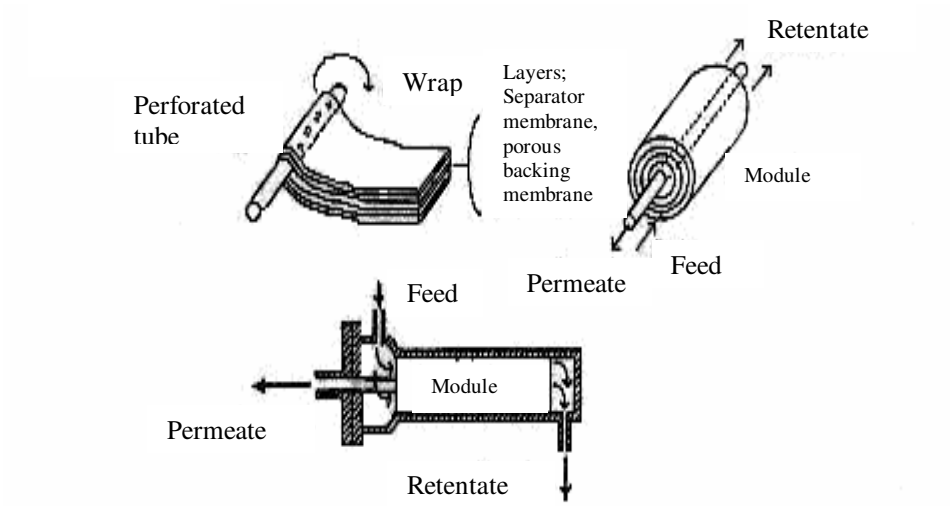

Figure 1.12 Spiral wound module (Seader and Henley, 1998).

d) Tubular membrane module: a tubular module is shown in Figure 1.11(e), this module also resembles a shell-and-tube heat exchanger, but the feed flows through the tubes. Permeate passes through the wall of the tubes into the shell side of the module. Tubular modules contain up to 30 tubes (Seader and Henley, 1998).

1.4.2 Desalination Technologies and Filtration Processes

For the removal of small particles and dissolved salts, crossflow membrane filtration is used. Crossflow membrane filtration (see Figure 1.13) uses a pressurized feed stream which flows parallel to the membrane surface. A portion of this stream passes through the membrane, leaving behind the rejected particles in the concentrated remainder of the stream. Since there is a continuous flow across the membrane surface, the rejected particles do not accumulate but instead are swept away by the concentrate stream. Thus, one feed stream is separated into two exit streams: the solution passing through the membrane surface (permeate) and the remaining concentrate stream (Dow Tech Manual, 2006).

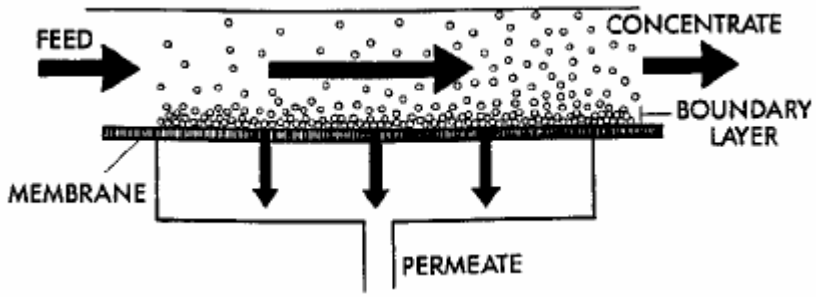

Figure 1.13 Crossflow membrane filtration (Dow Tech Manual, 2006).

There are four general categories of crossflow membrane filtration: microfiltration, ultrafiltration, nanofiltration, and reverse osmosis.

1.4.2.1 Microfiltration (MF)

Microfiltration removes particles in the range of approximately 0.1 to 1 micron. In general, suspended particles and large colloids are rejected while macromolecules and dissolved solids pass through the MF membrane. Applications include removal of bacteria, flocculated materials, or TSS (total

suspended solids). Transmembrane pressures are typically 10 psi (0.7 bar) (Dow Tech Manual, 2006).

1.4.2.2 Ultrafiltration (UF)

Ultrafiltration provides macro-molecular separation for particles in the 20 to 1,000 Angstrom range (up to 0.1 micron). All dissolved salts and smaller molecules pass through the membrane. Items rejected by the membrane include colloids, proteins, microbiological contaminants, and large organic molecules.

Most UF membranes have molecular weight cut-off values between 1,000 and 100,000. Transmembrane pressures are typically 15 to 100 psi (1 to 7 bars) (Dow Tech Manual, 2006).

1.4.2.3 Nanofiltration (NF)

Nanofiltration refers to a speciality membrane process which rejects particles in the approximate size range of 1 nanometer (10 Angstroms), hence the term “nanofiltration.” NF operates in the realm between UF and reverse osmosis. Organic molecules with molecular weights greater than 200-400 are rejected. Also, dissolved salts are rejected in the range of 20-98%. Salts which have monovalent anions (e.g. sodium chloride or calcium chloride) have rejections of 20-80%, whereas salts with divalent anions (e.g. magnesium sulfate) have higher rejections of 90-98%. Typical applications include removal of color and total organic carbon (TOC) from surface water, removal of hardness or radium from well water, overall reduction of total dissolved solids (TDS), and the separation of organic from inorganic matter in specialty food and wastewater applications. Transmembrane pressures are typically 50 to 225 psi (3.5 to 16 bars) (Dow Tech Manual, 2006).

1.4.2.4 Reverse Osmosis (RO)

Reverse osmosis is the finest level of filtration available. The RO membrane acts as a barrier to all dissolved salts and inorganic molecules, as well as organic molecules with a molecular weight greater than approximately 100. Water molecules, on the other hand, pass freely through the membrane creating a purified product stream. Rejection of dissolved salts is typically 95% to greater than 99% (Dow Tech Manual, 2006).

The applications for RO are numerous and varied, and include desalination of seawater or brackish water for drinking purposes, wastewater recovery, food and beverage processing, biomedical separations, purification of home drinking water and industrial process water (Dow Tech Manual, 2006).

Also, RO is often used in the production of ultrapure water for use in the semiconductor industry, power industry (boiler feed water), and medical/laboratory applications. Utilizing RO prior to ion exchange (IX) dramatically reduces operating costs and regeneration frequency of the IX system. Transmembrane pressures for RO typically range from 75 psig (5 bar) for brackish water to greater than 1,200 psig (84 bar) for seawater (Dow Tech Manual, 2006).

The normal range of filtration processes is shown in Figure 1.14.

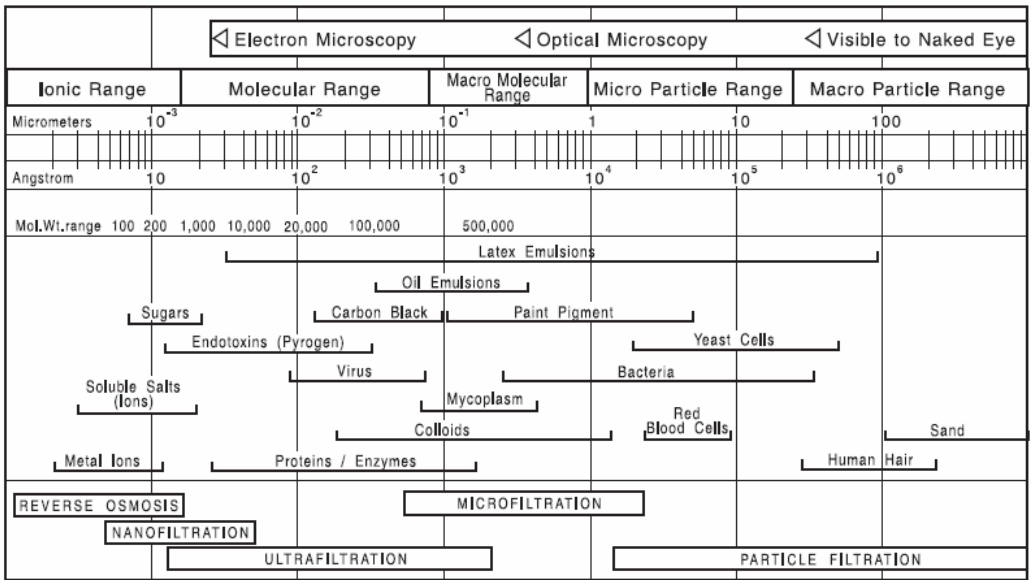

Figure 1.14 Ranges of filtration processes (Dow Tech Manual, 2006).

1.4.3 Principle of Reverse Osmosis

The phenomenon of osmosis occurs when pure water flows from a dilute saline solution through a membrane into a higher concentrated saline solution (Dow Tech Manual, 2006).

The phenomenon of osmosis is illustrated in Figure 1.15. A semi-permeable membrane is placed between two compartments. Then, place a salt solution in one compartment and pure water in the other compartment. The membrane will allow water to permeate through it to either side. But salt cannot pass through the membrane (Dow Tech Manual, 2006).

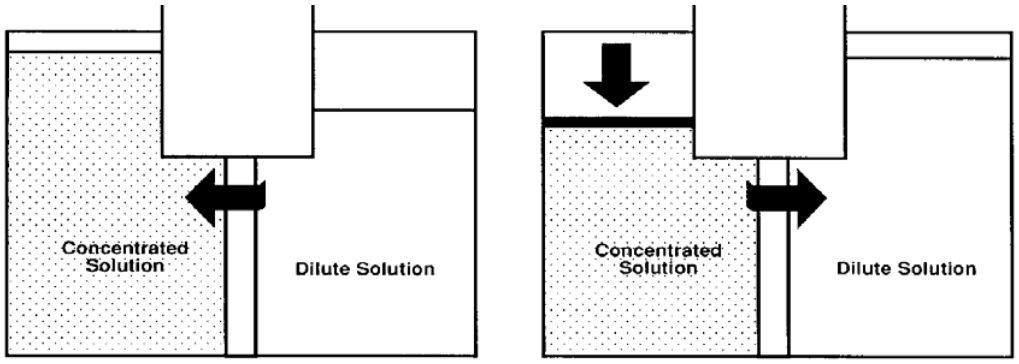

Osmosis

Water diffuses through a semi-permeable membrane toward region of higher concentration to equalize solution strength. Ultimate height difference between columns is "osmotic" pressure.

Reverse Osmosis

Applied pressure in excess of osmotic pressure reverses water flow direction. Hence the term "reverse osmosis"

Figure 1.15 Overview of osmosis and reverse osmosis (Dow Tech Manual, 2006).

As a fundamental rule of nature, this system will try to reach equilibrium. That is, it will try to reach the same concentration on both sides of the membrane. The only possible way to reach equilibrium is for water to pass from the pure water compartment to the salt-containing compartment, to dilute the salt solution (Dow Tech Manual, 2006).

Figure 1.15 also shows that osmosis can cause a rise in the height of the salt solution. This height will increase until the pressure of the column of water (salt solution) is so high that the force of this water column stops the water flow. The equilibrium point of this water column height in terms of water pressure against the membrane is called osmotic pressure (Dow Tech Manual, 2006).

Osmotic pressure is the hydrostatic pressure produced by a solution in a space divided by a semipermeable membrane due to a differential in the concentrations of solute.

$$\pi = MRT \tag{1.1}$$

where π is the osmotic pressure, M is molarity of the solution, R is the gas constant (0.0821 L atm/K mol) and T is temperature (K) (Kabay, 2001).

At the osmosis process, the solvent is transported throught the membrane because of a difference in trans-membrane concentration. If the system is not subject to any external influence such as removal of excess of solvent, then finally and hydrostatic pressure difference is establihed, at which point net material transport has reached zero. This condition is known as osmotic equilibrium, and the corresponding pressure is osmotic pressure. Osmotic equilibrium is a hydrodynamic equilibrium that solvent stil passes through the membrane but fluxes are statistically the same in both directions. The relationship between osmotic pressure and concentration is linear, at least for highly dilute solutions (Kabay, 2001). This rule is shown in eqn 1.2 that called as Van't Hoff equation.

$$\pi = \beta cRT \tag{1.2}$$

where β is Van't Hoff coefficient

If a force is applied to this column of water (as shown in Figure 1.15), the direction of water flow through the membrane can be reversed. The force must be overcome the osmotic force. This is the basis of the term reverse osmosis (Kabay, 2001).

In practice, reverse osmosis is applied as a crossflow filtration process. The simplified process is shown in Figure 1.16 (Dow Tech Manual, 2006).

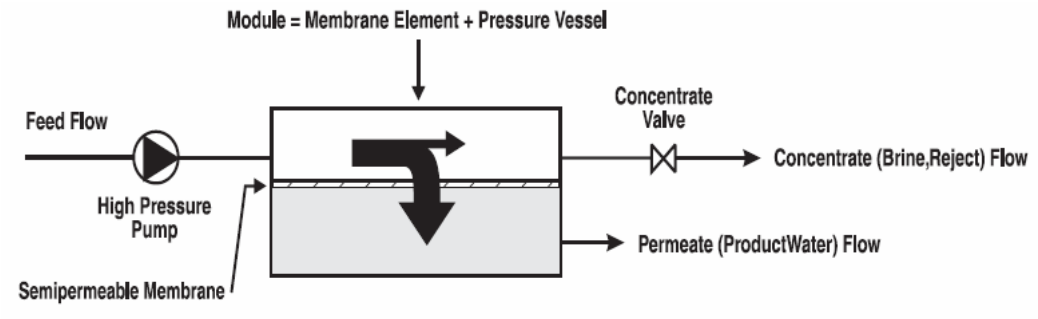

Figure 1.16 Reverse osmosis process (Dow Tech Manual, 2006).

With a high pressure pump, feed water is continuously pumped at elevated pressure to the membrane system. Within the membrane system, the feed water will be split into a low-saline and/or purified product, called permeates, and high saline or concentrated brine, called concentrate or reject. A flow regulating valve, called a concentrate valve, controls the percentage of feedwater that is going to the concentrate stream and the permeate which will be obtained from the feed (Dow Tech Manual, 2006).

1.5 Ion Exchange Separation

1.5.1 Ion Exchange

An ion exchange reaction may be defined as the reversible interchange of ions between a solid phase (the ion exchanger) and a solution phase, the exchanger being insoluble in the medium in which the exchanger is carried out. If an ion exchanger $M^- A^+$, carrying cations A^+ as the exchanger ions, is placed in an aqueous solution phase containing B^+ cations, an ion exchanger reaction takes place which may be represented by the following equation (Harland, 1994).

$$M^- A^+ + B^+ \Leftrightarrow M^- B^+ + A^+$$

An analogous representation of an anion exchanger reaction may be written (Harland, 1994).

$$M^+A^- + B^- \Leftrightarrow M^+B^- + A^-$$

The most important features characterizing an ideal exchanger are:

1. A hydrophilic structure of regular and reproducible form.
2. A controlled and effective ion exchange capacity.
3. A reversible and rapid rate of exchange.
4. Chemical stability towards electrolyte solutions.
5. Physical stability in terms of mechanical strength and resistance to attrition.
6. Thermal stability.
7. Consistent particle size and effective surface area compatible with the hydraulic design requirements for large scale plant (Harland, 1994).

1.5.2 Ion Exchanger Resins and Properties

Ion exchange resins are synthetic resins having a chemical structure based on a crosslinked three-dimensional polymer molecule into which functional groups such as sulfonic acid and quaternary ammonium are introduced. Most of polymer based used for ion exchange resins are copolymers consisting of styrene and divinylbenzene (DVB), the industrial product generally consisting of spherical particles of 14-50 mesh size (118-300 μm). The crosslinked copolymer is senthesized by mixing styrene, which has one vinyl group, with DVB, which has two vinyl groups, and carrying out a suspension polymerization in water. Figure 1.17 illustrates a model synthesis (Harland, 1994).

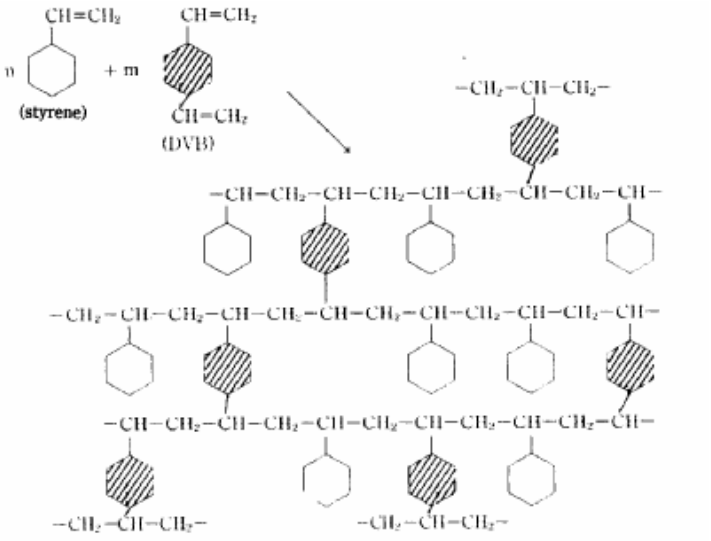

Figure 1.17 Chemical structure of styrene-divinylbenzene copolymer (Harland, 1994).

The ion exchange resin is then manufactured by introducing functional groups into this copolymer matrix by means of chemical reactions. The ion exchange groups introduced, for example sulfonic acid (-SO_3H) or quaternary ammonium ($\equiv N^+$), are chemically atteched to the polymer, and as they can not move freely, they are known as fixed ions. Mobile ions of opposite sign to the ion exchange groups (H^+ ion in the case of R-SO_3H) are known as counter ions (Harland, 1994).

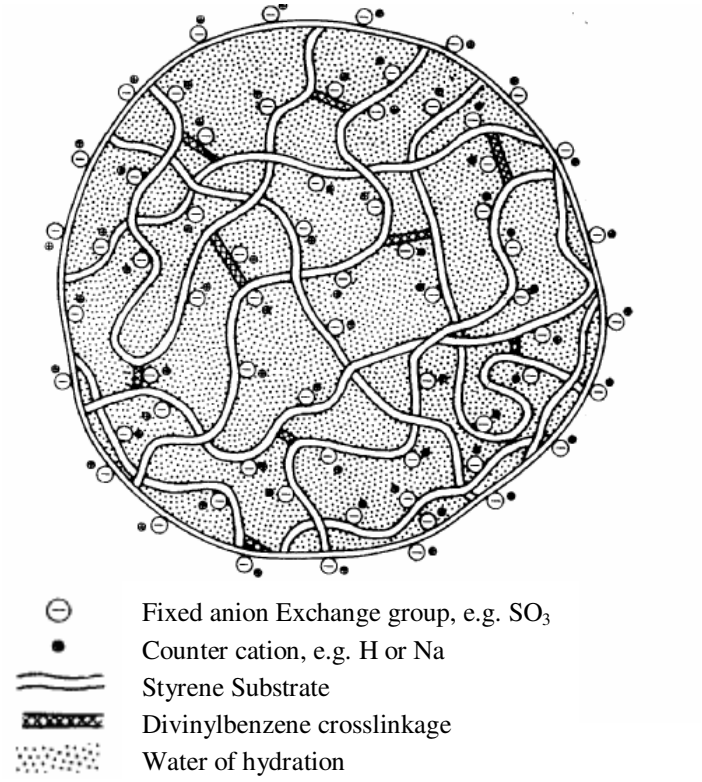

Figure 1.18 Structural model of ion exchange resin (Harland, 1994).

Figure 1.18 gives a structural model of an ion exchange resin. In Figure 1.18 the chemical structure of a resin in two dimensions are represented, but they are thought to have a rather irregular complex three dimensional structure in which polystyrene chains are crosslinked as shown in Figure 1.18 (Mitsubishi Kasei Corporation, 1992).

If the quantity of the bifunctional monomer DVB is increased in the polymerization, a fine mesh structure with considerable chain branching is obtained, whereas if, on the other hand, the quantity of DVB is decreased, a coarse mesh without much branching is obtained. The proportion of DVB in % is referred to as the crosslinkage (Mitsubishi Kasei Corporation, 1992).

The ion exchange resin manufactured by simple polimerization of styrene with DVB is transparent and has a gel structure; hence it is known as a gel type ion exchange resin. Using special polymerization techniques, however, ion exchange resins of higher porosity can be manufactured. Such a structure is termed gel-heteroporous or gel-microporous, and of a structure with respect to crosslinking shown schematically in Figure 1.19 (Harland, 1994).

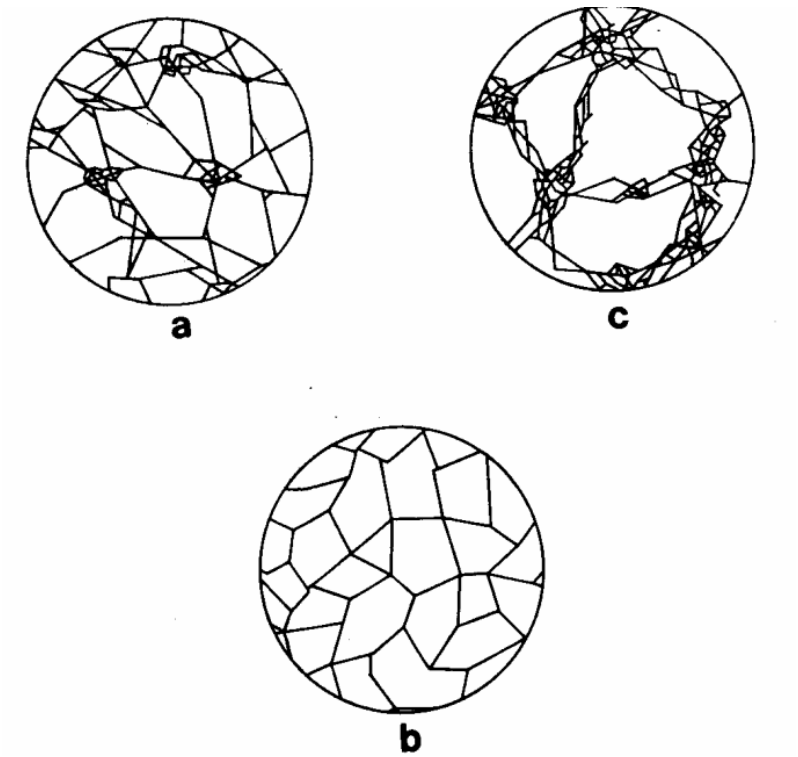

Figure 1.19 Shematic representation of resin structure. a) Gel-microporous, b) Gel-isoporous, c) Macroporous (Harland, 1994).

Typically, an ion exchange resin is described as “weak or strong”, acidic or basic”, and “cationic or anionic”.

1.5.2.1 Cation Exchange Resins

Cation exchange resins are resins which exchange positively charged ions such as Na^{+} and Ca^{2+}. They are classified as either strongly acidic or weakly acidic depending on their acidity (Mitsubishi Kasei Corporation, 1992).

Strongly acidic cation exchange resins

These resin, as shown by the structural Formula in Figure 1.20 have sulfonic acid groups as exchange groups. Due to the dissociation of these groups, they are strongly acidic like hydrochloric or sulfuric acid, and are, therefore known as strongly acidic cation exchange resins.

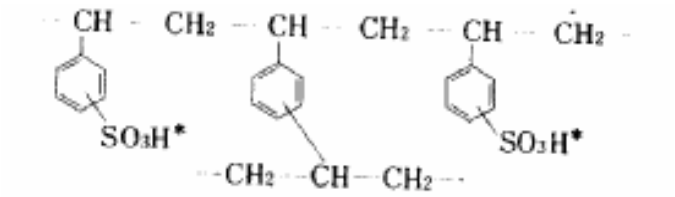

Figure 1.20 Chemical structure of strongly acidic cation exchange resin (Mitsubishi Kasei Corporation, 1992).

Weakly acidic cation exchange resins

Resin with carboxyl group (-COOH) which in its acid form is only very weakly ionized (pKa aproximately: 4-6), as an ion exchange groups as shown in Figure 1.21 and 1.22.

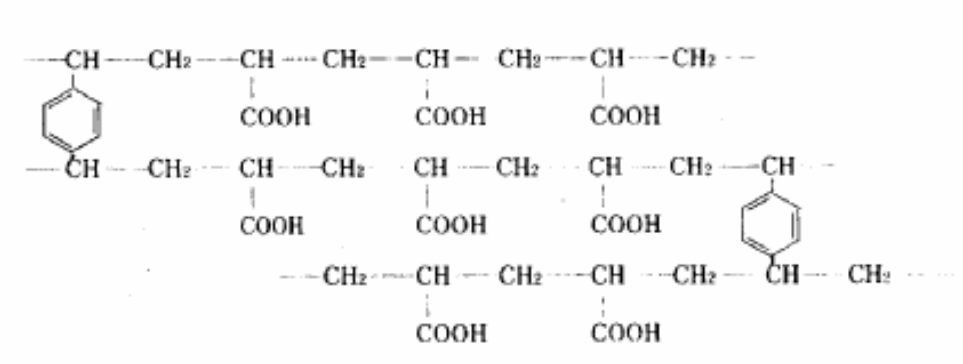

Figure 1.21 Chemical structure of acrylic acid type weakly acidic cation exchange resin (Mitsubishi Kasei Corporation, 1992).

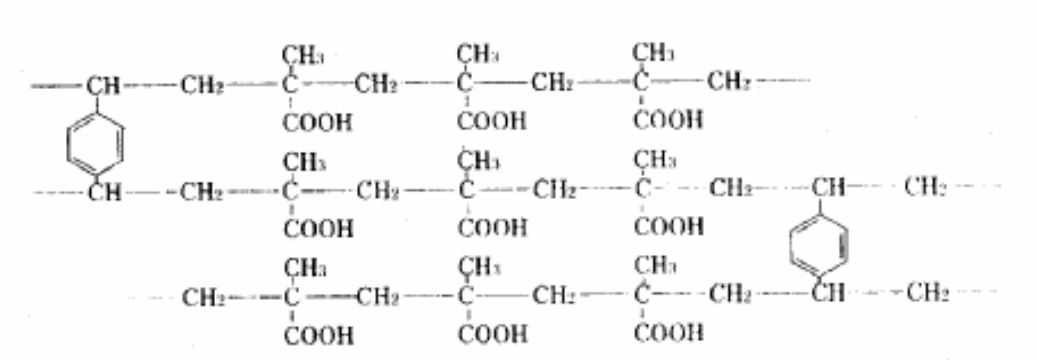

Figure 1.22 Chemical structure of metacrylic acid type weakly acidic cation exchange resin (Mitsubishi Kasei Corporation, 1992).

1.5.2.2 Anion Exchange Resins

These resin exchange ions like Cl^- or SO_4^{2-}. They are classified as strongly basic anion and weak basic anion exchange resins depending on the strength of their basicity (Mitsubishi Kasei Corporation, 1992).

Strongly basic anion exchange resins

Resins which have a quaternary ammonium group ($\equiv N^+$) as the exchanging group exhibiting strong basicity. They are known as strongly basic

ion exchange resins (as shown in Figure 1.23) (Mitsubishi Kasei Corporation, 1992).

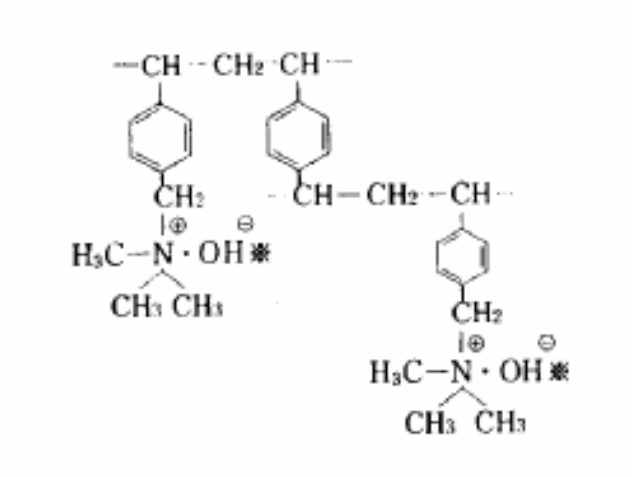

Figure 1.23 Chemical structure of strongly type anion exchange resin (Mitsubishi Kasei Corporation, 1992).

Weakly basic anion exchange resins

Resins with primary-tertiary amino groups as exchange groups exhibit weak basicity, and are, therefore, known as weakly basic ion exchange resins. Weakly basic ion exchange resins may be having a single exchange group, for example a tertiary amino group as shown in Figure 1.24, or a mixture of two or more amino groups (Mitsubishi Kasei Corporation, 1992).

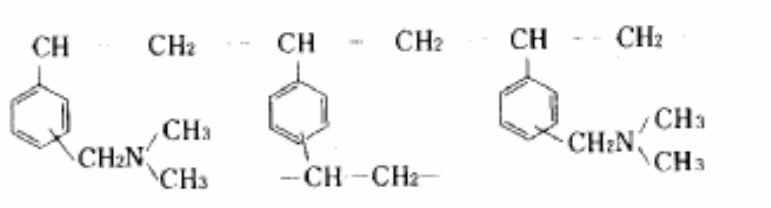

Figure 1.24 Chemical structure of tertiary amino weakly basic ion exchange resin (Mitsubishi Kasei Corporation, 1992).

1.5.2.3 Porous Ion Exchange Resins

If special methods are used are used to carry out the polymerization of styrene and DVB, resins of higher porosity can be manufactured. The chemical structure of these porous resins is identical to that of the gel type resins manufactured by ordinary polymerization techniques, but the polymer matrix contains a large number of macropores. They therefore have a far greater surface area than the gel type, which contains only micropores (Mitsubishi Kasei Corporation, 1992).

Various techniques have been reported for the manufacture of porous ion exchange resins. In all cases, however, there is definite relationship between the porosity of the resin obtained and its degree of crosslinkage. As illustrated in Figure 1.25, the porosity generally increases for resins of higher crosslinkage (Mitsubishi Kasei Corporation, 1992).

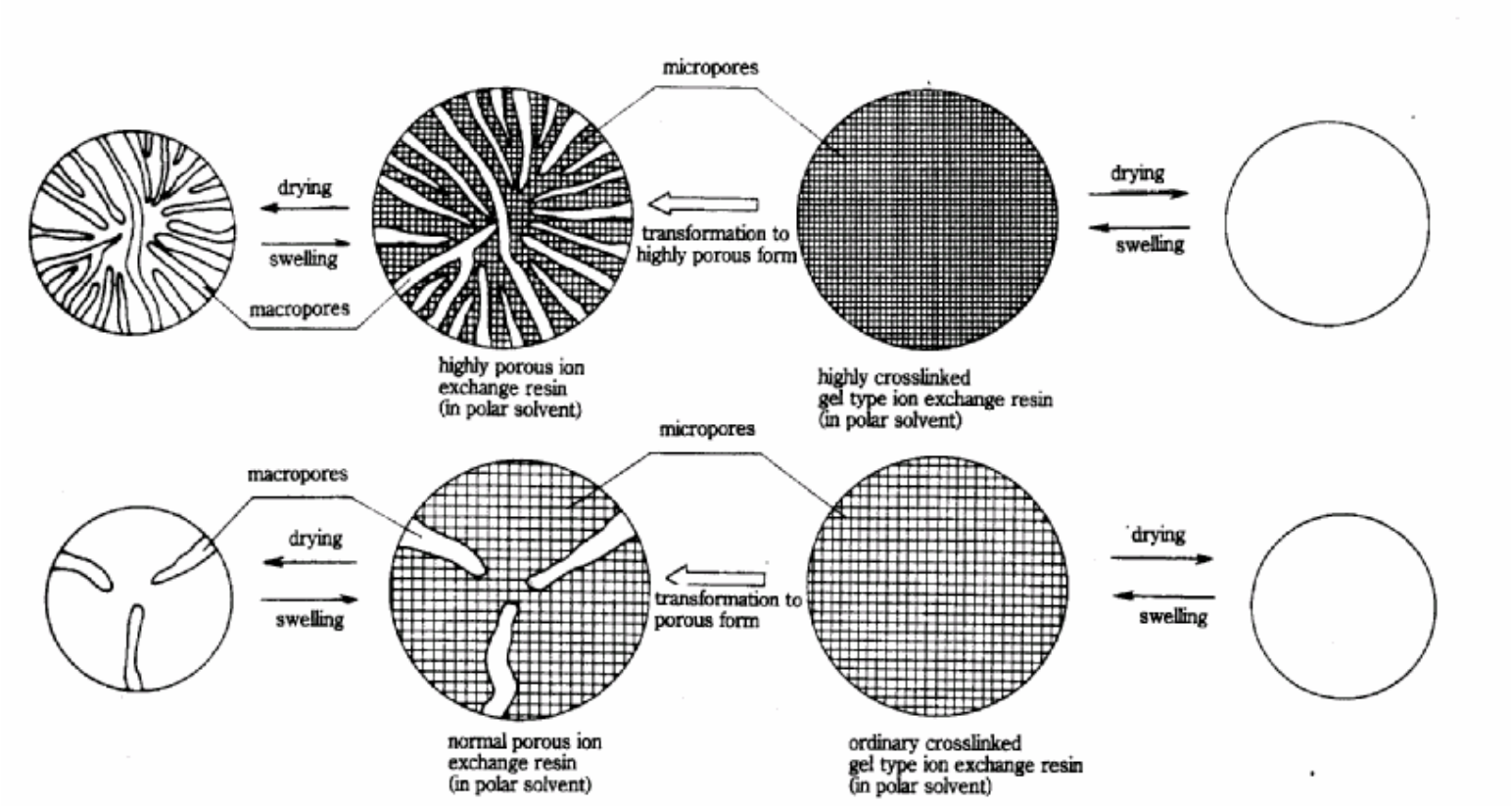

Figure 1.25 Schematic description of ion exchange resin structure (Mitsubishi Kasei Corporation, 1992).

Normal Porous Ion Exchange Resins

These are resins with only a moderate degree of crosslinkage. Although values of physical parameters, due to their porosity and specific surface area not so large, the size of the micropores in the resin matrix is large and they are, therefore, suitable for treatment of polar solvents such as aqueous solutions. Also they have excellent swelling and contraction strength, resistance to organic contamination and decolorizing properties, and thus these characteristics are desired (Mitsubishi Kasei Corporation, 1992).

Highly Porous Ion Exchange Resins

The resins have a high crosslinkage, and high values of physical parameters due to their porosity. They have a large specific surface area and pore volume, and are therefore, extremely useful for special applications where the resin surface is mainly used-for example, treatment of nonpolar solvents or adsorption of large counter ions which cannot diffuse in the micropores. Consequently, they are usually unsuitable for routine ion exchange in aqueous solution (Mitsubishi Kasei Corporation, 1992).

1.5.2.4 Special Resins

Apart from ion exchange resins which capture ions by ion exchange, there are also special resins such as chelating resins with functional groups that from chelates (Mitsubishi Kasei Corporation, 1992).

Chelating Resins

These are resins into which functional groups have been introduced that from chelates with metal ions, and they capture metal ions by this process (Mitsubishi Kasei Corporation, 1992).

Chelating resins have a far greater selectivity with respect to specific metal ions than ion exchange resins. An ion exchange resin may show higher selectivity for Ca^{2+}, Mg^{2+} or Sr^{2+} than for Na^{+}, but the difference is not so great (Mitsubishi Kasei Corporation, 1992).

The metal ions may normally be removed again by acids such as hydrochloric acid or sulphuric acid. This is due to the fact that metal chelates are unsuitable and tend to decompose at low pH (Mitsubishi Kasei Corporation, 1992).

1.6 Boron Problem in Seawater

Boron has various industrial uses, ranging from the glass and ceramic industries to detergents and soaps. The industrial applications of boron result in the accumulation of boron in industrial wastes that then permeate into the natural environment. The main industrial use of boron that affects the environment is the detergent industry (Waggott, 1969). Because sodium perborate is an excellent bleaching agent, detergent companies have added it to their washing powders for decades. Consequently, the high content of boron in detergents results in the accumulation of boron in domestic wastewater, particularly in industrial countries. Typically, the boron content in domestic wastewater ranges from 0.5 to 1mg/l. Surveys of boron concentration in rivers in the United Kingdom (Neal *et al.*, 1998) and other EU states (Wyness *et al.*, 2003) show that in most cases the boron concentration in rivers does not surpass the drinking water value of 1 mg/l. Furthermore, high levels of boron concentrations were found mostly in rivers that are associated with urban and industrial drainage relative to those from rural areas (Neal and Robson, 2000), thus indicating a direct link between boron contamination in rivers and sewage pollution. Since a large fraction of the rivers in Europe are polluted, over the last few decades many European countries have instead turned to ground water as

their main source of drinking water. At high levels (i.e. above 1mg/l), boron is considered a serious threat to the use of ground water for both drinking and agricultural purposes. Boron, for example, affects plant growth and yields because it is biologically an essential micronutrient for many plants; an overdose or an underdose of boron can result in toxicity or deficiency symptoms in plants, respectively. In fact, a level of boron in irrigation water exceeding 1mg/l can significantly affect the yield of sensitive crops such as citrus fruits. In contrast, borate minerals are added to fertilizers to compensate for boron deficiencies in areas where the natural soil lacks boron (Redondo et al, 2003).

Boron occurrence in seawater varies from 4 to 5.5 mg/L, proportionally to seawater salinity. Depending on location and seasonal effects, the boron concentration can exceed 7 mg/L (e.g. in the Arabian Gulf) (Charles, 1997).

There are two predominant reasons for limiting boron in water:

1. For humans, boron can represent reproductive dangers and has suspected teratogenic properties. The WHO has set a preliminary limit of 0.5 mg/L for drinking water The EU is suggesting a guideline of 1.0 mg/L (Busch, 2004).

2. In agriculture, a major limiting factor is the possible damage to plants and crops. Although boron is vital as a trace element for plant growth and is supplied in fertilizer it can be detrimental at higher concentrations. Amongst the more sensitive crops are citrus trees, which show massive leaf damage at boron levels of more than 0.3 mg/L in the irrigation water. Excess boron also reduces fruit yield and induces premature ripening on other species such as kiwi (Busch, 2004).

1.7 Methods for Boron Removal from Seawater

Boron is usually present in water as boric acid, a weak acid which dissociates according to the following equations:

$$H_3BO_3 \leftrightarrow H^+ + H_2BO_3^- \qquad pK_a \ 9.14 \qquad (1.3)$$

$$H_2BO_3^- \leftrightarrow H^+ + HBO_3^{2-} \qquad pK_a \ 12.74 \qquad (1.4)$$

$$HBO_3^{2-} \leftrightarrow H^+ + BO_3^{3-} \qquad pK_a \ 13.8 \qquad (1.5)$$

In the usual pH operating range of reverse osmosis elements, Equation 1.3 is the one with the highest importance. Thus there are both dissociated and non-dissociated boric acid species in the water (Redondo et al, 2003).

The dominant form of boron species depends on the pH of the water. The pKa of $H_3BO_3/H_2BO_3^-$ is 9.2, therefore the equilibrium 1.3, is typically towards the left at standard seawater pH 8 (Figure 1.26).

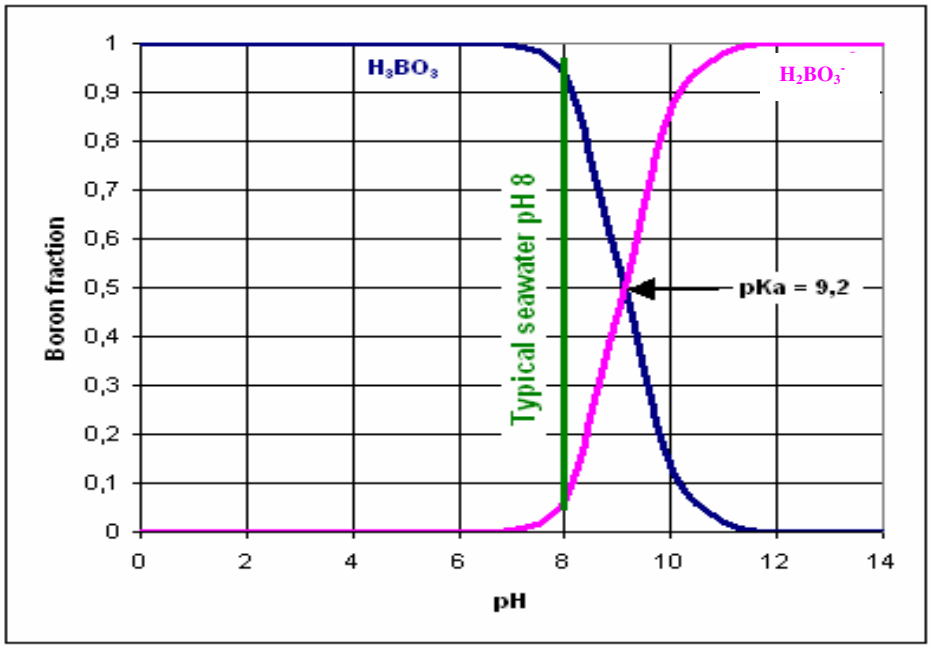

Figure 1.26 Distribution of $H_3BO_3/H_2BO_3^-$ in function of pH.

Seawater contains nearly 5 mg B/L. However, for many crops, too high concentration of boron is harmfull and causes a significant reduction in crop yield. Boron may be removed from water by membrane system using one or two stages and/or increasing pH of the water on the feed side of the membrane (Kabay, 2007).

The performance of boron selective resins is less sensitive to pH and temperature than that of membranes. Currently available, commercial boron selective resins typically comprise macroporous cross linked poly-styrene resins, functionalized with N-Methyl-D-glucamine, also called 1-amino-1-deoxy-D-glucitol. Figure 1.27 illustrates a structure for N-methyle-D-glucamine. The N-methyl-D-glucamine moieties of been selective resins capture boron via a covalent chemical reaction and an internal coordination complexation, rather than simple ion exchange. Over a wide range of pH, boric acid “adds” across one of the cis-diol pairs of the functional group to form this relatively stable cis-

diol borate ester complex. Figure 1.28 illustrates the structure of such an ester complex (Charles, 2006).

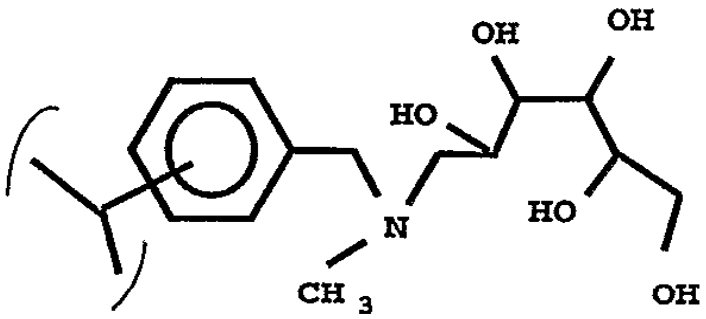

Figure 1.27 N-Methyl-D-glucamine functionality on a polystyrene matrix (Charles, 2006).

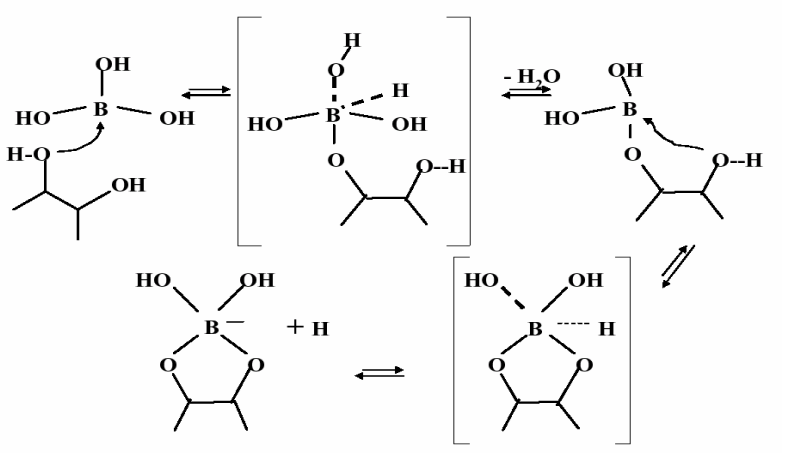

Figure 1.28 N-Methyl-D-glucamine functionality capturing boric acid (Charles, 2006).

In a boron removal process, once the boron selective resins has achieved its maximum boron loading, N-Methyl-D-glucamine is regenerated, typically in a 2-stage elution/regeneration treatment process employing acid (i.e. sulfuric

acid of HCl) for elution of boron. The polymer-bound cis-diol borate ester complex, described above, is subsequently hydrolyzed and the boron eluted from the resin via an acid rinse. This boron liberating hydrolysis is relatively facile at pH less than about 1.0; therefore, relatively high concentrations of acid are required for the complete and rapid elution of the boric acid from boron selective resins. The resin is then treated with base, (i.e. sodium hyroxide) to return the conjugate acid salt of the typically followed by water rinse to remove excess hydroxide subsequent to another boron loading cycle (Charles, 2006).

In the literature, several processes have been suggested for boron elimination from seawater. These processes are shown in Figure 1.29.

- Process A 2-pass SWRO:

In Figure 1.29, it is mentioned about the process that produces B-free water from seawater. In the 1st drawing there is 2 pass Reverse Osmosis (RO) desalination processes. The 1st RO unit is used to keep some minerals and disturbities in the 1st pass. The blue ways that pass through 1st RO unit called "Permeate" and it contains diluted seawater. The red way shows concentrated part of seawater and it called as "concentrate".

The permeate of 1st RO unit is divided two part. One part of permeate goes to 2nd RO unit that contains boron selective membranes. Before this process caustic is added to increase pH of 1st permeate of RO unit, because boron removal increases in base medium as mentioned before. Another reason of adding caustic, to be precipitates some ions such as calcium and magnesium. The final water that joins the second part of permeate contains between 0.3 to 1.0 mg/L boron as shown in Table 1.6.

- Process B SWRO+ IX:

The second processes that can be seen in Figure 1.29 concludes 1 pass RO unit and two columns with boron selective ion exchange resins. After seawater pass through the RO unit, salinity and other disturbities in water are hold on. Then boron is removed using ion exchange resins. An important parameter for the resin column is flow rate. The flow rate of the column must be slow, because of that permeate does not goes to columns directly. It divided to three parts. Two divided part goes through the ion exchange resin columns. The other part joins directly to product water. As can be seen in Table 1.6, boron level is smaller than process A.

Selective Boron Ion Exchange Resin with or without by-pass, depending on the residual boron concentration needed. The selective resin must be on-site regenerated with caustic soda and hydrochloric acid. A double column system is often required to ensure a continuous production.

Because some chemicals are used for regeneration of resin columns, the chemical cost is more expensive than process A. On the other hand, the energy and investment costs of process A are higher than process B.

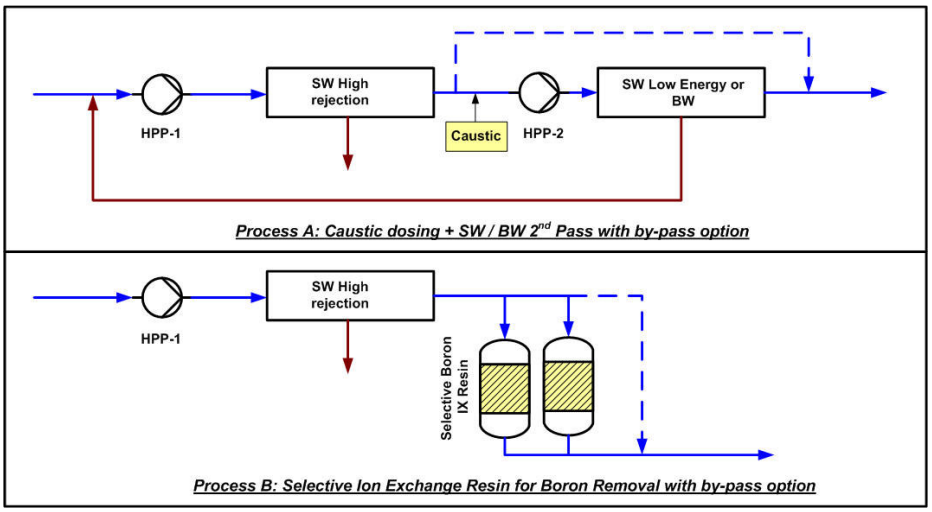

Figure 1.29 The main processes are used to produce B-free water from seawater

Table 1.6 Comparisons parameters between Process A (2 pass process) and Process B (combination of 1 pass and ion exchange process).

Comparison Parameters	**Process A**	**Process B**
Boron residual concentration	0.3-1.0 mg/L	0-1.0 mg/L
Energy costs	Higher - HPP2 power consumption	
Investment costs	Higher - Second Pass RO	
Chemicals costs		Higher - Resin Regeneration by NaOH, HCl
Footprint	Larger	
Water quality	Poor mineralization without by-pass, low sodium chloride content	High mineralization with or without by-pass due to resin selectivity, high sodium chloride content
Recommendations	Cost efficient for drinking water production at 0.5 mg/L Boron residual max.	Cost efficient for irrigation water for sensitive crops with Boron residual tolerance between 0.5 and 1.0 mg/L

2. EXPERIMENTAL

2.1 Materials

2.1.1 Chemicals

- Curcumine: $C_{21}H_{26}O_6$, Acros Organics
- Azomethine-H, Fluka
- Ascorbic Acid, Acros Organics
- Ammonium Acetate, Merck
- EDTA di-Sodium Salt, Analar
- CH_3COOH: 99-100%, d: 1.06 g/L, Merck
- HCl :37 %, d: 1.19 g/L, Merck
- H_3BO_3: 99.8 %, Merck

2.1.2 Preparation of Solutions

Curcumine Solution (0.075%): the solution was prepared on the day of use by dissolving 0.075 g curcumine in 100 mL of glacial acetic acid and stored in a polyethylene bottle. covered with aluminum foil on the day of use.

H_2SO_4: CH_3COOH (1:1) Solution: Equal volumes of the two acids are mixed.

Sodium Acetate Buffer Solution: 200 g sodium acetate is dissolved with 250 mL acetic acid and diluted to 1 L with deionized water.

100 mg B/L H_3BO_3:. 0.5719 g H_3BO_3 is dissolved in deionized water and diluted to 1L

2 ppm Model boron solution: 20 mL supernatant form a stock solution (100mg B/L) is diluted to 1000 mL with deionized water.

Standard boric acid solutions (0.0-2.00 mg B/L): 5mg B/L solution is prepared from a stock B solution (100 mg B/L). Finally, 0.1, 0.5, 1.0 and 2.0 mg B/L are prepared from 5 mg B/L of standard solution.

2.1.3 Ion exchange resins

Two type of ion exchange resin which are N-glucamine type chelating resins; Diaion CRB 02 and Dowex-XUS 43594.00 (supplied by Mitsubishi Chemicals, Japan and Dow Chemicals, Germany respectively) were used Their characteristics are summarized in Tables 2.1 and 2.2.

Table 2.1 Typical chemical and physical characteristic of Diaion CRB 02

Constitutional type	Highly porous
Ion form as shipped	OH-form
Shipping density (g/dm^3) (app.)	635
Moisture content (%)	50-60
Exchange capacity	Acid 0.6 meq/cm^3 (min)
Screen grading	118-300 μ
Effective size (mm)	0.355-0.500
Uniformity coefficient	1.6 (max)
Operating temperature (^oC)	100 ^oC (max) OH-form
Effective pH range	6-10

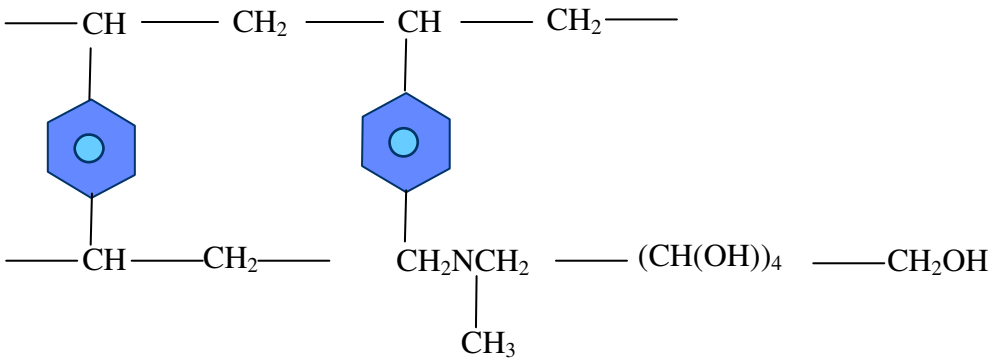

Figure 2.1 Structure of Diaion CRB02

Table 2.2 Typical chemical and physical characteristic of Dowex-XUS 43594.00

Total exchange capacity (min)	0.7 eq/L
Water retention capacity (%)	51-59
Mean particle size (µm)	550 ± 50
Uniformity coefficient	1.1 (max)
Whole uncracked beads (min) (%)	90
Total swelling (%)	24-28
Shipping weight (lbs/ft^3) (app.)	41
Total boron capacity (g B/L)	3.4-4.0

2.1.4 Equipments

Vacuum oven: Gallen Kamp

Shaker: Memmert

Spectrophotometer: Jasco, V-530 UV-VIS Spectrophotometer SSE 343

Magnetic Stirrer: Ikamag

2.2 Batch Sorption Tests

2.2.1 Optimum Resin Concentration

Optimum resin amounts for boron removal from model solution were determined by using Diaion CRB 02(45-125 µm and 0.355-0.500 mm resin size) and Dowex-XUS 43594.00 (45-125 µm and 0.355-0.500 mm resin size).

At the experiments, various dry resin amounts, that are (0.01 g, 0.02 g, 0.03 g, 0.04 g, 0.05 g, 0.06 g, 0.07 g, 0.1 g for (45-125 µm) particle size of

resin) (0.01 g, 0.02 g, 0.03 g, 0.04 g, 0.05 g,0.06 g, 0.07 g, 0.1 g, 0.15 g, 0.2 g, 0.3 g and 0.4 g for (0.355-0.500 mm) particle size of resin), were contacted with 100 mL of model solution at 25°C for 48 h with continuous shaking in shaker.

2.2.2 Kinetic Tests

Kinetic tests were carried out in a 1 L of three neckled glass flask placed in a water bath. The model solution in the flask was agitated on a mechanical stirrer to prevent the resin settling. Samples were withdrawn from the vessel at regular time intervals (3, 5, 10, 15, 20, 30, 45, 60, 90, 120, 150, 180, 240, 300, 360, 420, 480, 1440 min.). Kinetic tests were performed by using 0.5 g of dry Diaion CRB02 and Dowex-XUS 43594.00 (45-125 µm). At the experiments the temperature effect (for 25°C, 30°C, 35°C), stirring rate effect (for 200 RPM, 250 RPM, 300 RPM) and particle size effect (45-125 µm, 125-250 µm, 0.355-0.500 mm) were observed.

2.2.3 Sorption-Elution Tests

In this study, the elution performance of HCl on the resin was observed. First of all a batch study with 0.5 g resin, which is Diaion CRB02 (0.355-0.500 mm), was perfomed with model boron solution of 100 mL in a polyethylene bottle. For this study 4 parallel samples have been used. Batch study was done at 25°C for 48h with continuous shaking.

After batch study, the resins were filtered to separate from solution. Then washed with pure water. After that each four resin in bottles were eluted for 2 h with 0.1 M, 0.25 M, 0.5 M and 1.0 M 25 mL of HCL solution respectively. Then the resins were filtered from acid solution and washed with pure water. The same process was repeated twice. Finally the acid solutions collected were combined in a 100 mL volumetric flask. The solution was analysed with

curcumine method to find the elution capacity of HCl with different molarity. To find the elution capacity (%) of resin, Equation 2.1 was used,

$$E(\%) = \left(\frac{m_{eluted}(g)}{m_{sorbed}(g)}\right) x100 \qquad (2.1)$$

2.3 Sorption Tests with RO Permeate

In this study the Reverse Osmosis (RO) permeate collected at Urla RO plant was used as sample solution. The properties of used RO permeate solution is shown in Tables 2.3, 2.4 and 2.5, respectively.

In batch study, 0.05 mg of Diaion CRB 02 (45-125μm and 0.355-0.500mm) and Dowex XUS 43594.00 (45-125μm and 0.355-0.500mm) were contacted with 100 mL of RO permeate at 25°C for 48 h with continuous shaking in shaker.

A kinetic study was performed in a 1 L of three-necked glass flask placed in a water bath at 25°C for 24 h, using 0.25 g of dry resin Diaion CRB 02 (45-125 μm). The RO permeate solution in the flask was agitated by a mechanical stirrer with 250 RPM to prevent the resin from settling. Samples were withdrawn from the vessel at regular time intervals (3, 5, 10, 15, 20, 30, 45, 60, 90, 120, 150, 180, 240, 300, 360, 420, 480, 1440 min.).

Table 2.3 The data obtained for RO process at Urla SWRO plant.

Operation Time (min) Parameters		20	40	60	80	100
Pressure (bar)	**Feed**	60	60	60	60	60
Temperature (°C)	**Feed**	11.6	11.6	11.6	11.6	11.6
	Permeate	15.6	16	15.7	15.9	16.1
	Concentrate	16.6	17	16.7	16.9	17.2
Flow Rate (L/h)	**Feed**	262.2	262.8	264.6	263.4	263.4
	Permeate	46.2	46.8	46.2	46.2	46.2
	Concentrate	216	216	218.4	217.2	217.2
pH	**Feed**	8.2	8.2	8.2	8.2	8.2
	Permeate	7.9	7.8	7.8	7.7	7.8
	Concentrate	8.1	8.1	8.1	8.1	8.1
Conductivity (mS/cm)	**Feed**	60.3	60.3	60.3	60.3	60.3
	Permeate	0.449	0.446	0.437	0.432	0.429
	Concentrate	70.3	70.2	70.1	70.1	70.2
TDS (mg/L)	**Feed**	30150	30150	30150	30150	30150
	Permeate	223	224	220	217	215
	Concentrate	35150	35100	35050	35050	35100
Salinity (‰)	**Feed**	39.5	39.5	39.5	39.5	39.5
	Permeate	0	0	0	0	0
	Concentrate	47.8	47.8	47.7	47.7	47.7
Boron Concentration (mg/L)	**Feed**	5.275	5.275	5.275	5.275	5.275
	Permeate	0.8	0.825	0.825	0.825	0.9
	Concentrate	6	6	6.1	6.1	5.4

Table 2.4 The data obtained for RO process at Urla SWRO plant (continued).

Parameters \ Operation Time (min)		120	140	160	180
Pressure (bar)	**Feed**	60	60	60	60
Temperature (°C)	**Feed**	11.6	11.6	11.6	11.6
	Permeate	16.1	16.5	16.4	16.5
	Concentrate	17.2	17.2	17.6	17.9
Flow Rate (L/h)	**Feed**	263.4	262.8	264	263.4
	Permeate	46.2	46.8	46.8	46.2
	Concentrate	217.2	216	217.2	217.2
pH	**Feed**	8.2	8.2	8.2	8.2
	Permeate	7.9	7.8	7.8	7.8
	Concentrate	8.1	8	8	8
Conductivity (mS/cm)	**Feed**	60.3	60.3	60.3	60.3
	Permeate	0.427	0.429	0.426	0.421
	Concentrate	70.2	70.1	70.2	70
TDS (mg/L)	**Feed**	30150	30150	30150	30150
	Permeate	214	215	213	211
	Concentrate	35100	35050	35100	35000
Salinity (‰)	**Feed**	39.5	39.5	39.5	39.5
	Permeate	0	0	0	0
	Concentrate	47.8	47.8	47.8	47.7
Boron Concentration (mg/L)	**Feed**	5.275	5.275	5.275	5.275
	Permeate	0.775	0.725	0.875	0.775
	Concentrate	5.85	6	5.95	6

Table 2.5 The average properties of RO permeate used in batch tests.

RO ProcessPressure: 60 bar	
Used Membrane: one-left (**Filmtec SW30-2540 membrane**)	
Temperature [°C]	29.9 °C
Conductivity [µS/cm]	482
Salinity [‰]	0.0
TDS [mg/L]	239
pH	6.4
B-concentration [mg/L]	0.814 (is adjusted to 2 mg/L by spiking with H_3BO_3 solution)

The membrane used for RO process at Urla SWRO plant was the Filmtec SW30-2540 membrane of Dow Chemicals.

2.4 Boron Analysis

Boron analysis was performed using two different methods. The first one, Spectrophotometric Curcumine Method, is more sensible than the second one, which is Azomethine-H Method. Because of that, for the samples having low B concentration, Curcumine Method has been applied.

2.4.1 Spectrophotometric Curcumine Method

In this method, firstly a solution Curcumine is prepared. 0.5 mL of collected sample from kinetic study and 3 mL Curcumine solution are added in a polyethylene bottle. Then 3 mL H_2SO_4:CH_3COOH (1:1) is added into this solution. After that, the mixture is taken on a shaker at 30 °C for 1 h. The aim is to obtain a homogeneous solution. 1 h later 10 mL CH_3COONa buffer solution is added into the mixture.

At the same time 0, 0.1, 0.5, 1.0, 2.0 mg B/L of standard solutions are also prepared for getting calibration curve.

Samples are left to cool for a while and then absorbance values of samples are measured at λ_{max} = 543 nm by means of Jasco SSE-343, V-530 UV/VIS model Spectrophotometer.

All samples, which collected from kinetic experiments, were analysed with Curcumine Method.

2.4.2 Spectrophotometric Azomethine-H Method

In this method, an Azomethine-H solution and standard solutions are prepared. 10 mL of collected sample from kinetic study is put into 25 mL of plastic bottle. Then 2.5 mL Azomethine-H solution and 2.5 mL buffer solution are added respectively. Samples are left to a dark medium for 1 hour and then absorbance values of samples are measured at λ_{max} = 415 nm by means of Jasco SSE-343, V-530 UV/VIS model Spectrophotometer.

The prepared standard solutions for calibration curve are 0, 0.1, 0.5, 1.0, 2.0 mg B/L.

All samples, which collected from batch studies with continuous shaking during 48 h, were analysed with Azomethine-H Method.

3. RESULTS AND DISCUSSION

3.1 Optimum Resin Concentration for Boron Removal

Optimum resin amounts for removal of boron from model solution were determined by batch studies using Diaion CRB02 at a particle size range of (45-125 µm) and (0.355-0.500 mm) and Dowex-XUS 43594.00 at a particle size range of (45-125 µm) and particle size (0.355-0.500 mm).

As shown in Figure 3.1, boron removal increased with increasing resin amounts from 0.01g to 0.1g/100 mL for both Diaion CRB 02 (45-125 µm) and Diaion CRB 02 (0.355-0.500 mm). As can be seen in results, (45-125 µm) sized resins adsorbed nearly 90% boron from model solution. Boron removal had a plateau for the resin amounts between 0.05 g/100 mL and 0.1 g/100 mL for Diaion CRB 02 (45-125 µm). According to these results, the optimum resin amount for Diaion CRB 02 (45-125 µm) was found as 0.05 g resin/L for both resins with (45-125 µm) and (0.355-0.500 mm) particle size range.

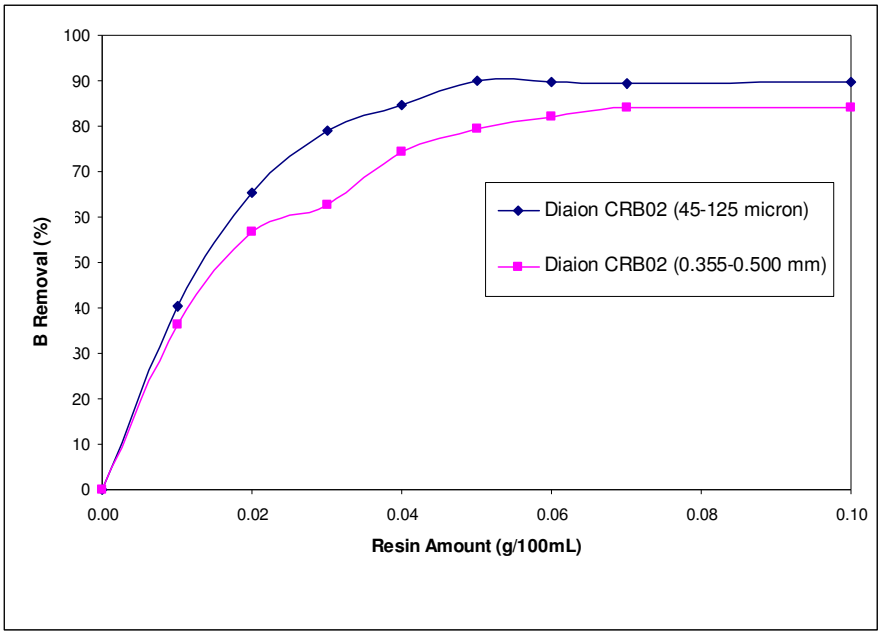

Figure 3.1 Effect of Resin Amount on Removal of Boron from Model B Solution by Diaion CRB02 as a function of resin particle size (25°C, 48h).

Figure 3.2 shows that boron removal increased with increasing resin amounts from 0.01 g to 0.1 g/100 mL for Dowex-XUS 43594.00 (45-125 µm) and Dowex-XUS 43594.00 (0.355-0.500 mm); however boron removal had a plateau for the resin amounts between 0.05 g to 0.10 g/100 mL for both sized resin. According to these results, optimum resin amount was found as 0.05 g resin/100 mL for Dowex-XUS 43594.00 (45-125 µm).

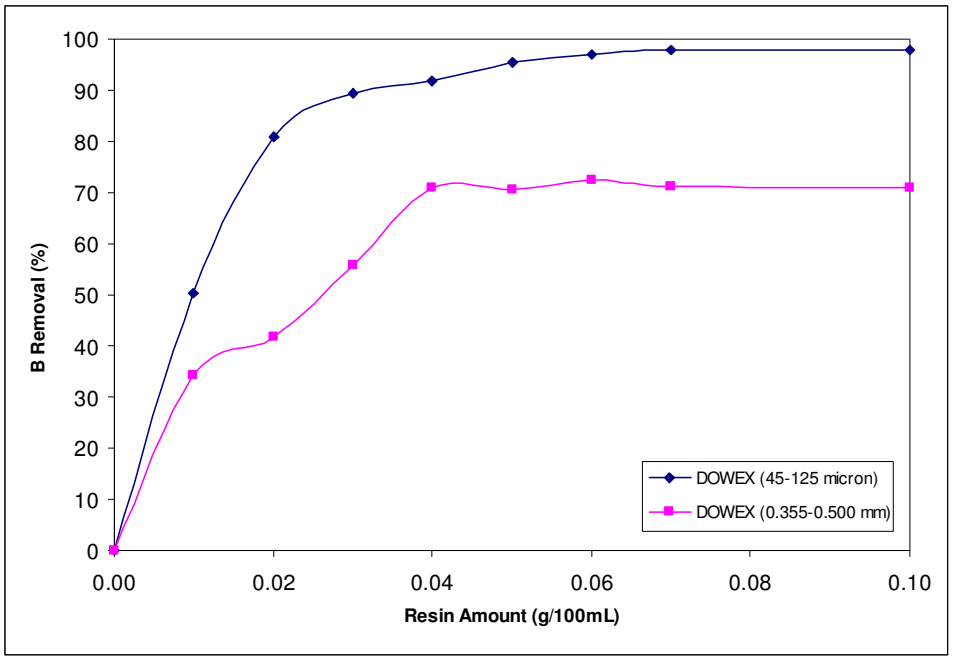

Figure 3.2 Effect of Resin Amount on Removal of Boron from Model B Solution by Dowex XUS (43592.00) as a function of resin particle size (25°C, 48h).

Since percent removal of boron with resins at particle size range of (0.355-0.500 mm) was lower than the resins with (45-125 µm), a separate study was performed using resin concentration range of 0.00-0.40 g/ 100 mL. As shown in Figure 3.3 a plateau was observed with both resins at a resin concentration of 0.15 g/100 mL.

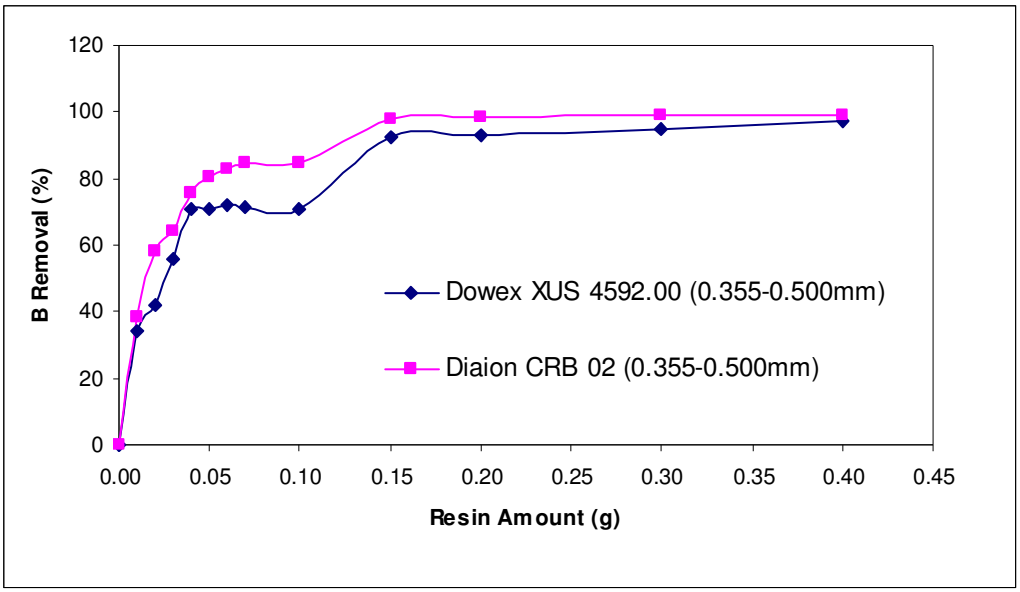

Figure 3.3 Effect of Resin Amount on Removal of Boron from Model B Solution by Dowex XUS (43592.00) and Diaion CRB 02 with resins size of (0.355-0.500 mm), (25°C, 48h).

3.2 Kinetic Tests

In kinetic studies, effect of temperature, stirring rate and particle size has been investigated. All experiments were done using optimum resin amount (0.05 g/100 mL) for Diaion CRB 02 (45-125 µm) resin with 1 L of 2 ppm Model B Solution.

3.2.1 Temperature Effect

Figure 3.4 and 3.5 show the kinetic study results of Diaion CRB 02 (45-125 micron) at 25°C, 30°C and 35°C. 250 RPM stirring rate was used for all kinetic studies to find temperature effect (The results were also tabulated in appendix section). According to these results, boron removal rate increased with an increase in temperature.

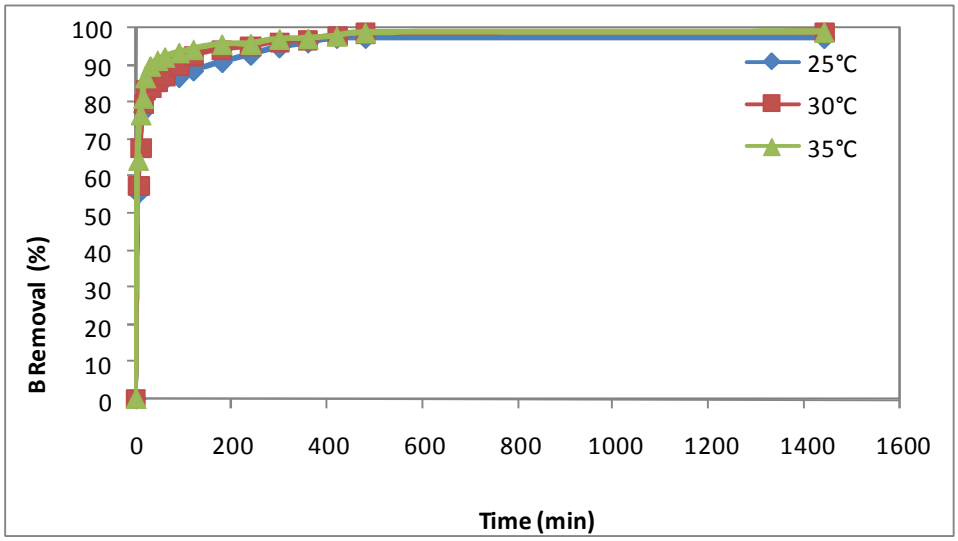

Figure 3.4 Effect on temperature on kinetic behaviour of Diaion CRB02 (45-125 µm) resin for boron removal with 250 RPM stirring rate.

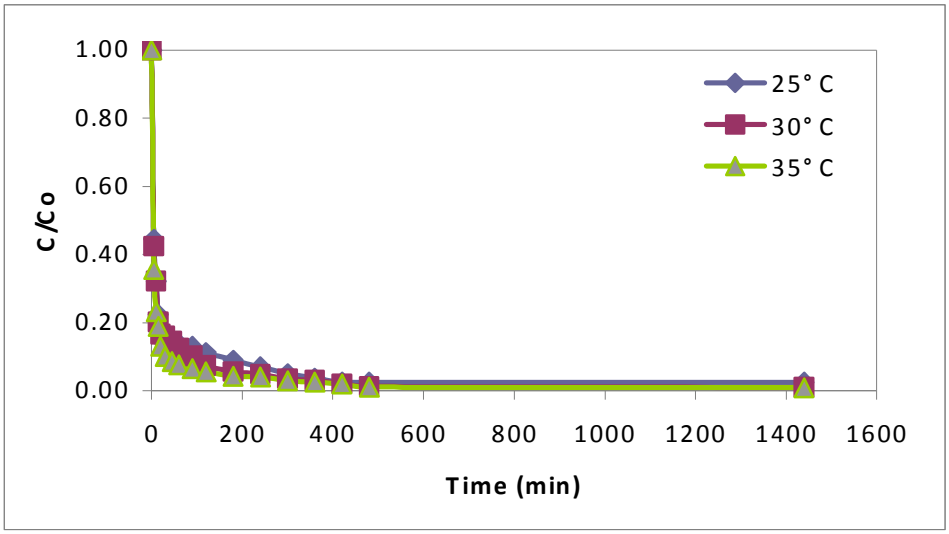

Figure 3.5 C/Co vs. time graph as a function of temperature for Diaion CRB02 (45-125 µm) resin with 250 RPM stirring rate.

3.2.2 Stirring Rate Effect

Figures 3.6 and 3.7 show the effect of stirring rate on boron removal by Diaion CRB02 (45-125 μm) (The results were also tabulated in Appendix.) As shown in Figures 3.6 and 3.7, the effect of stirring rate was not so remarkable on boron removal.

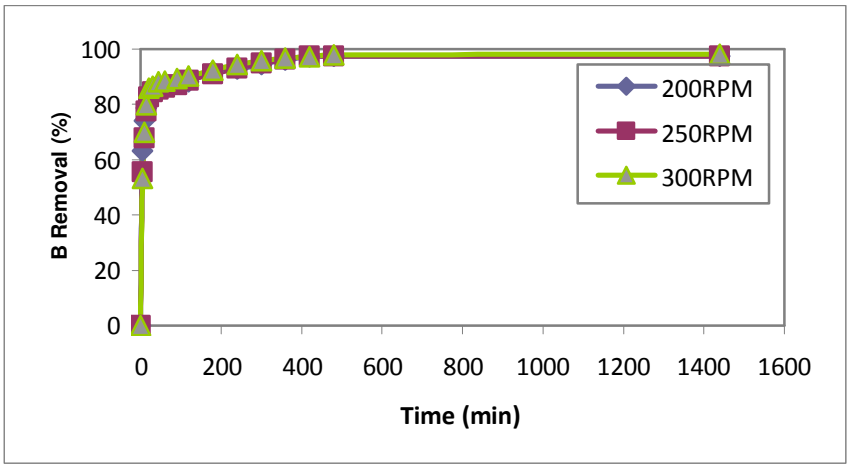

Figure 3.6 Effect of stirring rate on boron removal by Diaion CRB02 (45-125 μm) resin with amount of 0.05 g/ 100 mL at 25°C

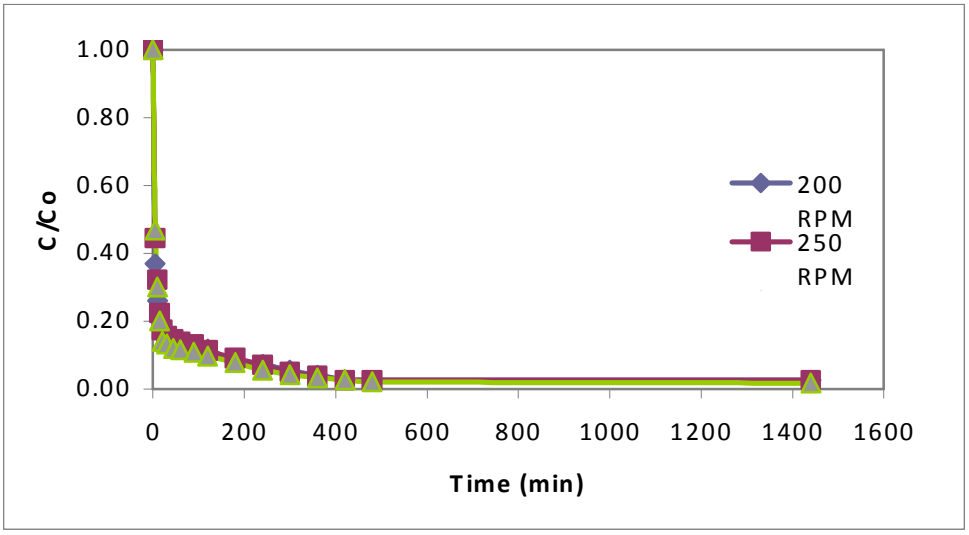

Figure 3.7 C/Co vs. time graph as a function of stirring rate for Diaion CRB02 (45-125 µm) resin with amount of 0.05 g/ 100 mL at 25°C.

3.2.3 Particle Size Effect

The effect of particle size on boron removal was studied using resin amount of 0.05 g/100 mL of Diaion CRB 02 resin at particle size range (45-125 µm), (125-250 µm) and (0.355-0.500 mm).

As shown in Figures 3.8 and 3.9, boron sorption rate of Diaion CRB 02 (45-125 µm) was the largest. On the other hand, the boron sorption rate of Diaion CRB 02 (0.355-0.500 mm) was too low because 0.05g resin/100 mL of resin concentration was not the optimum resin amount for particle range of (0.355-0.500 mm).

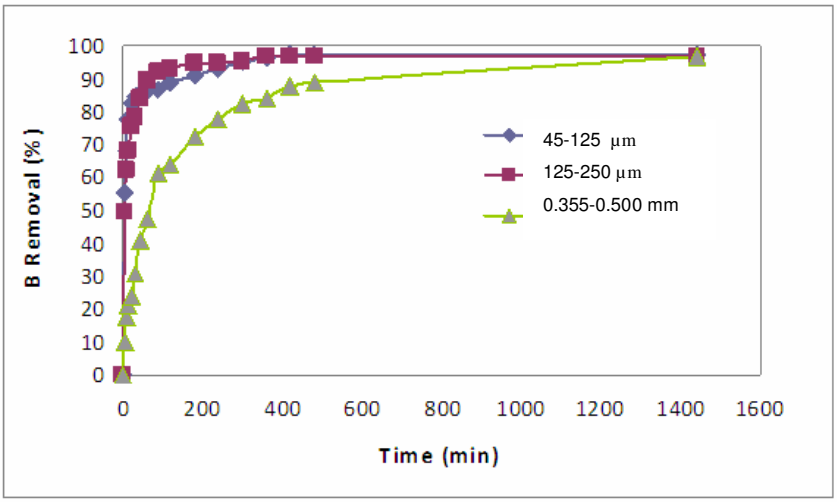

Figure 3.8 Effect of particle size of Diaion CRB 02 on boron removal using 0.05 g/100 mL resin amount at 25ºC and with 250 RPM stirring rate.

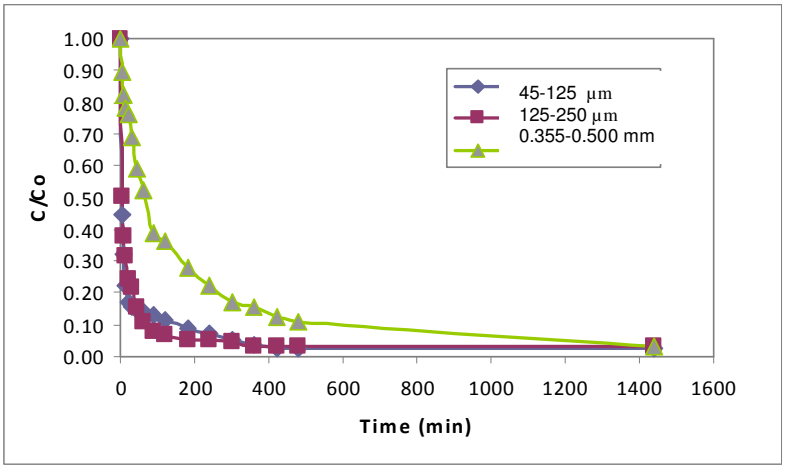

Figure 3.9 C/Co vs. time graph as a function of particle size of Diaion CRB 02 using 0.05 g/100 mL resin amount at 25ºC and with 250 RPM stirring rate.

Figures 3.10 and 3.11 show the kinetic study requests that performed with using 0.15 g/L (0.355-0.500 mm) particle sized Diaion CRB 02 resin. When compared Figure 3.10 with Figure 3.11, it is shown that the sorption rate of

Diaion CRB 02 (0.355-0.500 mm) increased using the optimum amount of resin (0,15g/L), which that was 0.15 g resin/100 mL.

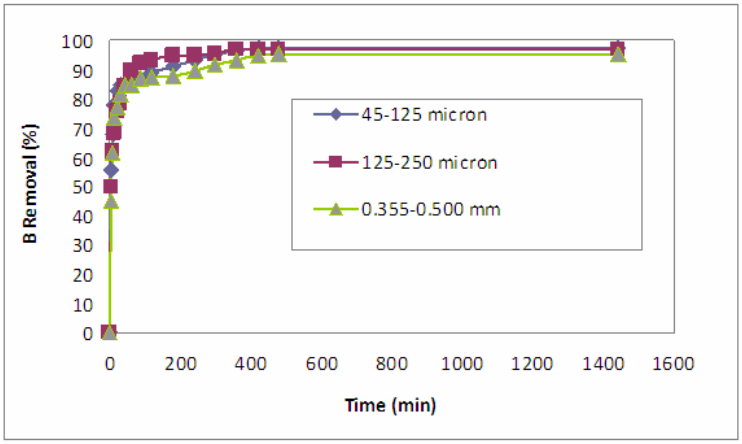

Figure 3.10 Effect of particle size of Diaion CRB 02 on boron removal using 0.15 g/100 mL for (0.355-0.500 mm) particle sized Diaion CRB 02 resin and 0.05 g/100 mL for (45-125 µm) and (125-250 µm) (25ºC, 250 RPM)**.**

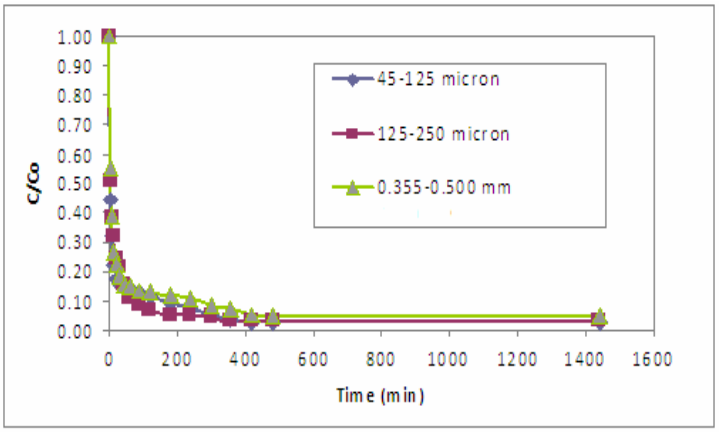

Figure 3.11 C/Co vs. time graph as a function of particle size of Diaion CRB 02, using 0.15 g/100 mL for (0.355-0.500 mm) particle sized Diaion CRB 02 resin and 0.05 g/100 mL for (45-125 µm) and (125-250 µm) (25ºC, 250 RPM).

3.3 Kinetic Theory

3.3.1 Classical Kinetic Models

Pseudo first- and second-order equations

A simple kinetic of sorption is the pseudo-first-order equation in the form (Ozacar and Sendil, 2004);

$$\frac{dq}{dt} = k_1(q_e - q_t) \tag{3.1}$$

where q_t and q_e represent the amount of adsorbed (mg/g) at any time t and at equilibrium time, respectively, and k_1 is rate constant of pseudo-first-order sorption process (min^{-1}) (Ozacar and Sendil, 2004).

The amount of boron absorbed at equilibrium, q_e (mg/g) was computed by using the following expression:

$$q_e = \frac{C_0 - C_e}{m} \times V \tag{3.2}$$

where C_0 and C_e are boron concentrations (mg/L) before and after adsorption, V is the volume of adsorbate (L) and m is the weight of the adsorbent (g).

Integrated eq. (3.1) with respect to boundary conditions

q = 0 at t = 0
and $q = q_t$ at t = t ,

Then Equation 3.1 becomes

$$\log(q_e - q_t) = \log(q_e) - \frac{k_1 t}{2.303} \quad (3.3)$$

Straight line plots of $\log(q_e - q_t)$ against time were used to determine the rate constant k_1 (min^{-1}) and correlation coefficients R^2 (Ngah and Hanafiah, 2008).

Pseudo-second-order kinetics

The kinetic data can be analysed by means of pseudo second order kinetics, which is represented by (Kabay et. al, 2007):

$$\frac{dq}{dt} = k_2 (q_e - q_t)^2 \quad (3.4)$$

where k_2 is the pseudo-second-order rate constant (g/mg.min), q_e and q_t represent the amount of the adsorbed (mg/g) at equilibrium and at any time t .

Separating the variables in Eqn. 3.4 gives;

$$\frac{dq}{(q_e - q_t)^2} = k_2 dt \quad (3.5)$$

Integrating Eqn. 3.5 for the boundary conditions

t = 0 to t = t
and q = 0 and q = q_e gives;

$$\frac{t}{q_t} = \frac{1}{k_2 q_e^2} + \frac{1}{q_e} t \quad (3.6)$$

A plot between t/q versus t gives a straight line if pseudo-second-order model is suitable. The value of the constants k_2 (g/mg h) and also predicted q_e (mg/g) can

be calculated from the slope and intercept of the plot, respectively. The constant k_2 is used to calculate the initial sorption rate r, at t →0, as follows (Kabay et. al, 2007).

$$r = k_2 q_e^2 \tag{3.7}$$

Thus the rate constant k_2, initial sorption rate r can be calculated from the plot of t/q versus time t using Eqn. 3.6 (Kabay et. al, 2007).

3.3.2 Diffusional and Reaction Models

The ion exchange between the counter ion (in solution) and the exchangeable ion (on the resin) is well described by a heterogeneous process. The models for process dynamic cover both the diffusional steps (bulk solution, a film layer at the external surface of the particle, pores) and the exchange reaction on the active sites. Since the resistance in bulk solution is easily controlled and negligible, three resistances, such as film diffusion, particle diffusion and chemical reaction, usually determine the overall rate of the ion-exchange process. One approach to the kinetic study is based on Fick's first law of integration of material balance for infinitive solution volume (ISV), whereas the other method uses the unreacted core model (UCM) in which ion exchange is treated as a heterogeneous reaction first occurs at the skin of the particle, then within a zone moving into the particle through the unreacted core (Badruk et. al., 1999). Five kinetic models developed for spherical particles in different cases of the rate-determining steps are given in Table 3.1.

Table 3.1 Diffusional and reaction models (Samuelson, 1963).

Method	**Equation**	**Rate Controlling Step**
ISV	**-ln (1-X)**=kt, where k=Dr$_{\text{Л}}^2$/r$_o^2$	Film Diffusion
	-ln (1-X^2) =k$_{li}$t, where k=3DC/r$_o$δCr	Particle Diffusion

UCM	$\mathbf{X}=(3C_{Ao}K_{MA}/ar_oC_{So})t$	Liquid Film
	$\mathbf{3-3(1-X)^{2/3}-2X} = (6D_{CR}C_{Ao}/ ar_o^2 C_{So})t$	Reacted Layer
	$\mathbf{1-(1-X)^{1/3}}= (k_sC_{Ao}/ r_o)t$	Chemical Reaction

3.3.2.1 Infinite Solution Volume Models (ISV)

Particle Diffusion

Manipulating Vermeulen's approximation given by Eqn. (1.11), a simple expression can be obtained (Vermeulen, 1952):

$$-\ln(1-X^2) = 2kt \qquad (3.7)$$

where $k = \dfrac{D_r \pi^2}{r_o^2}$

If the particle diffusion is the rate controlling mechanism, a plot of $-\ln(1-X^2)$ versus time should result in a straight line. The value of diffusion coefficient can be found from the slope.

Film Diffusion

If the film diffusion is the rate controlling mechanism, derivation of Eqn. (1.20) results in;

$$\ln(1-X) = k_{li}t$$

where $k_{li} = \dfrac{3DC}{r_o \delta \overline{C}}$

3.3.2.2 Unreacted Core Model (UCM)

Film Diffusion

When the fluid is the rate controlling layer, Eqn. (1.24) can be modified to represent the fractional attainment of equilibrium as a function of time.

$$X = \frac{3C_{Ao}K_{MA}}{ar_oC_{so}}t \qquad (3.9)$$

In the case of the film diffusion is in control of the ion exchange mechanism, the extent of the resin conversion X, plotted against t should produce a straight line and its slope is given by the expression $3\ C_{Ao}K_{MA}/ar_oC_{so}$.

Reacted Layer Diffusion

If reacted layer diffusion controls the ion exchange process, Eqn. (3.9) can be used to find the mass transfer coefficient

$$\left[3-3(1-X)^{2/3}-2X\right]=\frac{6D_{e,r}C_{Ao}}{ar_o^2C_{so}}t \qquad (3.10)$$

A straight line should be obtained by plotting $\left[3-3(1-X)^{2/3}-2X\right]$ against time, t if reacted layer diffusion controls. The slope is given by the expression $6\overline{D_e}C_{Ao}/ar_o^2C_{so}$.

Chemical Reaction

By manipulating the Eqn. (1.10) the following equation can be obtained to represent the rate controlling mechanism, in the case of the slowest step is the chemical reaction,

$$\left[1-(1-X)^{1/3}\right]=\frac{k_s C_{Ao}}{r_o} \qquad (3.11)$$

Then, a plot of $\left[1-(1-X)^{1/3}\right]$ versus time should produce a straight line. The slope is given by $C_{Ao}\, k_s / r_o$.

3.3.3 Evaluation of Kinetic Data Using Classical Kinetic Models and Diffusional Models

The kinetic behaviour of Diaion CRB 02 ion exchange resin was examined in order to get a measure of the relative kinetic performance of the resin as a function of temperature, stirring rate and particle size of resin.

3.3.3.1 Effect of Temperature on Kinetic Behaviour

The pseudo-first and second order models were applied to the kinetic data obtained in Figures 3.12 and 3.13. Table 3.2 shows the results of first and second order models.

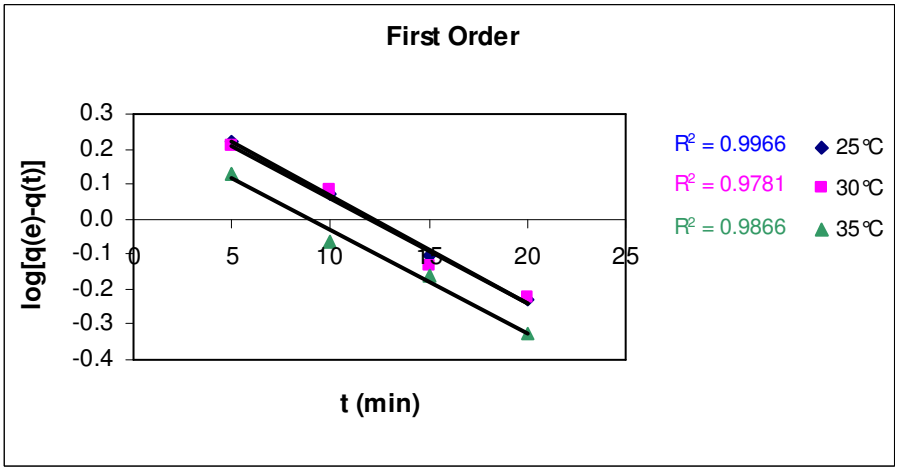

Figure 3.12 Applying pseudo-first-order kinetic model to kinetic data obtained at various temperatures.

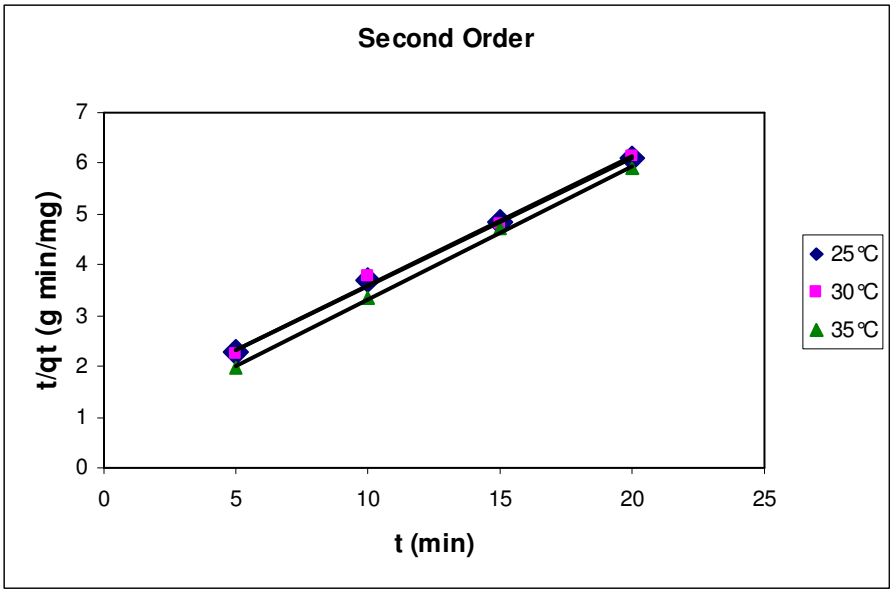

Figure 3.13 Applying pseude-first-order kinetic model to kinetic data obtained at various temperatures.

Table 3.2 Kinetic data evaluation using classical kinetic models (Temperature effect).

	$q_{e,exp}$ (mg/g)	1st Order Kinetic Model			2nd Order Kinetic Model		
		k_1 (1/min)	$q_{e,cal}$ (mg/g)	R^2	k_2 (g/mg min)	$q_{e,cal}$ (mg/g)	R^2
25°C	3.8800	0.0705	2.3616	0.9966	0.0591	3.9683	0.9977
30°C	3.8600	0.0691	2.2861	0.9781	0.0626	3.9154	0.9945
35°C	3.8700	0.0677	1.8298	0.9866	0.0970	3.8153	0.9986

The obtained kinetic data at different temperatures were fitted to sorption kinetics using the pseudo first order and pseudo second order kinetic model equations for Diaion CRB 02 (45-125 μm). Figure 3.12 was obtained by plotting

$\log(q_e - q_t)$ versus time and Figure 3.13 was obtained by plotting t/q versus time. Predicted sorption capacity values $q_{e,cal}$ were also calculated from the graphs by using Equation 3.3 and 3.6 for first order model and second order models, respectively. The experimental sorption capacity values, $q_{e,exp}$ for 25°C, 30°C and 35°C were found from experimental results as 3.88, 3.86, 3.87 respectively. The agreement between $q_{e,exp}$ and $q_{e,cal}$ is much greater for the pseudo second-order model than for the pseudo first-order model.

The calculated pseudo first and second order rate parameters k_1 and k_2, and correlation coefficients R^2 are given in Table 3.2. The R^2 values obtained were greater for second order model than those of first order model. As shown in Table 3.2, the rate parameter, k_2 increased with increasing temperature according to 2nd order model.

As shown in Figures 3.14, 3.15, 3.16 and Table 3.3, the kinetic studies were also evaluated using diffusional and reaction models.

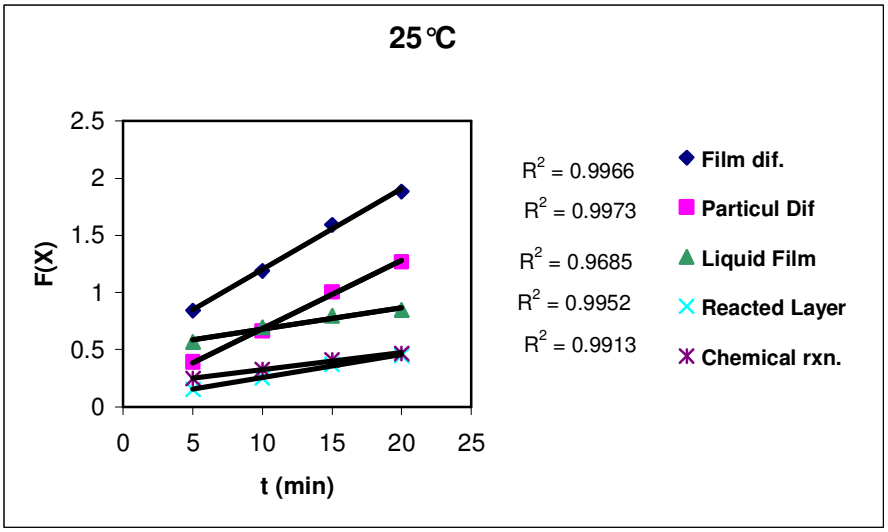

Figure 3.14 Applying kinetic data obtained with Diaion CRB 02 (45-125 μm) at 25°C to diffusional models.

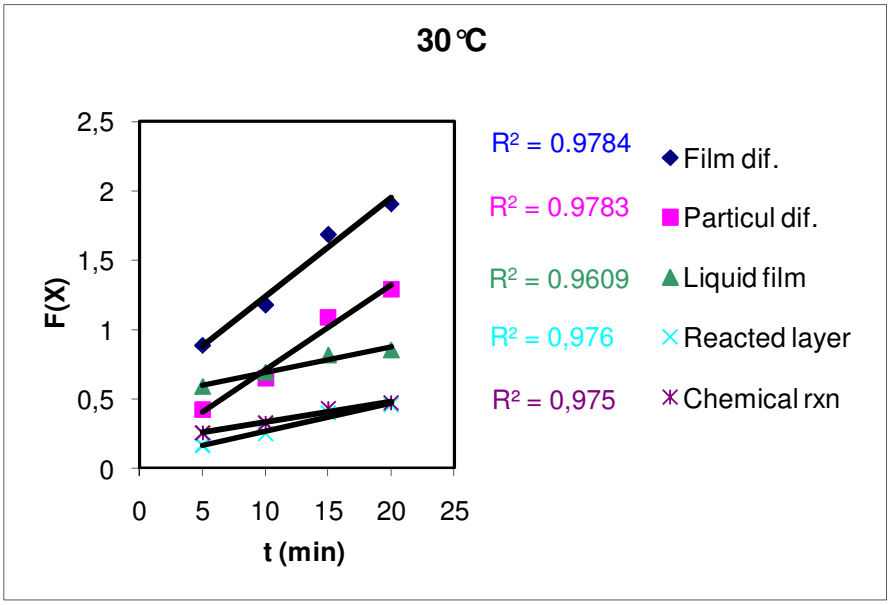

Figure 3.15 Applying kinetic data obtained with Diaion CRB 02 (45-125 µm) at 30°C to diffusional models.

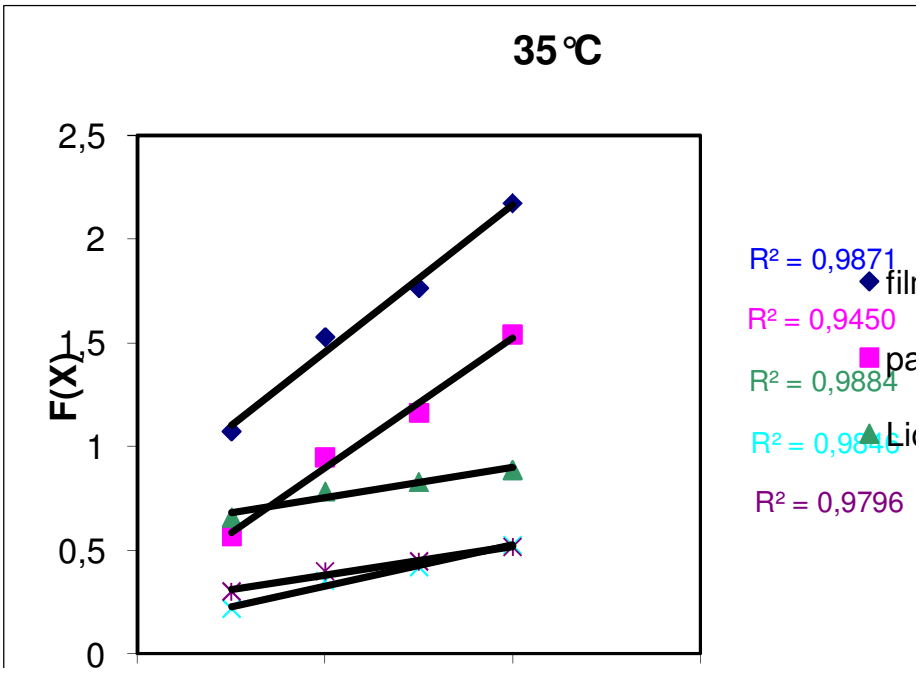

Figure 3.16 Applying kinetic data obtained with Diaion CRB 02 (45-125 µm) at 35°C to diffusional models.

Table 3.3 Evaluation of diffusional models for kinetic data obtained at various temperatures.

Model	25°C		30°C		35°C	
	Slope	R^2	*slope*	R^2	*slope*	R^2
-ln (1-X)	0.4964	0.9666	0.5216	0.9784	0.7471	0.9871
-ln (1-X^2)	0.0886	0.9973	0.1045	0.9783	0.2703	0.9884
X	0.4936	0.9685	0.5078	0.9609	0.6054	0.9450
3-3(1-X)$^{2/3}$-2X	0.0517	0.9952	0.0588	0.9760	0.1297	0.9846
1-(1-X)$^{1/3}$	0.1756	0.9913	0.1828	0.9750	0.2418	0.9796

The correlation coefficients for the linear models show that the rate is particle diffusion controlled according to ISV model at 25°C, 30°C and 35°C. According to UCM, the rate is controlled by reacted layer.

3.3.3.2 Effect of Stirring Rate on Kinetic Behaviour

The pseudo-first and second order models were applied to the kinetic data obtained in Figures 3.17 and 3.18. Table 3.4 shows the results of first and second order models.

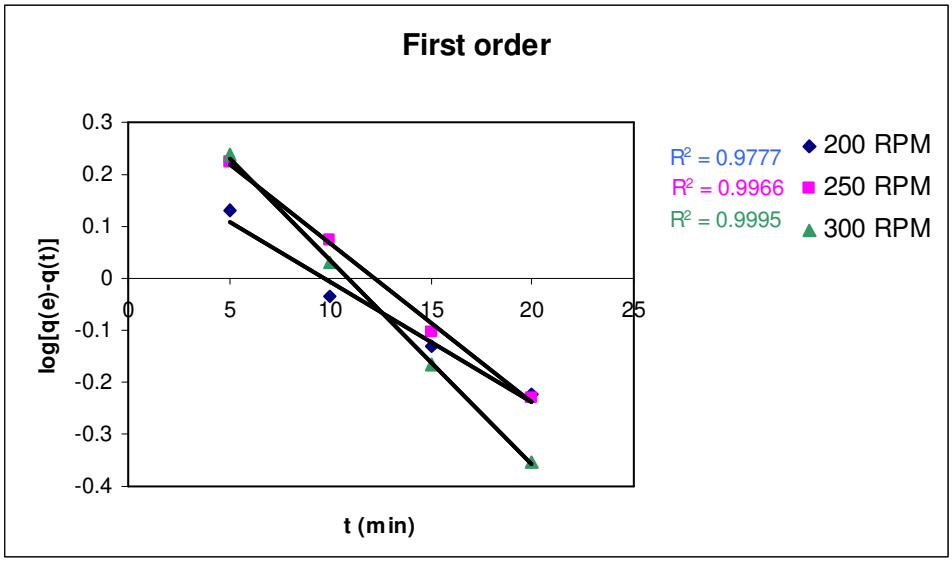

Figure 3.17 Applying pseude-first-order kinetic model to kinetic data obtained at various stirring rate level.

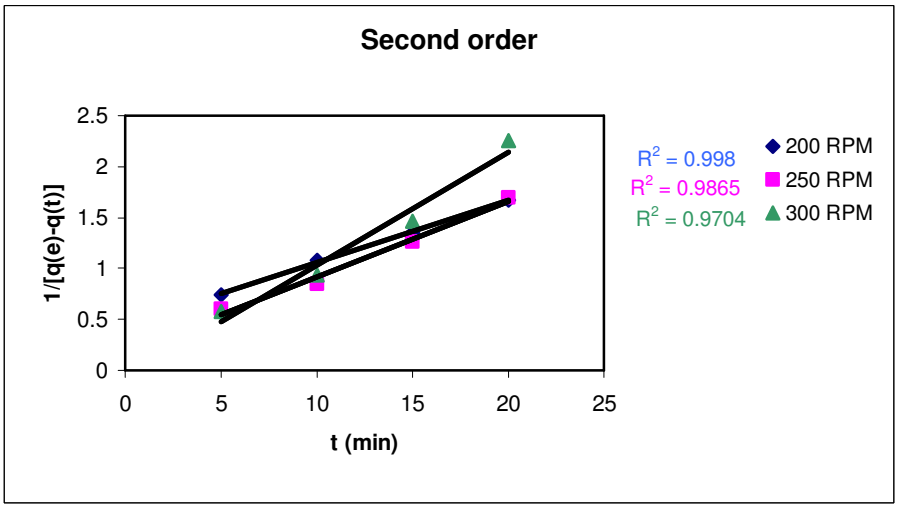

Figure 3.18 Applying pseude-first-order kinetic model to kinetic data obtained at various stirring rate level.

Table 3.4 Kinetic data evaluation using classical kinetic models (Stirring rate effect).

	$q_{e,exp}$ (mg/g)	1st Order Kinetic Model			2nd Order Kinetic Model		
		k_1 (1/min)	$q_{e,cal}$ (mg/g)	R^2	k_2 (g/mg min)	$q_{e,cal}$ (mg/g)	R^2
200RPM	3.8200	0.0532	1.6757	0.9777	0.1209	3.5817	0.9998
250RPM	3.8800	0.0705	2.3616	0.9966	0.0591	3.9683	0.9977
300RPM	3.8100	0.0905	2.6847	0.9995	0.0441	4.2499	0.9995

The obtained kinetic data were fitted to sorption kinetics using the pseudo first order and pseudo second order kinetic model equations for studying the effect of with Diaion CRB 02 (45-125 μm). The kinetic studies were performed with 200 RPM, 250 RPM and 300 RPM. Figure 3.17 was plotted in order to observe first order reactions by plotting $\log(q_e - q_t)$ versus time and Figure 3.18 was plotted in order to observe second order reactions by plotting t/q versus time. Predicted sorption capacity values $q_{e,cal}$ were also calculated from the graphs by using Equations 3.3 and 3.6 for first order model and second order models, respectively. The experimental sorption capacity values, $q_{e,exp}$ for 200 RPM, 250 RPM and 300 RPM found from experimental results were 3.82, 3.88, 3.81, respectively. The agreement between $q_{e,exp}$ and $q_{e,cal}$ is much greater for the pseudo second-order model than for the pseudo first-order model.

The calculated pseudo first and second order rate constants k_1 and k_2, and correlation coefficients R^2 are given in Table 3.4. R^2 values for 200 RPM, 250 RPM and 300 RPM were (0.9966, 0.9977, 0.9995, respectively)for pseudo-second order plots. They were a little bit larger than R^2 values obtained first-order model plots. The comparison of the experimental and theoretical sorption

capacity values for second order kinetics showed similarity as a proof of the better fitting to the pseudo-second-order mechanism. As shown in Table 3.4, the rate constant, k_2 decreased with increasing stirring rate.

As shown in Figures 3.19, 3.20, 3.21 and Table 3.5, the kinetic studies were also evaluated using diffusional and reaction models.

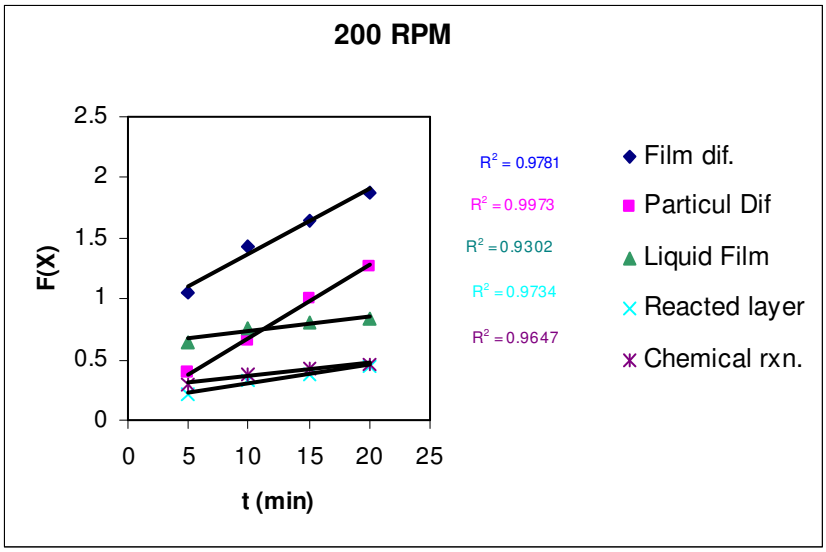

Figure 3.19 Applying kinetic data obtained with Diaion CRB 02 (45-125 μm) with a stirring rate of 200 RPM to diffusional models.

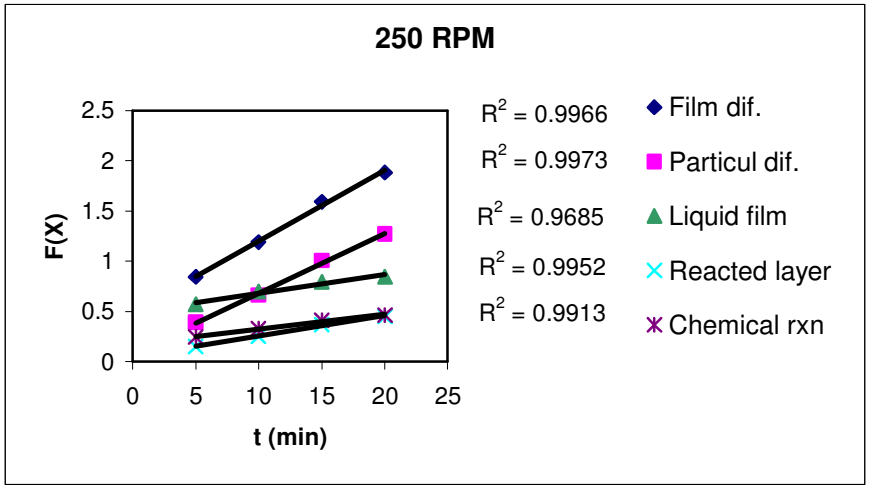

Figure 3.20 Applying kinetic data obtained with Diaion CRB 02 (45-125 μm) with a stirring rate of 250 RPM to diffusional models.

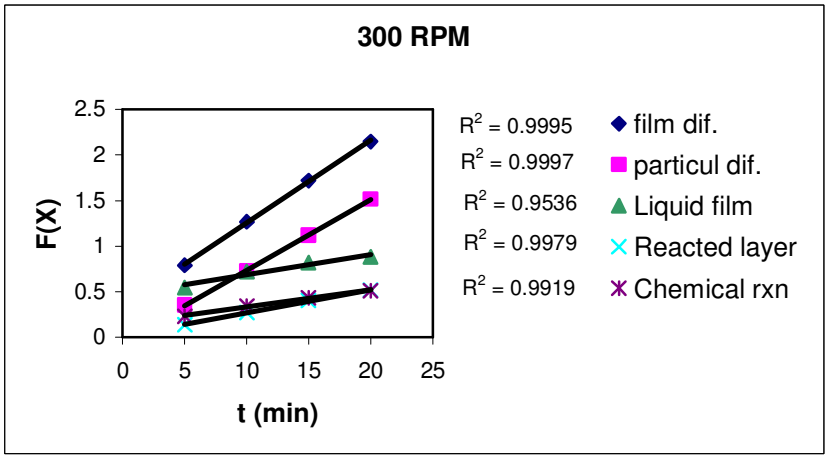

Figure 3.21 Applying kinetic data obtained with Diaion CRB 02 (45-125 μm) with a stirring rate of 300 RPM to diffusional models.

Table 3.5 Evaluation of diffusional models for kinetic data obtained at various stirring rates.

Model	200 RPM		250 RPM		300 RPM	
	Slope	R^2	***slope***	R^2	***Slope***	R^2
$-ln\ (1-X)$	0.8261	0.9781	0.4964	0.9966	0.3501	0.9995
$-ln\ (1-X^2)$	0.0886	0.9973	0.0886	0.9973	0.0402	0.9997
X	0.6060	0.9302	0.4936	0.9685	0.4643	0.9536
$3-3(1-X)^{2/3}-2X$	0.1472	0.9734	0.0517	0.9952	0.0148	0.9979
$1-(1-X)^{1/3}$	0.2520	0.9647	0.1756	0.9913	0.1484	0.9919

The correlation coefficients for the linear models show that the rate is particle diffusion controlled according to both ISV and UCM models with 200 RPM, 250 RPM and 300 RPM.

3.3.3.3 Effect of Particle Size on Kinetic Behaviour

The pseudo-first and second order models were applied to the kinetic data obtained in Figure 3.22 and 3.23. Table 3.6 shows the results of first and second order models.

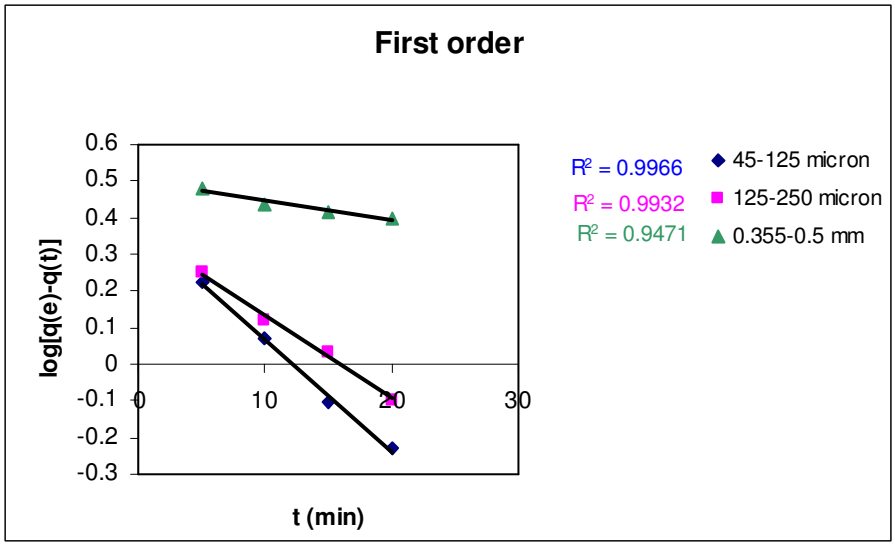

Figure 3.22 Applying pseude-first-order kinetic model to kinetic data obtained at various particle size of Diaion CRB 02 resin.

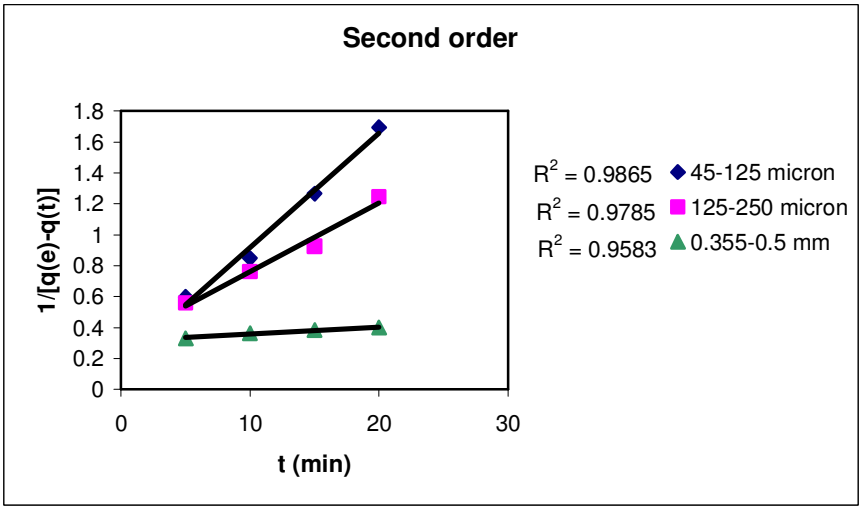

Figure 3.23 Applying pseude-first-order kinetic model to kinetic data obtained at various particle size of Diaion CRB 02 resin.

Table 3.6 Kinetic data evaluation using classical kinetic models (Particle size effect).

	$q_{e,exp}$ (mg/g)	1st Order Kinetic Model			2nd Order Kinetic Model		
		k_1 (1/min)	$q_{e,cal}$ (mg/g)	R^2	k_2 (g/mgmin)	$q_{e,cal}$ (mg/g)	R^2
45-125 µm	3.8800	0.0705	2.3616	0.9966	0.0591	3.9683	0.9977
125-250 µm	3.6600	0.0520	2.2914	0.9932	0.0487	3.4412	0.9956
0.355-0.500 mm	3.6000	0.0714	2.6903	0.9471	0.0379	4.029	0.9822

The obtained kinetic data were fitted to sorption kinetics using the pseudo first order and pseudo second order kinetic model equations for particle size effect of kinetic study with Diaion CRB 02. The kinetic studies were performed with (45-125 µm), (45-125 µm) and (0.355-0.500 mm) of resin size. Figure 3.22 was obtained by plotting $\log(q_e - q_t)$ versus time and Figure 3.23 was obtained by plotting t/q versus time. Predicted sorption capacity values $q_{e,cal}$ were also calculated from the graphs by using Equation 3.3 and 3.6 for first order model and second order models, respectively. The experimental sorption capacity values, $q_{e,exp}$ for (45-125 µm), (125-250 µm) and (0.355-0.500 mm) were found from experimental results as 3.88, 3.66, 3.60 respectively. The agreement between $q_{e,exp}$ and $q_{e,cal}$ is much greater for the pseudo second-order model than for the pseudo first-order model.

The calculated pseudo first and second order rate parameters k_1 and k_2, and correlation coefficients R^2 are given in Table 3.6. R^2 values for (45-125 µm), (125-250 µm) and (0.355-0.500 mm) were (0.9977, 0.9956, 0.9822, respectively) fit to pseudo-second-order mechanism in each case. The comparison of the experimental and theoretical sorption capacity values for second order kinetics showed similarity as a proof of the fitting of the obtained data to the pseudo-second-order mechanism. As shown in Table 3.6, the rate constant, k_2 decreased with increasing particle size.

As shown in Figures 3.24, 3.25, 3.26 and Table 3.7, the kinetic studies were also evaluated using diffusional and reaction models.

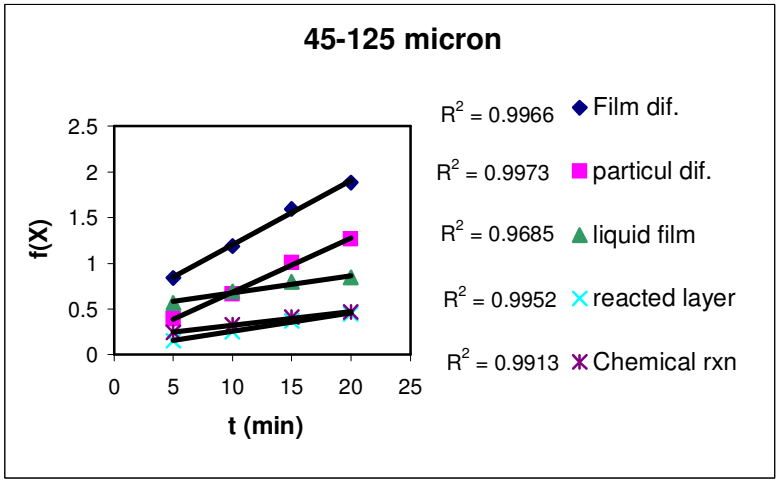

Figure 3.24 Applying kinetic data obtained with Diaion CRB 02 (45-125 μm) at 25°C to diffusional models.

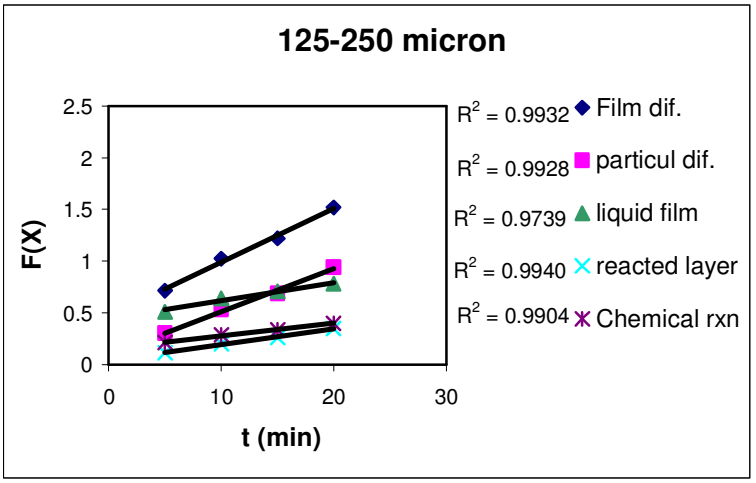

Figure 3.25 Applying kinetic data obtained with Diaion CRB 02 (125-250 μm) at 25°C to diffusional models.

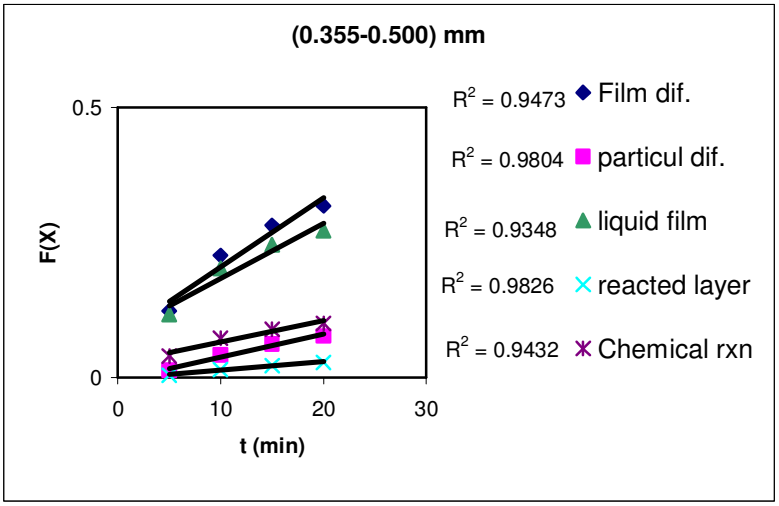

Figure 3.26 Applying kinetic data obtained with Diaion CRB 02 (0.355-0.500 mm) at 25°C to diffusional models.

Table 3.7 Evaluation of Diffusional Models for kinetic data obtained at various particle size using the resin of Diaion CRB 02 at 25°C.

Model	45-125 micron		125-250 micron		0.355-0.500 mm	
	slope	R^2	*Slope*	R^2	*slope*	R^2
$-ln\ (1-X)$	0.4964	0.9666	0.4679	0.9932	0.0781	0.9473
$-ln\ (1-X^2)$	0.0886	0.9973	0.0961	0.9943	0.0039	0.9804
X^*	0.4936	0.9685	0.4408	0.9739	0.0816	0.9348
$3-3(1-X)^{2/3}-2X$	0.0517	0.9952	0.0431	0.9940	0.0018	0.9826
$1-(1-X)^{1/3}$	0.1756	0.9913	0.1591	0.9904	0.0265	0.9432

The correlation coefficients for the linear models show that the rate is particle diffusion controlled according to ISV and UCM models for (45-125 µm), (125-250 µm) and (0.355-0.500 mm) resin size.

3.4 Adsorption Isotherms for Boron Removal

In batch experiment, three well-known models, namely the Langmuir, Freundlich and Dubinin-Radushkevich (DR) adsorption equilibrium models were used to analyse the experimental data.

3.4.1 Langmuir Model:

The Langmuir isotherm, which is valid for monolayer sorption onto a surface with a finite number of identical sites and uniform adsorption energies, is given by equation 3.12.

$$Q_e = \frac{K_L Q_{\max} C_e}{1 + bC_e} \tag{3.12}$$

where Q_{max} is the amount of adsorption corresponding to monolayer coverage (mg/g). C_e is the equilibrium concentration of boron solution (mg/L), and Q_e is the amount of ion (such as B) sorbed on the resins (mg B/g-dry resin), Q_{max} is a constant indicates the adsorption capacity of resins (mg B/g-dry resin), b is a constant indicates energy of adsorption (L/mg) (Seki et. al., 2006).

Figure 3.27 shows the plot of Qe vs Ce for Diaion CRB 02 (45-125 μm).

The nonlinear form equation can be linearized as below:

$$\frac{C_e}{Q_e} = \frac{1}{Q_{\max} b} + \frac{C_e}{Q_{\max}} \tag{3.13}$$

Q_m and b can be calculated from the slope and intercept of Langmuir plots of C_e/Q_e versus C_e (Seki et. al., 2006).

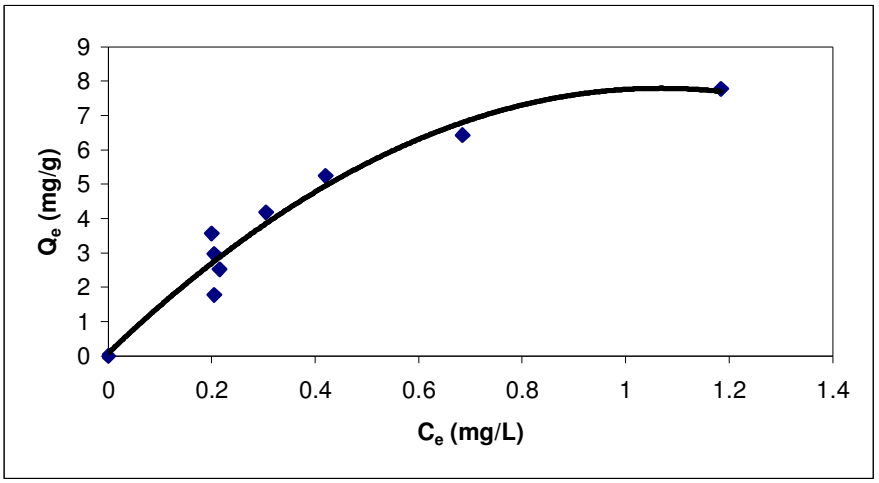

Figure 3.27 Equilibrium isotherm for loading B on to Diaion CRB 02 (45-125 μm).

The linearized plot of Langmuir isotherm for Diaion CRB 02 (45-125 μm) was given in Figure 3.28.

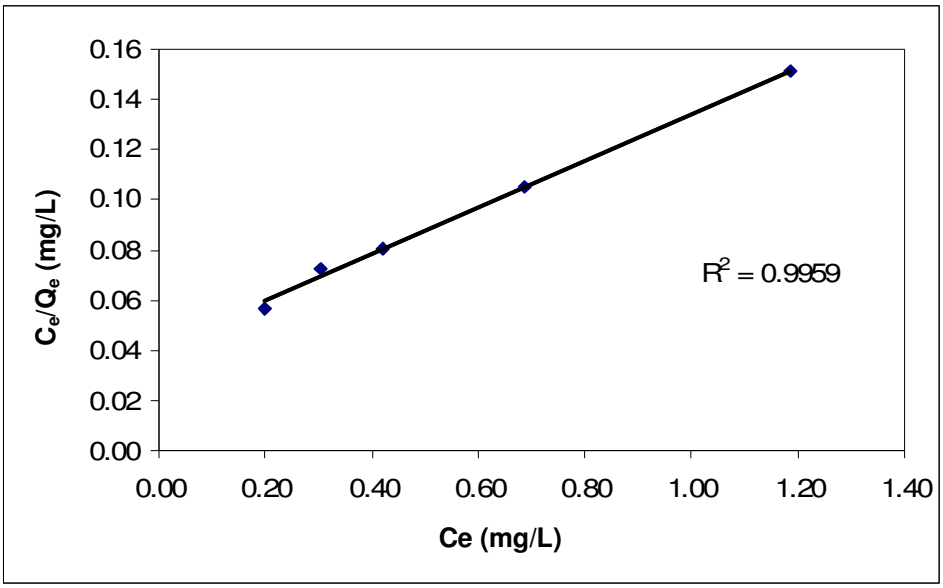

Figure 3.28 Linearized form of Langmuir isotherm for Diaion CRB02 (45-125 micron).

The calculated results are summarized in Table 3.8.

Table 3.8 The Langmuir equation constants for boron removal using Diaion CRB 02 (45-125 micron) resin.

Q_{max} (mg/g)	B (L/mg)	R^2
10.73	2.27	0.9959

3.4.2 Freundlich Model:

Freundlich equation is employed for boron adsorption from aqueous solution. The freundlich equation is applied to describe heterogeneous system and reversible adsorption and is not restricted to the formation of monolayer. It

describes reversible adsorption. The freundlich adsorption isotherm has the form of:

$$Q_e = K_f C_e^{1/n}$$

where C_e is the equilibrium concentration (mg/L), Q_e is the amount of ion (such as B) sorbed on the resins (mg B/g-dry resin), K_f is a constant indicates the rate of adsorption, n is a constant indicates the degree of favourability of adsorption.

This equation can be rearranged to the following linear form:

$$\log Q_e = \log K_f + \frac{1}{n} \log C_e \qquad (3.13)$$

When the sorption data were analyzed according to equation 3.13, as shown in Figure 3.29, a plot of log Q_e versus log C_e enables to determine the values of 1/n and K_f. The results were presented in Table 3.9.

When compared the Freundling and Langmuir isotherms, the R^2 value of Freundlich seems to better than R^2 value of Langmuir isotherm.

The constant is also known a measurement of linearity. If 1/n is equal to unity, the absorption is linear and adsorption sites are homogeneous in energy and no interaction takes place between the adsorbed species. If the value of 1/n smaller than 1, adsorption is favourable. It shows that the sorption capacity increases and new adsorption sites occur. If the value if 1/n is greater than 1, adsorption bond becomes weak; unfavourable adsorption capacity decreases.

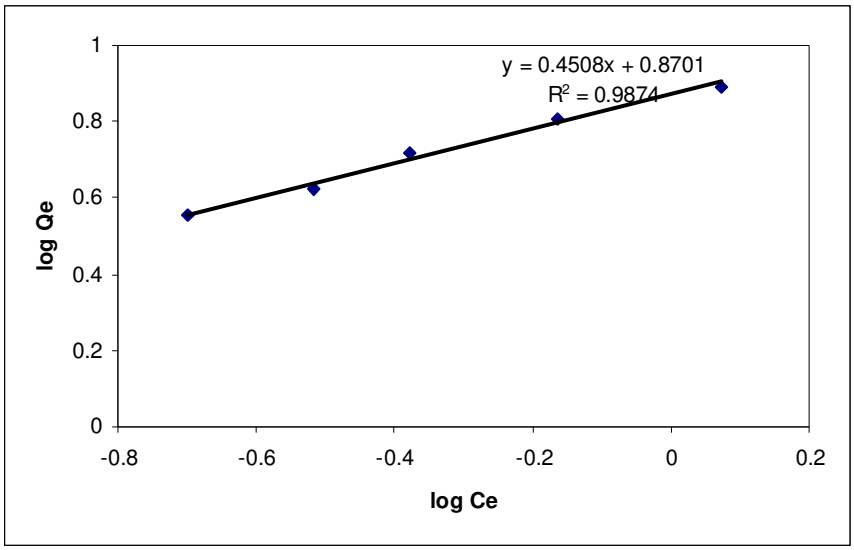

Figure 3.29 Linearized form of Freundlich isotherm for Diaion CRB 02 (45-125 micron).

Table 3.9 The Freundlich equation constants for boron removal with Diaion CRB 02 (45-125 micron) resin.

1/n	**K_f**	**R^2**
0.45	7.41	0.9874

3.4.3 Dubinin-Radushkevich Model

In DR isotherm, the equation used for adsorptions type can be given as below (Seki et. al., 2006)

$$\ln Q_e = \ln X_m - k\varepsilon^2$$

Where ε (polanyi potential) is RTln(1+1/C_e), C_e the equilibrium concentration of boron is solution (mol/L) and Q_e is the equilibrium

concentration of boron on adsorbent(mol/g). X_m is the adsorption capacity (mol/g) and R is the gas constant 8.314 x 10^{-3} kJ/(mol K). T is the temperature (K) (Seki et. al., 2006).

The value of k is a constant and is used to calculate adsorption energy (mol^2/kj^2)

The mean energy change of adsorption (E) can be calculated using the following expression (Seki et. al., 2006):

$$E = (2k)^{-0.5}$$

The magnitude of E can be used for estimating the type of adsorption. According to, the magnitude of E is between 8 kJ/mol and 16 kJ/mol, adsorption type can be explained by ion-exchange. It is accepted that when the adsorption is lower than 8 kJ/mol, the type of adsorption can be considered as physical adsorption (Seki et. al., 2006).

As can be seen in Table 3.10, all E values are between 8-16 kj/mol. It obviously shows the type of sorption is considered as ion-exchange adsorption.

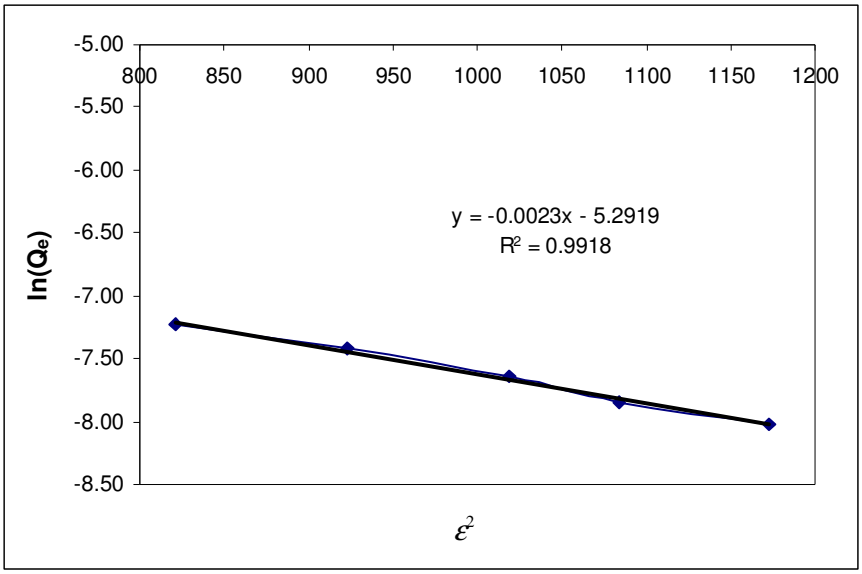

Figure 3.30 Linearized form of DR model isotherm for Diaion CRB 02 (45-125 micron).

Table 3.10 The DR isotherm equation constants for boron removal with different type and size of resins.

k	Xm	E (kj/mol)	R^2
0.0023	0.0050	14.7442	0.9918

The value of k is a constant and is used to calculate adsorption energy (mol^2/kj^2). Plots of ln Qe versus ε^2 (in Figure 3.30) yield a straight line of slope k and intercept ln X_m. The results are tabulated in Table 3.10.

3.5 Thermodynamic Parameters

In engineering practice, values of thermodynamic parameters such as enthalpy change (ΔH°), entropy change (ΔS°) and free energy change (ΔG°) must be taken into consideration in order to determine the spontaneity of a process. A spontaneous process will show a decrease in ΔH° and ΔG° values with increasing temperature (Ngah and Hanafiah, 2008).

The kinetic experiments were carried out at temperatures of 298, 303 and 305 K. All the thermodynamic parameters can be calculated from the following equations (Bekçi et. al., 2006):

$$K_C = \frac{Q_e}{C_e} \tag{3.14}$$

Where Kc is the equilibrium constant, Qe is the concentration of boron adsorbed on resin at equilibrium (mg/L), Ce is the equilibrium concentration of boron in the solution (mg/L)

Gibbs free energy change ΔG° is calculated by;

$$\Delta G° = -RT \ln Kc \tag{3.15}$$

$$\ln Kc = \frac{\Delta S°}{R} - \frac{\Delta H°}{RT} \tag{3.16}$$

Where, R is the gas constant (8.314 J/K mol) and T is the temperature in Kelvin. Van't Hoff equation (eqn : 3.16) can be used with the experimental data

to evaluate entropy change of adsorption (ΔS°) and enthalpy change of adsorption ΔH° from the intercept and slope by plotting ln Kc versus 1/T. Additionally, the values of Gibbs free energy change ΔG° is calculated from equation (3.15) at 298, 303 and 308K.

As can be seen in Figure 3.31, the ln Kc versus 1/T graph was plotted and the values of ΔH° and ΔS° can be obtained from slope and intercept of Van't Hoff equation (eqn. 3.16). The results were tabulated in Table 3.11.

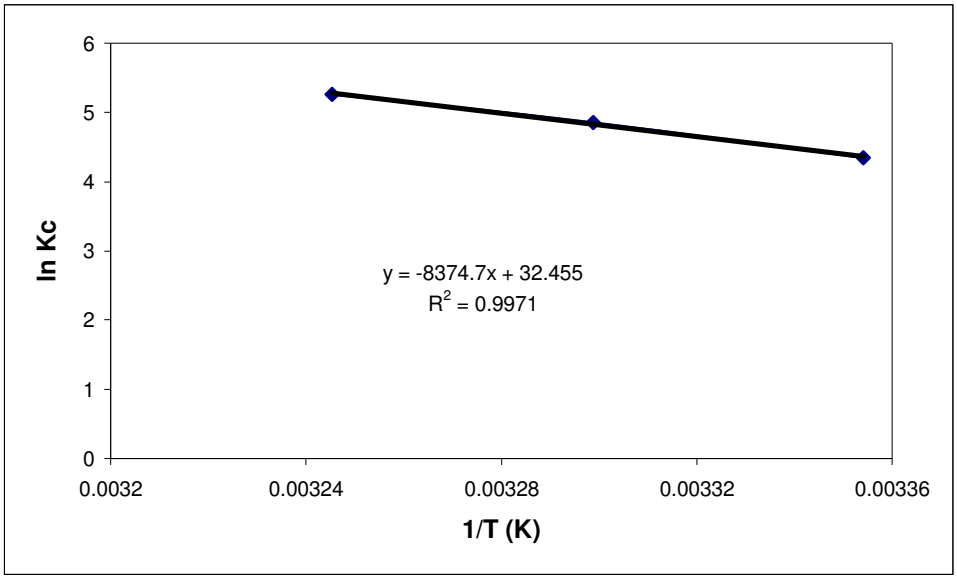

Figure 3.31 Van't Hoff equation plot of ln Kc versus 1/T.

Table 3.11 The values of ΔG° ΔH° and ΔS° obtained using Van't Hoff equation.

T (K)	ΔG° (kj/mol)	ΔH° (kj/mol)	ΔS° (kj/mol K)
298.14	-10.79	69.63	0.26
303.14	-12.24		
308.14	-13.48		

It is known that the absolute magnitude of the change in free energy for physisorption is between -20 and 0 kj/mol, chemisorption has a range of -80 to -400 kj/mol (Bekçi et al., 2006). ΔG° values calculated are -10.79 kj/mol for 298.14 K, -12.24 for 303.14 K, -13.48 kj/mol for 308.14 K, respectively. The results show that the sorption of boron using both resins may occur as physically. Also the negative values of ΔG° at various temperature indicate that the adsorption process is spontaneous.

The positive value of standard enthalpy change (ΔH°) (as shown in Table 3.11) for boron sorption using Diaion CRB 02 resin implies the endothermic nature of the sorption process.

As seen in Table 3.11, the ΔS° value is 0.26 kj/mol K. The positive values ΔS◦ suggests increased randomness during adsorption (Bekçi et. al., 2006). Also, positive ΔS◦ value for boron sorption using Diaion CRB 02 resin indicate an increase in degree of freedom of the boron species.

3.6 Removal of Boron from RO Permeate

In this section, natural sewater RO permeate solution was used.

Figure 3.32 shows the kinetic study results of Diaion CRB 02 (45-125 μm) by using RO permeate solution at 25°C and 250 PRM (The results also tabulated in Appendix section).

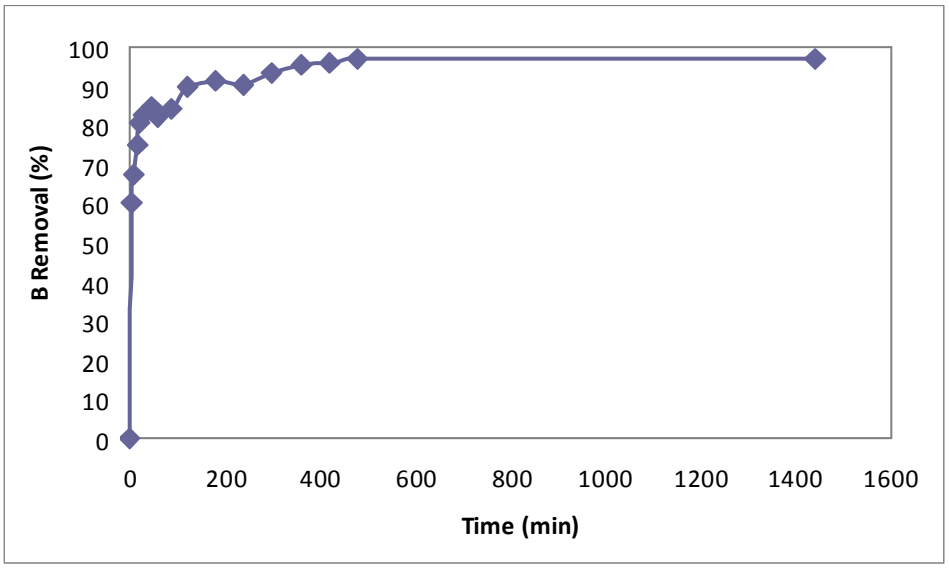

Figure 3.32 Kinetic Behaviour of Diaion CRB 02 on Removal of Boron from RO Permeate Solution at 25°C with 250 RPM stirring rate.

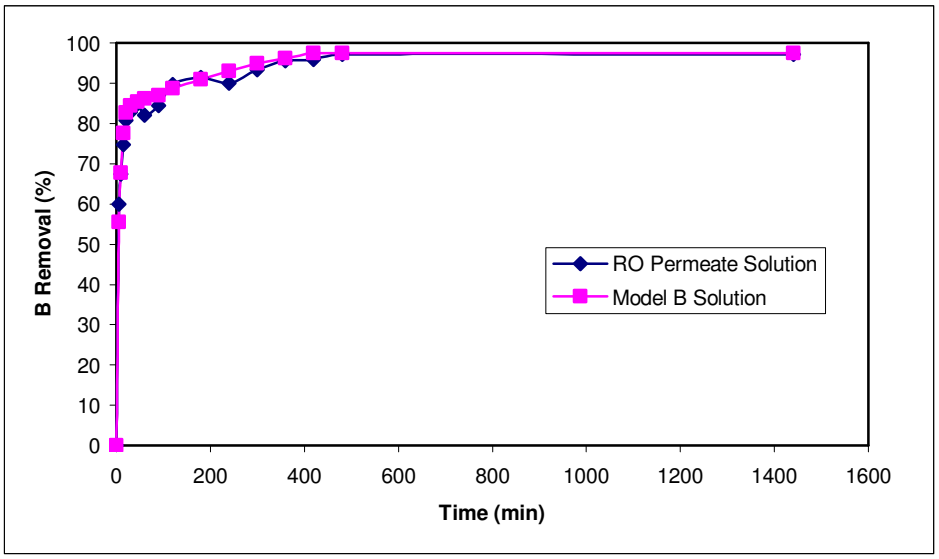

Figure 3.33 Comparision of Kinetic Behaviour of Diaion CRB 02 on Removal of Boron from RO Permeate Solution and Model B Solution.

As shown in Figure 3.33 (results were also tabulated in appendix section), boron removals from RO Permeate and from model B solution, were nearly the same.

Figure 3.34 shows the results of batch study with different size of both resins using SWRO permeate. Figure 3.35 shows the results of batch study with different size of both resins using model B solution.

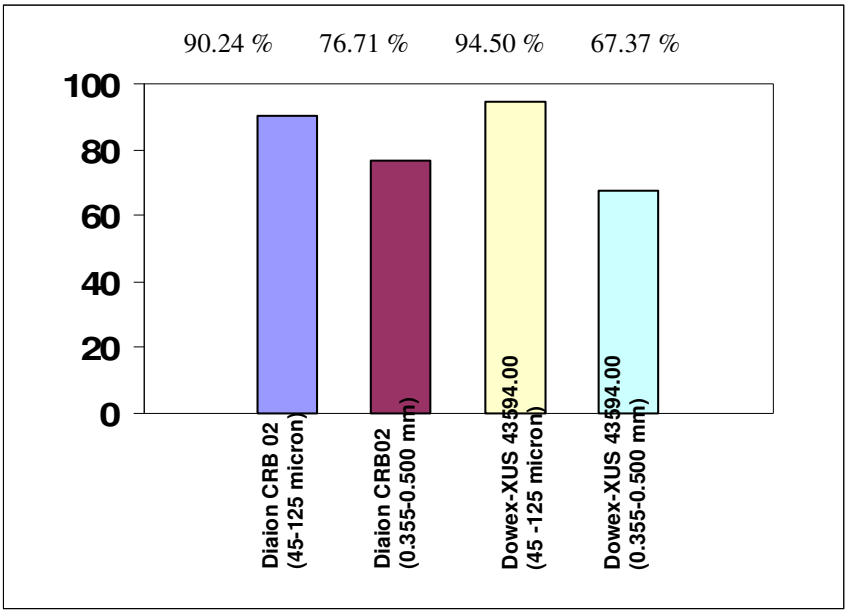

Figure 3.34 Effect of resin particle size for boron removal from SWRO permeate.

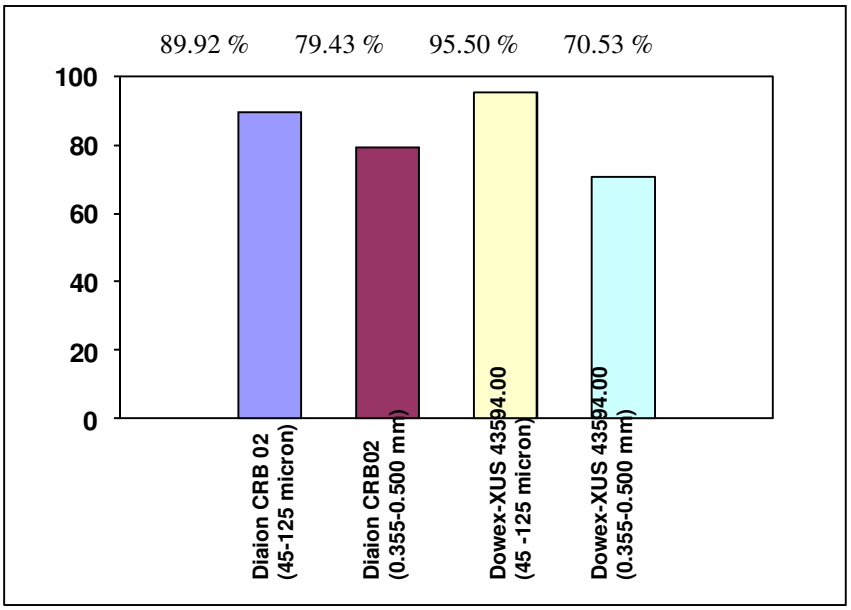

Figure 3.35 Effect of resin particle size for boron removal from model solution.

As shown in Figure 3.34 and 3.35, effect of resin particle size for boron removal from SWRO solution and model solution are nearly the same. The experiment results are tabulated in Table 3.12.

Table 3.12 A comparison between the batch study results using RO Permeate Solution and Model Solution.

Resin Size and Type	RO Permeate Solution			Model Solution		
	C_e (mg/L)	C/Co	B Removal (%)	C_e (mg/L)	C/Co	B Removal (%)
Diaion CRB02 45-125 µm	0.19	0.10	90.24	0.20	0.10	89.92
Diaion CRB02 0.355-0.5 mm	0.46	0.23	76.71	0.40	0.20	79.43
Dowex 45-125 µm	0.11	0.05	94.51	0.09	0.05	95.50
Dowex 0.355-0.5 mm	0.64	0.33	67.37	0.59	0.29	70.53

3.7 Batch Elution of Boron

The aim of this study was to obtain the elution capacity of HCl solution for boron by Diaion CRB 02 resin (0.355-0.500 mm).

The results are shown in Table 3.13. The elution (%) increased with increasing concentration of HCl solution.

Table 3.13 The result of batch elution of boron.

Concentration of HCl (M)	Elution of B (%)
0.10	69.76
0.25	73.61
0.50	74.36
1.00	77.83

4. CONCLUSIONS

Requirement for fresh water increases worldwide and there is a need for more and more plants that are able to treat non-conventional water sources. Seawater has become an important source of fresh water in many arid regions. According to drinking water regulations and health effect of the boron against human and plants, removal of boron from seawater has become key subject for researchers.

In this study, boron removal from reverse osmosis desalinated seawater was investigated by using ion exchange method. The batch sorption tests were conducted using:

1. Model seawater
2. Reverse osmosis desalinated seawater

Two types of N-methyl glucamine type chelating commercial resins (Diaion CRB 02 and Dowex-XUS 43594.00) with different particle size range of (45-125 μm) and (0.355-0.500 mm) were used for sorption studies.

Optimum resin amount for removal of boron from model seawater was determined using Diaion CRB 02 and Dowex-XUS 43594.00 resins with two different particle size (0.355-0.500 mm and 45-125 μm). By reducing the resin particle size, the optimum resin amounts decreased from 0.15 g resin/100mL to 0.05 g resin/100 mL for both Diaion CRB 02 and Dowex-XUS 43594.00 for boron removal from 2 ppm model solution.

The batch-mode boron removal results of Diaion CRB 02 performed with model B solution are 82.92% and 79.43% for (45-125 μm) and (0.355-0.500 mm) particle sizes, respectively. The boron removal of Dowex-XUS 43594.00 are 82.92% and 79.43% for (45-125 μm) and (0.355-0.500 mm) particle sizes,

respectively. Removal of boron with the (0.355-0.500mm) particle-sized resin is less than powdered-sized resin for both resins.

The batch-mode boron removal results of Diaion CRB 02 performed with SWRO permeate are % for (45-125 µm) and (0.355-0.500mm) respectively. The boron removal of Dowex-XUS 43594.00 are 94.5% and 67.37% for (45-125 µm) and (0.355-0.500mm), respectively. Removal of boron with the particle-sized resin (0.355-0.500mm) is less than powdered-sized resin for both resins.

The batch elution study performed with Diaion CRB 02 (0.355-0.500mm). According to experimental results, % elutions of boron are 69.76, 73.61, 74.36 and 77.83 with 0.1 M HCl, 0.25 M HCl, 0.5 M HCl and 1.0 M HCl, respectively. The % elution incresed with increasing concentration of HCl.

As kinetic experiment, temperature effect, stirring rate effect and particle size effect on boron removal was investigated.

According to result of temperature effect, the equilibrium half-times for B removal from model B solution was between 0-5 minute that was nearly same for 25°C, 30°C and 35°C. On the other hand, the kinetic performance of Diaion CRB 02 increased with increasing of temperature degree.

Stirring rate effect was investigated with 200 RPM, 250RPM and 300 RPM using Diaion CRB 02 (45-125 µm). Stirring rate did not affect the kinetic performance of the resin.

According to kinetic tests, the equilibrium half-times for B removal from model boron solution were between 60-90 minutes with Diaion CRB 02 (0.355-0.500 mm). The corresponding values for powdered resin (45-125 µm) were less than 5 minutes. Kinetic performance of the (0.355-0.500 mm) particle sized resin was relatively slower than powdered sized resin (45-125 µm). Kinetic performances of resins improved effectively by decreasing the particle size.

Sorption kinetics in model B solution fit to pseudo-first-order mechanism. In the comparision of the experimental and theoretical q values for second order kinetics showed similarity as a proof of the fitting to the pseudo-second-order mechanism. The same results are obtained for stirring rate effect and particle size effect.

The data obtained from kinetic studies with model B solution were applied to the kinetic models known as Infinitive Solution Volume and Unreacted Core Models. The correlation coefficients for the linear models show that the rate is particle diffusion controlled according to bothe ISV and UCM models.

Using the result of temperature study, the thermodynamic parameters were obtained. Free energy change ($\Delta G°$) values found as -10.79 kj/mol, -12.24 kj/mol and -13.48 kj/mol at 25°C, 30°C and 35°C respectively. The negative results show the reactions occured spontaneously. Enthalpy change ($\Delta H°$) found as 69.63 (kj/kmol). The positive value of $\Delta H°$ indicates endothermic nature of adsorption.

The batch study of Diaion CRB 02 (45-125 µm) resin was applied to Langmuir, Freundlich and Dubinin-Radushkevich (DR) Adsorption Isotherms. The correlation for the linear regression fit of DR model equation was found to be 0.9918 for Diaion CRB 02 (45-125 µm) in model B solution.

APPENDIX-I

Batch Studies:

Table A.1 Effect of Resin Amount on Removal of Boron from Model B Solution by Diaion CRB 02 (45-125 µm) (Figure 3.1).

Resin Amount (g/100mL)	C (mg/L)	B removal (%)
0.00	0.00	0.00
0.01	1.19	40.30
0.02	0.69	65.49
0.03	0.42	78.84
0.04	0.31	84.63
0.05	0.20	89.92
0.06	0.21	89.67
0.07	0.22	89.17
0.10	0.21	89.67

Table A.2 Effect of Resin Amount on Removal of Boron from Model B Solution by Diaion CRB02 (Particle size: 0.355-0.500 mm) (Figure 3.1).

Resin Amount (g/100mL)	C (mg/L)	B removal (%)
0.00	0.00	0.00
0.01	1.22	36.46
0.02	0.84	56.51
0.03	0.72	62.76
0.04	0.49	74.48
0.05	0.40	79.43
0.06	0.35	82.03
0.07	0.31	83.85
0.10	0.31	83.85

Table A.3 Effect of Resin Amount on Removal of Boron from Model B Solution by Dowex XUS (43592.00) (45-125 micron) (Figure 3.2).

Resin Amount (g/100mL)	C (mg/L)	B removal (%)
0.00	0.00	0.00
0.01	1.00	50.25
0.02	0.38	81.00
0.03	0.22	89.25
0.04	0.17	91.75
0.05	0.09	95.50
0.06	0.06	97.00
0.07	0.04	98.00
0.10	0.04	98.00

Table A.4 Effect of Resin Amount on Removal of Boron from Model B Solution by Dowex XUS (43592.00) (0.355-0.500 micron) (Figure 3.2).

Resin Amount (g/100mL)	C (mg/L)	B removal (%)
0.00	0.00	0.00
0.01	1.31	34.26
0.02	1.16	41.81
0.03	0.88	55.67
0.04	0.58	70.78
0.05	0.59	70.53
0.06	0.55	72.29
0.07	0.57	71.28
0.10	0.58	70.78

Table A.5 Effect of Resin Amount on Removal of Boron from Model B Solution by Dowex XUS (43592.00) (0.355-0.500 micron) (Figure 3.3).

Resin Amount (g/100mL)	**C (mg/L)**	**B removal (%)**
0.00	0.00	0.00
0.01	1.31	34.26
0.02	1.16	41.81
0.03	0.88	55.67
0.04	0.58	70.78
0.05	0.59	70.53
0.06	0.55	72.29
0.07	0.57	71.28
0.10	0.58	70.78
0.15	0.15	92.34
0.20	0.11	93.01
0.30	0.07	94.62
0.40	0.03	97.11

Table A.6 Effect of Resin Amount on Removal of Boron from Model B Solution by Diaion CRB02 (0.355-0.500 micron) (Figure 3.3).

Resin Amount (g/100mL)	C (mg/L)	B removal (%)
0.00	0.00	0.00
0.01	1.22	36.46
0.02	0.84	56.51
0.03	0.72	62.76
0.04	0.49	74.48
0.05	0.40	79.43
0.06	0.35	82.03
0.07	0.31	83.85
0.10	0.31	83.85
0.15	0.04	98.02
0.20	0.03	98.28
0.30	0.03	98.70
0.40	0.02	98.91

Kinetic Studies:

Table A.7 Results of kinetic studies for Diaion CRB 02 (45-125 micron) with Model B Solution at 25°C (Figure 3.4 and 3.5).

Time (min)	C (mg/L)	C/Co	B Removal (%)
0	1.99	1.00	0.00
5	0.89	0.44	55.53
10	0.64	0.32	67.84
15	0.45	0.22	77.64
20	0.35	0.17	82.66
30	0.31	0.16	84.42
45	0.29	0.15	85.43
60	0.28	0.14	86.18
90	0.26	0.13	86.93
120	0.23	0.11	88.69
180	0.18	0.09	90.95
240	0.14	0.07	92.96
300	0.10	0.05	94.97
360	0.08	0.04	96.23
420	0.05	0.03	97.49
480	0.05	0.03	97.49
1440	0.05	0.03	97.49

Table A.8 Results of kinetic studies for Diaion CRB 02 (45-125 micron) with Model B Solution at 30°C (Figure 3.4 and 3.5).

Time (min)	C (mg/L)	C/Co	B Removal (%)
0	1.96	1.00	0.00
5	0.83	0.42	57.54
10	0.63	0.32	67.77
15	0.40	0.20	79.80
20	0.33	0.17	83.38
30	0.32	0.16	83.89
45	0.29	0.15	85.42
60	0.25	0.13	87.47
90	0.20	0.10	89.77
120	0.15	0.07	92.58
180	0.11	0.06	94.37
240	0.10	0.05	95.14
300	0.07	0.04	96.42
360	0.06	0.03	96.93
420	0.04	0.02	97.95
480	0.03	0.01	98.72
1440	0.02	0.01	98.98

Table A.9 Results of kinetic studies for Diaion CRB 02 (45-125 micron) with Model B Solution at 35°C (Figure 3.4 and 3.5).

Time (min)	C (mg/L)	C/Co	B Removal (%)
0	1.95	1.00	0.00
5	0.70	0.36	64.39
10	0.46	0.23	76.68
15	0.37	0.19	81.17
20	0.26	0.13	86.82
30	0.20	0.10	89.92
45	0.17	0.09	91.43
60	0.15	0.08	92.36
90	0.13	0.07	93.47
120	0.11	0.06	94.41
180	0.08	0.04	95.79
240	0.08	0.04	95.85
300	0.06	0.03	97.13
360	0.05	0.03	97.34
420	0.04	0.02	97.99
480	0.02	0.01	98.87
1440	0.02	0.01	99.04

Table A.10 Results of kinetic studies for Diaion CRB 02 (45-125 micron) with Model B Solution at 25°C and 200RPM (Figure 3.6 and 3.7).

Time (min)	C (mg\L)	C/Co	Removal (%)
0	1.96	1.00	0.00
5	0.72	0.37	63.09
10	0.51	0.26	73.97
15	0.42	0.21	78.63
20	0.35	0.18	82.26
30	0.28	0.15	85.50
45	0.27	0.14	86.07
60	0.25	0.13	87.27
90	0.24	0.12	87.97
120	0.23	0.12	88.27
180	0.16	0.08	91.87
240	0.14	0.07	92.73
300	0.11	0.06	94.50
360	0.08	0.04	95.95
420	0.05	0.03	97.27
480	0.05	0.03	97.49
1440	0.05	0.03	97.49

Table A.11 Results of kinetic studies for Diaion CRB 02 (45-125 micron) with Model B Solution at 25°C and 250RPM (Figure 3.6 and 3.7).

Time (min)	C (mg\L)	C/Co	Removal (%)
0	1.99	1.00	0.00
5	0.89	0.44	55.53
10	0.64	0.32	67.84
15	0.45	0.22	77.64
20	0.35	0.17	82.66
30	0.31	0.16	84.42
45	0.29	0.15	85.43
60	0.28	0.14	86.18
90	0.26	0.13	86.93
120	0.23	0.11	88.69
180	0.18	0.09	90.95
240	0.14	0.07	92.96
300	0.10	0.05	94.97
360	0.08	0.04	96.23
420	0.05	0.03	97.49
480	0.05	0.03	97.49
1440	0.05	0.03	97.49

Table A.12 Results of kinetic studies for Diaion CRB 02 (45-125 micron) with Model B Solution at 25°C and 300RPM (Figure 3.6 and 3.7).

Time (min)	C (mg\L)	C/Co	Removal (%)
0	1.96	1.00	0.00
5	0.92	0.47	53.19
10	0.59	0.30	69.86
15	0.39	0.20	79.87
20	0.28	0.14	85.93
30	0.26	0.13	86.68
45	0.23	0.12	88.09
60	0.23	0.12	88.49
90	0.21	0.11	89.26
120	0.19	0.10	90.26
180	0.15	0.08	92.25
240	0.11	0.06	94.42
300	0.08	0.04	95.84
360	0.06	0.03	96.71
420	0.05	0.03	97.27
480	0.04	0.02	97.92
1440	0.03	0.02	98.26

Table A.13 Results of kinetic studies for Diaion CRB 02 (125-250 micron) with model B Solution at 25°C and 250RPM (Figures 3.8, 3.9, 3.10 and 3.11).

Time (min)	C (mg/L)	C/Co	B Removal (%)
0	1.89	1.00	0.00
5	0.95	0.50	49.51
10	0.72	0.38	62.10
15	0.60	0.32	68.30
20	0.46	0.24	75.68
30	0.41	0.22	78.31
45	0.30	0.16	84.28
60	0.20	0.11	89.19
90	0.15	0.08	92.01
120	0.13	0.07	93.28
180	0.10	0.05	94.86
240	0.10	0.05	94.94
300	0.09	0.05	95.18
360	0.06	0.03	96.94
420	0.06	0.03	96.90
480	0.06	0.03	96.96
1440	0.06	0.03	97.07

Table A.14 Results of kinetic studies for Diaion CRB 02 (0.355-0.500 mm) with Model B Solution at 25°C and 250 RPM (Figures 3.8 and 3.9).

Time (min)	C (mg/L)	C/Co	B Removal (%)
0	1.92	1.00	0.00
5	1.73	0.90	10.22
10	1.58	0.82	17.76
15	1.51	0.78	21.53
20	1.46	0.76	23.89
30	1.32	0.69	31.09
45	1.14	0.59	40.75
60	1.01	0.52	47.53
90	0.74	0.39	61.38
120	0.70	0.36	63.65
180	0.53	0.28	72.20
240	0.43	0.22	77.56
300	0.33	0.17	82.64
360	0.30	0.16	84.29
420	0.24	0.12	87.67
480	0.21	0.11	89.07
1440	0.06	0.03	96.78

Table A.15 Results of kinetic studies for 0.15 g/100 mL Diaion CRB 02 (0.355-0.500 mm) with model B Solution at 25°C and 250RPM (Figures 3.10 and 3.11).

Time (min)	C (mg/L)	C/Co	B Removal (%)
0	1.95	1.00	0.00
5	1.08	0.55	44.86
10	0.76	0.39	61.17
15	0.52	0.27	73.32
20	0.45	0.23	77.13
30	0.36	0.19	81.43
45	0.30	0.16	84.43
60	0.29	0.15	84.92
90	0.26	0.13	86.72
120	0.25	0.13	87.36
180	0.23	0.12	88.09
240	0.21	0.11	89.37
300	0.16	0.08	91.70
360	0.14	0.07	93.00
420	0.10	0.05	94.79
480	0.09	0.05	95.43
1440	0.09	0.05	95.37

Table A.16 Results of kinetic studies for Diaion CRB 02 (45-125 micron) with RO Permeate Solution at 25°C and 250 RPM (Figures 3.32 and 3.33).

Time (min)	C (mg/L)	C/Co	B Removal (%)
0	1.98	1.00	0.00
5	0.79	0.40	60.01
10	0.64	0.33	67.48
15	0.50	0.25	74.80
20	0.38	0.19	80.79
30	0.34	0.17	82.81
45	0.30	0.15	84.85
60	0.36	0.18	81.99
90	0.31	0.16	84.43
120	0.20	0.10	89.72
180	0.17	0.09	91.49
240	0.20	0.10	90.06
300	0.13	0.07	93.40
360	0.09	0.04	95.51
420	0.08	0.04	95.83
480	0.06	0.03	97.10
1440	0.06	0.03	97.10

Table A.15 Results of kinetic studies for Diaion CRB 02 (45-125 micron) with Model B solution at 25°C with 250 RPM (Figures 3.12 and 3.3).

Time (min)	qt (mg / g-resin)	Log (q_e-q_t)	t/q_t
5	2.21	0.22	2.26
10	2.70	0.07	3.70
15	3.09	-0.10	4.85
20	3.29	-0.23	6.08
30	3.36	-0.28	8.93
45	3.40	-0.32	13.24
60	3.43	-0.35	17.49
90	3.46	-0.38	26.01
120	3.53	-0.46	33.99
180	3.62	-0.59	49.72
240	3.70	-0.74	64.86
300	3.78	-1.00	79.37
360	3.83	-1.30	93.99

Table A.16 Results of kinetic studies for Diaion CRB 02 (45-125 micron) with Model B solution at 30°C with 250 RPM (Figures 3.12 and 3.13).

Time (min)	qt (mg / g-resin)	Log (q_e-q_t)	t/q_t
5	2.25	0.21	2.22
10	2.65	0.08	3.77
15	3.12	-0.13	4.81
20	3.26	-0.22	6.13
30	3.28	-0.24	9.15
45	3.34	-0.28	13.47
60	3.42	-0.36	17.54
90	3.51	-0.46	25.64
120	3.62	-0.62	33.15
180	3.69	-0.77	48.78
240	3.72	-0.85	64.52
300	3.77	-1.05	79.58
360	3.79	-1.15	94.99
420	3.83	-1.52	109.66

Table A.17 Results of kinetic studies for Diaion CRB 02 (45-125 micron) with Model B solution at 35°C with 250 RPM (Figures 3.12 and 3.13).

Time (min)	q_t (mg / g-resin)	Log (q_e-q_t)	t/q_t
5	2.52	0.13	1.99
10	3.00	-0.06	3.34
15	3.17	-0.16	4.73
20	3.39	-0.33	5.89
30	3.52	-0.46	8.53
45	3.57	-0.54	12.59
60	3.61	-0.59	16.62
90	3.65	-0.68	24.63
120	3.69	-0.76	32.51
180	3.75	-0.92	48.06
240	3.75	-0.93	64.04
300	3.80	-1.17	78.99
360	3.81	-1.22	94.58
420	3.83	-1.46	109.62

Table A.18 Results of kinetic studies for Diaion CRB 02 (45-125 micron) with Model B solution with 200 RPM at 25°C (Figures 3.17 and 3.18).

Time (min)	qt (mg / g-resin)	Log (q_e-q_t)	t/q_t
5	2.47	0.13	2.02
10	2.90	-0.04	3.45
15	3.08	-0.13	4.87
20	3.22	-0.22	6.20
30	3.35	-0.33	8.95
45	3.37	-0.35	13.34
60	3.42	-0.40	17.54
90	3.45	-0.43	26.10
120	3.46	-0.44	34.68
180	3.60	-0.66	49.97
240	3.64	-0.73	66.02
300	3.70	-0.93	80.98
360	3.76	-1.22	95.70
420	3.81	-2.08	110.13

Table A.19 Results of kinetic studies for Diaion CRB 02 (45-125 micron) with Model B solution with 250 RPM at 25°C (Figures 3.17 and 3.18).

Time (min)	qt (mg / g-resin)	Log (q_e-q_t)	t/q_t
5	2.21	0.34	2.26
10	2.70	0.43	3.70
15	3.09	0.49	4.85
20	3.29	0.52	6.08
30	3.36	0.53	8.93
45	3.40	0.53	13.24
60	3.43	0.54	17.49
90	3.46	0.54	26.01
120	3.53	0.55	33.99
180	3.62	0.56	49.72
240	3.70	0.57	64.86
300	3.78	0.58	79.37
360	3.83	0.58	93.99

Table A.20 Results of kinetic studies for Diaion CRB 02 (45-125 micron) with Model B solution with 300 RPM at 25°C (Figures 3.17 and 3.18).

Time (min)	qt (mg / g-resin)	Log (q_e-q_t)	t/q_t
5	2.08	0.24	2.40
10	2.74	0.03	3.65
15	3.13	-0.17	4.79
20	3.37	-0.35	5.94
30	3.40	-0.38	8.84
45	3.45	-0.44	13.04
60	3.47	-0.46	17.31
90	3.50	-0.50	25.74
120	3.54	-0.56	33.94
180	3.61	-0.71	49.81
240	3.70	-0.95	64.89
300	3.75	-1.25	79.92
360	3.79	-1.66	95.04

Table A.21 Results of kinetic studies for Diaion CRB 02 (45-125 micron) with Model B solution with 250 RPM at 25°C (Figures 3.22 and 3.23).

Time (min)	Qt (mg / g-resin)	Log (q_e-q_t)	t/q_t
5	2.21	0.22	2.26
10	2.70	0.07	3.70
15	3.09	-0.10	4.85
20	3.29	-0.23	6.08
30	3.36	-0.28	8.93
45	3.40	-0.32	13.24
60	3.43	-0.35	17.49
90	3.46	-0.38	26.01
120	3.53	-0.46	33.99
180	3.62	-0.59	49.72
240	3.70	-0.74	64.86
300	3.78	-1.00	79.37
360	3.83	-1.30	93.99

Table A.22 Results of kinetic studies for Diaion CRB 02 (125-250 micron) with Model B solution with 250 RPM at 25°C (Figures 3.22 and 3.23).

Time (min)	Qt (mg / g-resin)	Log (q_e-q_t)	t/q_t
5	1.87	0.25	2.68
10	2.34	0.12	4.27
15	2.58	0.03	5.82
20	2.86	-0.10	7.00
30	2.96	-0.15	10.15
45	3.18	-0.32	14.15
60	3.37	-0.53	17.83
90	3.47	-0.73	25.92
120	3.52	-0.86	34.09
180	3.58	-1.10	50.28
240	3.58	-1.12	66.99
300	3.59	-1.18	83.52

Table A.23 Results of kinetic studies for Diaion CRB 02 (0.355-0.500 mm) with Model B solution with 250 RPM at 25°C (Figures 3.22 and 3.23).

Time (min)	qt (mg / g-resin)	Log (q_e-q_t)	t/q_t
5	0.39	0.48	12.73
10	0.68	0.44	14.65
15	0.83	0.41	18.13
20	0.92	0.40	21.78
30	1.19	0.35	25.11
45	1.57	0.27	28.73
60	1.83	0.20	32.84
90	2.36	0.03	38.15
120	2.45	-0.01	49.05
180	2.77	-0.19	64.87
240	2.98	-0.35	80.51
300	3.18	-0.61	94.45
360	3.24	-0.74	111.13
420	3.37	-1.27	124.65

REFERENCES

Alkan, M., Demirbaş, Ö., Çelikçapa, S., Doğan, M., 2004, Sorption of acid red 57 from aqueous solution onto sepiolite, J. Hazard Mater, B116, 135-145.

ANZECC, 1992, Australian water quality guidelines for fresh and marine waters, National Water Quality Management Strategy Paper No 4, Australian and New Zealand Environment and Conservation Council, Canberra.

Ayers R.S., Westcot D.W., 1994, Water quality for agriculture**,** Food and Agriculture Organization of the United Nations Rome.

Ayers, R.S., 1977, Quality of Water for Irrigation, Jour, ASCE. Vol 103, No. IR2.

Badruk, M., Kabay N., Demircioğlu, M., Mordoğan, H., İpekoğlu, U., 1999, Removal of boron from wastewater of geothermal power plant by selective ion exchange resins, Separation and Science Technology.

Bauder T.A, 2007, Colorado State University Extension water quality specialist; R.M. Waskom, Extension water resource specialist; and J.G. Davis, Extension soils specialist and professor, soil and crop sciences.

Charles, M R, 2006, Alkaline Regeneration of N-Methyl-D- Glıukamine Functional Resins, Patent Application Number, WO2006/110574.

Dasch, E. Julius, 1996, Encyclopedia of Earth Sciences. New York: Macmillan Reference USA.

Dow Tech Manual, 2006, Form No. 609-02002-504.

Dow Tech Manual, 2006, Form no: 609-02003-1004.

Fry, Al., 2006, Facts and Trend water, brochure of World Business Council for Sustainable Development.

Gleick, P. H., Schneider, S. H., 1996, Water resources. In Encyclopedia of Climate and Weather, ed., Oxford University Press, New York, vol. 2, pp.817-823.

Harland, C.E., 1994, Ion Exchange Theory and Practice, UK, Royal Society of Chemistry.

Howard G., Gartram J., 2003, Domestic water quantity, service level and health, World Health Organization, Geneva.

Kabay, N. Sarp, S., Yüksel, M., Arar, Ö., Bryjak, M., 2007, Removal of Boron From Seawater by Selective Ion Exchange Resins, Reactive & Functional Polymers, p. 1643-1650.

Kabay, N., 2001, Membrane Processes Course Notes.

Markus Busch, William E. Mickols, Steve Jons, Jorge Redondo, Jean De Witte, 2004, Boron Removal in Seawater Desalination, International Desalination and Water Reuse Quarterly.

Mesmer, R. E., Baes, C. F., Jr., Sweeton, F.H., 1972, Inorganic Chemistry.

Miles, Lawrence D, 1979, McGraw-Hill Encyclopedia of Science and Technology, 5th edition, McGraw-Hill.

Millennium Ecosystem Assessment, 2005, Ecosystems and Human Well-being: Synthesis.

Mitsubishi Kasei Corporation, 1992, Diaion Ion Exchange Resin Manual.

Ngah, W.S., Hanafiah, M. A., 2008, Adsorption of Cupper on Rubber leaf Powder: Kinetic, Equilibrium and Thermodynamic Studies, Biochemical Engineering Journal, p. 521-530.

Özacar, M., Şengil, I., A., 2004, Two-stage batch sorber design using second-order kinetic model for the sorption of metal complex dyes onto pine sawdust, Biochemical Engineering Journal, p. 39-45.

Pilson, Michael E. Q., 1998, An Introduction to the Chemistry of the Sea, Upper Saddle River, NJ: Prentice Hall.

Post, J.C. and Ochs, W.J. 1995, Agricultural salinity assessment and management *(*K.K. Tanji*,* ed*).* ASCE Manual No 71. New York*,* ASCE.

Redondo, J., Busch, M., 2003, Boron removal from seawater using Filmtech high rejection membrane, Malta, Desalination.

Saeijs, H.F.L, Van Berkel, M.J., 1995, Global Water Crisis, the Major Issue of the 21st Century", European Water Pollution Control.

Saeijs, H.F.L., Van Berkel, M.J., 2003, Global Water Crisis, the Major Issue of the 21st Century, European Water Pollution Control, 1995. Vol. 5.4 pp. 26-40; cited by Corporate Water Policies, Dec.

Samuelson, O, 1963, Ion Exchannge Separations in Analytical Chemistry, John Willey and Sons, New York.

Seader, J. D., Henley, E. J., 1998, Separation Process and Principles, John willey and Sons. Inc., New York.

Seader, J.D., Hendley, E, J., 1998, Seperation Process & Principles, John Wiley & Sons inc, New York.

Seki, Y., Seylan, S., Yurdakoç, M., 2006, Removal of Boron form Aqueous Solution by Adsorption Al2O3 Base Materials Using Ful Factoial Design, Journal of Hazardous Materials.

The British Dietetic Association, 2003, Food Facts. Fluid: Why you need it and how to get enough. BDA, November.

The United Nations World Water Development Report, 2008.

TIFAC, 1997, Membrane Separation System Study Report.

UNESCO, 2003, World Water Development Report, Part II: A look at the world's freshwater resources.

WBCSD and UNEP, 1998, Industry fresh water and sustainabled development.

Yilmaz, I., Kabay, N., Brjyak, M., Yüksel, M., Wolska, J., Koltuniewicz, A., 2006, A submerged membrane–ion-exchange hybrid process for boron removal DesalinationVolume 198, Issues 1-3.

CURRICULUM VITAE

Name:	Kırmızısakal ÖZLEM
Date of Birth:	June, 02, 1982
Place of Birth:	Adana, Turkey
Nationality:	Republic of Turkish
Marital Status:	Single
Adress:	Erzene Mah. 83. Sok. No: 25 D:9 Bornova, İzmir, Turkey
Phone Number:	+90 232 3739951
E-mail:	ozlem.kirmizisakal@gmail.com
Education:	2000-2005, BSc Degree in Chemical Engineering Department of Ege University, İzmir, Turkey 2006-2008, MSc Degree in Chemical Engineering Department of Ege University, İzmir, Turkey

Publications:

1) Removal of Boron from Balçova-Izmir Geothermal Water by Ion Exchange Process: Batch and Column Studies. I. Yılmaz İpek, N. Kabay, M.Yüksel, **Ö. Kırmızısakal**, M. Bryjak, Chem. Eng. Commun (in Press).
2) Removal of Bororn From Balçova Geothermal Water by Ion Exchange-Microfiltration Hybrid Process, N. KAbay, I. Yılmaz İpek, I. Soroho, M. Makowski, **Ö. Kırmızısakal**, S.Yağ, M. Bryjak, M. Yüksel, Desalination (in Pres).

Presentation in National and International Conferences:

1) Removal of Boron from Balçova-Izmir Geothermal Water by Ion Exchange Process: Batch and Column Studies, I. Yılmaz İpek, N. Kabay, M.Yüksel, **Ö. Kırmızısakal**, M. Bryjak, Somer - Chemical Engineering Conferences-METU (Poster Presentation)